Alternative splicing and RNA editing of the Complexin C-terminus regulates neurotransmitter release in *Drosophila*

by

Elizabeth A. Brija

B.A. Neuroscience and Behavior
Mount Holyoke College, 2016

Submitted to the Department of Brain and Cognitive Sciences
in partial fulfillment of the requirements for the degree of

Doctor of Philosophy in Neuroscience

at the

MASSACHUSETTS INSTITUTE OF TECHNOLOGY

June 2023

Authored by……
Department of Brain and Cognitive Sciences
April 11th, 2023

Certified by…….
J. Troy Littleton
Menicon Professor of Neuroscience
Thesis Supervisor

Accepted by……
Mark Harnett
Graduate Officer, Department of Brain and Cognitive Sciences

Alternative splicing and RNA editing of the Complexin C-terminus regulates neurotransmitter release in *Drosophila*

by

Elizabeth A. Brija

Submitted to the Department of Brain and Cognitive Sciences on April 11th, 2023
in partial fulfillment of the requirements for the degree of
Doctor of Philosophy in Neuroscience

Abstract

Chemical synaptic transmission is an essential and highly regulated step in neuronal communication. Changes in the strength of synaptic transmission mediate several forms of plasticity associated with learning and memory. Functional regulation of Complexin (Cpx) provides an entry point for altering presynaptic output since the protein controls spontaneous and evoked neurotransmitter release through its effects on SNARE complex assembly. The *Drosophila cpx* locus undergoes alternative splicing to produce two isoforms (Cpx7A and Cpx7B) that differ in the C-terminal ~20 amino acids of Cpx. Although PKA phosphorylation of Cpx7B C-terminal residue S126 enhances spontaneous release and synaptic growth in *Drosophila*, the more abundant Cpx7A does not undergo PKA phosphorylation, but is subject to RNA editing that produces three alternative C-terminal domain residues (N130S, N130D, N130G). Edit variant N130S contains a phospho-competent residue located in a similar C-terminal region to the Cpx7B PKA phosphorylation site, but the functional significance of Cpx7A RNA editing in regulating neurotransmission and structural plasticity is unknown.

In this thesis, I characterized the role of alternative splicing and RNA editing in Cpx function. I found that Cpx7A and Cpx7B splice isoforms have largely redundant roles in regulating neurotransmitter release despite significant expression level differences. Single-cell RNAseq data revealed multiple Cpx7A RNA editing variants are co-expressed, indicating editing acts stochastically to generate a range of edited Cpx proteins within individual cells. To determine if RNA editing alters Cpx7A function, I compared synaptic transmission and growth properties in *cpx* null mutants rescued with unedited or edited Cpx7A transgenes. N130S variants displayed a dramatic reduction in spontaneous fusion clamping compared to unedited Cpx7A. In addition, N130S can dominantly function when co-expressed with unedited Cpx7A, suggesting the abundance of edited proteins within single neurons can fine-tune their baseline neurotransmission. N130S displayed altered subcellular localization, suggesting altered ability of the edited protein to tether to synaptic vesicles. Additionally, casein kinase 2 was found to phosphorylate the N130S variant. Together, these findings indicate Cpx7A and Cpx7B have redundant roles in controlling baseline neurotransmission, while differential RNA editing of Cpx7A alters Cpx's clamping properties and functionally changes presynaptic output by enhancing spontaneous neurotransmitter release.

Thesis Supervisor: J. Troy Littleton
Title: Menicon Professor of Neuroscience

Acknowledgements

My PhD journey would not have been possible without my thesis supervisor, J. Troy Littleton, MD, PhD, who provided invaluable patience and guidance over the years. I also could not have completed this journey without my committee chair, Li-Huei Tsai, PhD, and my defense committee, Myriam Heiman, PhD and Adam Martin, PhD, who kindly provided advice, knowledge, and expertise. Additionally, this research would not have been possible without the generous financial support from the National Science Foundation Graduate Research Fellowship Program.

I am also grateful to the Littleton lab members for teaching me countless experimental skills and for making every day in the lab enjoyable. Special thanks to Zhuo Guan, PhD and Suresh K. Jetti, PhD for their experimental contributions to my research, and to Dina Volfson for keeping the lab running in pristine order. Many thanks to my fellow graduate students for coffee chats and editing help on various proposals and applications, and especially to Chad Sauvola, for always being happy to talk all things neurobiology with me over appetizers while we figured out cloning strategies and virtual teaching.

I'd like to thank my friends and family back home for always welcoming me with open arms even after years apart. Thank you to my MHC circle for providing space to share our accomplishments and struggles as we strive to establish our careers, even across four time zones! Thanks to all of Team Wildwood for keeping me sane and encouraging me to become a better athlete every day. Above all, I thank Michael for supporting me through all of life's adventures. Thank you.

Table of Contents

List of Figures

Chapter 1

Chapter 2

Chapter 3

Chapter 1

Regulation of Synaptic Vesicle Fusion by Complexin

Elizabeth A. Brija[1]

[1]The Picower Institute for Learning and Memory, Department of Brain and Cognitive Sciences, Massachusetts Institute of Technology, Cambridge, MA 02139

1.1 Overview

Neuronal communication requires the propagation of action potentials into presynaptic terminals to open voltage-gated calcium channels (VGCCs) clustered at presynaptic release sites known as active zones (AZs). The subsequent influx of calcium triggers synaptic vesicle (SV) fusion and neurotransmitter release. Calcium-dependent SV fusion is mediated by vesicle and target membrane SNARE (soluble *N*-ethylmaleimide–sensitive factor attachment protein receptor) proteins that zipper together, bringing the vesicle and plasma membrane into close proximity for fusion (Harris & Littleton, 2015; Rizo & Südhof, 2002). SVs occasionally undergo fusion independent of action potentials, resulting in spontaneous single vesicle fusion events known as "minis" (Fatt & Katz, 1952). In mammals, these spontaneous release events can regulate dendritic spine morphogenesis and protein synthesis (McKinney et al., 1999; M. A. Sutton et al., 2004). Moreover, changes in the frequency of minis can trigger synaptic growth and activity-dependent plasticity at *Drosophila* NMJs (Cho et al., 2015; Choi et al., 2014; Huntwork & Littleton, 2007), indicating spontaneous fusion events play an important role in structural and function synaptic plasticity in addition to the well-established role of evoked neurotransmitter release.

Due to the critical function of fast stimulus-dependent vesicular release in neuronal signaling, it is imperative to tightly regulate SV fusion by controlling the timing and localization of SNARE complex assembly (Südhof & Rothman, 2009). One key regulatory protein for neurotransmitter release is the calcium sensor Synaptotagmin 1 (Syt1), a SV protein that interacts with SNAREs and lipid membranes to facilitate fast and synchronous calcium-dependent vesicle fusion in response to an action potential (Littleton et al., 1993; Yoshihara & Littleton, 2002). Another key modulator of neurotransmission is the small cytosolic protein, Complexin (Cpx), which serves a dual regulatory role: Cpx binds the assembling SNARE complex and holds the complex in a partially zippered state, allowing the protein to facilitate action potential-dependent fusion while also acting as a molecular "fusion clamp" to block premature exocytosis in the absence of calcium (Bera et al., 2022; Cho et al., 2010; Huntwork & Littleton, 2007).

The *Drosophila* neuromuscular junction (NMJ) has proven to be a powerful model synapse to study neurotransmission. The extensive genetic tools available in *Drosophila*, along with highly stereotyped synaptic organization and ease of access for imaging and electrophysiology, makes the glutamatergic NMJ a particularly useful system to characterize evolutionarily-conserved regulators of SV exocytosis (Banerjee et al., 2021; Cho et al., 2015; Choi et al., 2014; Huntwork

& Littleton, 2007; Newman et al., 2022; Yoshihara & Littleton, 2002). This chapter explores evoked and spontaneous SV fusion, with a focus on the conserved role for Cpx in regulating neurotransmission. I review structural and functional studies of Cpx in vertebrate and invertebrate model systems, concentrating on recent work that characterizes how different modifications of the unstructured Cpx C-terminus, including prenylation and phosphorylation, give rise to various regulatory changes in the protein's function. Finally, I discuss how RNA editing generates protein diversity and changes in neuronal function, with focus on the potential effects of RNA editing of the Cpx C-terminus on synaptic transmission in *Drosophila*.

1.2 Synaptic Vesicle Fusion and the SNARE complex

Synaptic vesicle lifecycle and the canonical SNARE proteins

Vesicles are small, secretory structures that carry cellular cargo enclosed by a lipid bilayer. In the case of SVs, this cargo is usually small neurotransmitters such as glutamate, acetylcholine or GABA, which are released from the vesicle into the synaptic cleft when exocytosis occurs. For SVs to release their contents into the cleft, both vesicle and plasma membrane lipid bilayers must interact to form a fusion pore between the two bilayers. To bring lipid bilayers into close apposition for fusion, this energetically unfavorable event due to repulsive forces between the bilayers must be overcome (Israelachvili et al., 1977; McNew et al., 2000; Südhof, 2013b). The binding and assembly of the evolutionarily-conserved SNARE complex into a highly structured coiled-coiled helix is thought to provide the necessary free energy to drive membrane fusion (Pobbati et al., 2006; Weimbs et al., 1997). Vesicular v-SNAREs (Synaptobrevin (Syb)/VAMP (vesicle-associated membrane protein)) provide one alpha-helix to interact with three alpha-helices from target membrane t-SNARES (Syntaxin-1 (Syx1) and synaptosomal-associated protein of 25 kDa (SNAP-25)). Syx1 provides one helix while SNAP-25 provides two helices that assemble with the v-SNARE, zippering together and forming a four-helix coiled-coil complex that provides the necessary energy to overcome lipid repulsion (Fasshauer et al., 1998; Littleton et al., 1998; Söllner, Whiteheart, et al., 1993; Söllner, Bennett, et al., 1993; R. B. Sutton et al., 1998; Weber et al., 1998). The v- and t-SNARE classification is also referred to by an R- and Q-SNARE scheme to account for homotypic fusion events, such as fusion between structurally and functionally equivalent vesicles (Fasshauer et al., 1998). R-SNAREs have an arginine (R) while Q-SNAREs have a glutamine (Q) at the central ionic layer (zero layer) of the SNARE coiled-coil structure

(Fasshauer et al., 1998; Weimbs et al., 1997). Previous work found that as few as one SNARE interaction is sufficient for liposome docking with a lipid bilayer (Bowen et al., 2004), however the number and arrangement of SNARE complexes required for proper SV fusion is unknown. Some models suggest that the physiological time scale of neurotransmission requires a circular arrangement of three to eight SNARE complexes zippering together between the two membranes, forming "spokes on a wheel" around a fusion pore (X. Han et al., 2004; Hua & Scheller, 2001; Montecucco et al., 2005; Shi et al., 2012).

In neurons, SV fusion can be initiated by an action potential that depolarizes the presynaptic terminal, leading to transient openings of VGCCs and subsequent influx of calcium into the terminal. These spikes in the local concentration of calcium at AZs trigger rapid fusion of the docked and primed SVs at these sites (Ghelani & Sigrist, 2018; Katz & Miledi, 1969; Zhai & Bellen, 2004). Calcium-dependent fusion is called evoked release and is comprised of a fast, synchronous phase of SV release (~60 μs after influx) followed by a slower, asynchronous phase where fewer SVs are released over several hundred milliseconds after calcium influx (Atluri & Regehr, 1998; Goda & Stevens, 1994; Sabatini & Regehr, 1996).

In addition to calcium-evoked fusion, spontaneous single SV fusion events can be observed in electrophysiological recordings as "mini" postsynaptic currents (Fatt & Katz, 1952). Minis can occur in the absence of a presynaptic calcium signal, though mini frequency can be modulated by external calcium concentrations (Miledi & Thies, 1971). Although most SVs undergo exocytosis through an action potential-evoked release pathway, spontaneous fusion events are thought to play a functional role in synapse development and maintenance, as well as normal synaptic signaling (Andreae & Burrone, 2018; Banerjee et al., 2021; Choi et al., 2014; McKinney et al., 1999). In addition to a role for minis in synaptogenesis, a few recent studies have identified a role for spontaneous fusion in various neuronal plasticity pathways, including activity-dependent structural plasticity and short-term homeostatic plasticity at *Drosophila* NMJs (Cho et al., 2015; Kavalali, 2015; Newman et al., 2017; M. A. Sutton et al., 2004). Genetic manipulations to key synaptic proteins, such as the calcium-sensing protein Syt1, have resulted in a genetic separation of spontaneous and evoked release events (Banerjee et al., 2021; Littleton et al., 1993), suggesting that although both fusion pathways are important for proper synaptic signaling, separate regulatory control may exist for each evoked versus spontaneous SV release, which will be further discussed in section 1.3.

After membrane fusion, the SNARE complex is disassembled and the vesicle membrane and its associated proteins are endocytosed for future fusion events. SNARE complex disassembly is mediated by the *N*-ethylmaleimide–sensitive factor (NSF), a hexameric ATPase, and the soluble NSF attachment proteins (SNAPs), that function as adapters to tether NSF to the SNARE complex. When NSF or SNAP activity is disrupted, SNARE complexes accumulate, resulting in reduced synaptic transmission (Babcock et al., 2004; Kawasaki & Ordway, 1999; Littleton et al., 1998; Söllner, Bennett, et al., 1993; Tolar & Pallanck, 1998). After SNARE proteins have been separated, v- and t-SNAREs must be correctly sorted and organized, though the protein sorting processes that mediate these events are still unclear. During this time, the synaptic vesicle membrane can also be recycled and sorted through several endocytic routes, including individual SV recovery through clathrin-mediated endocytosis, clathrin-independent kiss-and-run events, and bulk endocytosis to form intracellular endosomes (reviewed in: Chanaday et al., 2019; Gan & Watanabe, 2018; Soykan et al., 2016). Once SVs are reformed, they are reacidified through a vesicular proton-dependent ATPase to create a proton gradient, which allows for neurotransmitter loading through neurotransmitter-specific transporters, such as the vesicular glutamate transporter, VGLUT (Maycox et al., 1988; Stadler & Tsukita, 1984). Reformed SVs then move back into the cycling SV pool for further rounds of exocytosis.

SNARE chaperones and other SNARE regulatory proteins

Within the SV lifecycle, many regulatory proteins facilitate proper SV fusion and recycling. A few of these proteins, like NSF and the SNAP proteins, were briefly discussed in relation to SNARE disassembly. Other regulatory proteins, like Syt1 and Cpx, work to hold SNARE assembly in a partially-zippered state until a calcium stimulus is received, which will be discussed in the next section. Here, I will focus on several other proteins that act as SNARE chaperones and regulators to guide the localization and assembly of SNAREs to AZs, modulate SV priming through control of SNARE availability for complex assembly, and support SV target specificity.

Most SNARE proteins are comprised of a membrane anchor and contain a ~60 residue SNARE motif (Weimbs et al., 1997; Zhang & Hughson, 2021). A few SNAREs instead contain two SNARE motifs connected by a linker sequence, like SNAP-25, which contributes two motifs to the four-helix coiled-coil complex. In the absence of chaperone proteins, SNAREs can

misassemble into non-fusogenic off-pathway products or form a complex with anti-parallel SNARE motifs (Brunger, 2006; Weninger et al., 2003). Experiments *in vitro* suggest that cytosolic Syx1 can form homotetramers that are unable to bind other SNARE proteins (Lerman et al., 2000; Misura et al., 2001), while co-incubation of Syx1 and SNAP-25 form a possible off-pathway product containing 2:1 complexes of the t-SNAREs in addition to the on-pathway 1:1 product (Dawidowski & Cafiso, 2016; Fasshauer et al., 1997; Pobbati et al., 2006; Xiao et al., 2001). Other work has shown that 40% of SNARE complexes formed when all three SNARE proteins are co-incubated contained antiparallel helices (Lai et al., 2017). An anti-parallel configuration may prevent other SNARE complex regulators, such as Syt1 and Cpx, from properly interacting with the complex to modulate fusion (Zhou et al., 2015, 2017).

Studies of Syx1 and its yeast homolog Sso1p have suggested that the N-terminal domain of the protein inhibits SNARE assembly by binding intramolecularly to produce a "closed" conformation of Syx1 that cannot interact with other SNARE proteins (Calakos et al., 1994; Dulubova, 1999; Fiebig et al., 1999; Nicholson et al., 1998). This N-terminal domain binds other regulatory proteins like Munc13 (also called Unc-13), a protein essential for SV fusion (Augustin et al., 1999; Betz et al., 1997), and Munc18 (also called Sec1 or Unc-18), in which Munc18 can bind the closed Syx1 conformation (Dulubova, 1999; Pevsner et al., 1994; B. Yang et al., 2000). Munc13 can then open Munc18-bound closed Syx1, permitting Munc18-chaperoned SNARE assembly (Ma et al., 2011; S. Wang et al., 2017).

Experiments studying Sec1/Munc18 in several systems, including yeast, *C. elegans,* and mammals, demonstrated the essential role of these proteins in neurotransmission (Hata et al., 1993; Novick et al., 1980; Novick & Schekman, 1979; Verhage et al., 2000), forming a model for how the "SM" family of proteins interact with SNAREs and regulate fusion (Brenner, 1974; Hosono et al., 1992; Novick et al., 1980; Shen et al., 2007). Proteoliposome fusion assays demonstrate that Munc18-1 promotes fusion by interacting with R- and Q-SNAREs and enhances SNARE complex assembly (Shen et al., 2007), while mice lacking Munc18 exhibits a complete loss of neurotransmitter release, leading to paralysis and lethality after birth (Verhage et al., 2000). Interestingly, Munc18-1 can be phosphorylated in its SNARE-binding domain by Src family kinases (Meijer et al., 2018) and by protein kinase C (PKC) (Genç et al., 2014) to either inhibit or promote synaptic transmission, respectively, supporting the model that phosphorylation of SM and SNARE proteins can provide modulatory input into the SV fusion pathway (Laidlaw et al., 2017).

Munc18-1 and Munc13-1 can also work in concert to inhibit SNARE misassembly and increase evoked release probability by facilitating proper priming of SVs (Lai et al., 2017). In particular, the MUN domain of Munc13-1 interacts with Syx1 and VAMP2 to promote proper parallel-orientation of SNAREs in complex assembly (Lai et al., 2017). Munc13 also helps to facilitate docking and priming of SVs by tethering SVs to the AZ plasma membrane to promote synchronous fusion (Li et al., 2020; Liu et al., 2016; Quade et al., 2019; Reddy-Alla et al., 2017; Rothman et al., 2017; Shin et al., 2010). This Munc13 membrane tether is regulated by calcium and can bind RIM (Rab3-interacting molecule) and other synaptic proteins involved in neurotransmission (Camacho et al., 2017; Michelassi et al., 2017; Zikich et al., 2008). Taken together, Munc13 facilitates proper SV fusion by opening Syx1 for SNARE assembly while it orients parts of the SNARE complex and helps tether SVs to the AZ, where they are primed for fusion.

Another form of SNARE regulation is mediated by "decoy" SNAREs, which are SNARE proteins that are incompatible with membrane fusion (Lao et al., 2000; Scales et al., 2002). One known decoy SNARE across multiple model systems is Tomosyn (Tom), which can displace Syx1 from Munc18 and is thought to interact with Syx1 and SNAP-25 in a SNARE complex decoy pathway (Fujita et al., 1998; Masuda et al., 1998; Pobbati et al., 2004). Tom contains an R-SNARE motif which mimics other R-SNAREs like Syb, thus preventing R-SNAREs from binding to corresponding Q-SNAREs to form a fusogenic complex (Hatsuzawa et al., 2003; Pobbati et al., 2004; Sauvola & Littleton, 2021). In *Drosophila* mutants of *Tom*, a 50% increase in docked SVs per release site is observed and mutants display an increase in evoked and spontaneous fusion (Sauvola et al., 2021). Results in *C. elegans* are similar, with *Tom* mutants displaying increased synaptic transmission and a larger pool of primed vesicles. Interestingly, enhanced Unc-13 levels are also observed at synapses, suggesting that a balance of Tom and Unc-13 may be important for normal synaptic function (McEwen et al., 2006). Together, these results suggests that an enhanced pool of accessible t-SNAREs exists to increase SV docking when Tom is absent and unable to function as a decoy SNARE (McEwen et al., 2006; Pobbati et al., 2004; Sauvola et al., 2021).

Other SNARE regulatory proteins help facilitate vesicle-target recognition by recruiting and binding important synaptic proteins that specify membrane identity. Ras-associated binding (Rab) proteins and other Rab-associated proteins, like RIM, work as regulators of vesicle transport to help deliver the correct proteins to the proper intracellular location through specific affinities of

target proteins. Rab proteins are GTPases that cycle on and off of specific membranes, like SVs, where they recruit target-specific effector proteins, including tethering factors like RIM and SNAREs, to form protein complexes that drive efficient vesicle fusion (Betz et al., 2001; Y. Han et al., 2011; Koushika et al., 2001; Stenmark & Olkkonen, 2001; Y. Wang et al., 1997). RIM mutants demonstrate a reduction in SV docking and subsequently have impaired evoked release (Graf et al., 2012; Y. Han et al., 2011), while Rab3 mutants also show SV recruitment defects, but only a mild impairment of evoked release (Geppert et al., 1997; Graf et al., 2009; Nonet et al., 1997; Schlüter et al., 2006). These studies suggest both proteins are important for proper SV recruitment. Using various biochemical and biophysical approaches to define binding interactions between RIMs, Rab3, and Munc13, a model of a tripartite complex between these three proteins has emerged that supports SV release (Dulubova et al., 2005). In fact, disrupted Munc13-1 and RIM1 interactions leads to inefficient vesicle priming (Betz et al., 2001), supporting that the tripartite complex has important implications in the docking and priming of SVs and may be required for some forms of synaptic plasticity (Koushika et al., 2001; Rizo & Rosenmund, 2008). These targeting and tethering interactions play an important role in neurotransmission by mediating membrane fusion specificity and identity, after which partial SNARE complex assembly prepares SVs for fusion (Whyte & Munro, 2002; Yu & Hughson, 2010).

Overall, maintenance of proper SNARE assembly is essential to the speed and accuracy of SV fusion, providing strong support for the necessity of SNARE chaperones and other regulatory proteins in executing efficient SV release. Both Munc13 and Munc18 bind and stabilize different conformational forms of Syx1, functioning as points for SV docking or priming regulation (X. Wang et al., 2020; Weimer et al., 2003). Munc13 also facilitates parallel-orientation SNARE complex formation and participates in membrane targeting and vesicle tethering via its interaction with RIM and other synaptic molecules (Camacho et al., 2017; Lai et al., 2017). These interactions position SVs at AZs sites where docking and priming steps can occur to generate a fusion-ready vesicle that can be triggered to release during calcium influx.

1.3 Synaptotagmin 1 and Complexin regulation of SNARE complex assembly and function

Neurons maintain low intracellular calcium concentration, allowing influx of extracellular calcium to act as intracellular signal for numerous cellular processes. These spikes in local calcium concentration are important for synaptic transmission and synaptic plasticity pathways where fast,

coordinated signaling is critical. SNARE regulatory proteins like Syt1 and Cpx work to tightly couple full SNARE complex assembly to intracellular calcium signals. The cytosolic α-helical protein Cpx binds the assembling SNARE complex and arrests assembly in a partially-zippered state, thus acting as a fusion "clamp" (Bykhovskaia et al., 2013; Giraudo et al., 2006; Malsam et al., 2012; McMahon et al., 1995). Conversely, Syt1 is bound to the SV membrane and consists of two calcium-binding C2 domains, C2A and C2B, that allows Syt1 to act as a calcium sensor to trigger full zippering of the SNARE complex, leading to a synchronous evoked fusion event (Bowers & Reist, 2020; Chapman & Davis, 1998; Geppert et al., 1994; Perin et al., 1991; Südhof, 2013a). Although numerous studies on the role of Syt1 and Cpx in regulated SNARE assembly and SV fusion have been completed, the precise mechanisms by which these proteins mediate synaptic fusion are still unclear.

Synaptotagmin 1

Early studies of Syt1 across multiple model systems demonstrated that loss of Syt1 had detrimental effects on synchronous release, with alterations to its calcium binding abilities leading to changes in the calcium sensitivity of SV fusion and ultimately, a disruption of synaptic transmission (Davis et al., 1999; Fernández-Chacón et al., 2001; Geppert et al., 1994; Lee et al., 2013; Littleton et al., 1993, 1994; Mackler et al., 2002). These studies provided support for the role of Syt1 as a critical calcium sensor for neurotransmission, defining the roles of calcium-binding residues within the two Syt1 C2 domains. In many proteins, C2 domains function to coordinate calcium and lipid binding (Nalefski et al., 2001). As such, the C2 domains of Syt1 contain negatively-charged aspartate residues that become neutralized when bound to positively-charged calcium ions (Bykhovskaia, 2021; Fernandez et al., 2001; Ubach et al., 1998, 2001). Neutralization of these domains allows the protein to partially insert into the plasma membrane, which may aid full SNARE zippering and SV fusion (Brose et al., 1992; Bykhovskaia, 2021; Chapman & Davis, 1998; Davis et al., 1999; Fernández-Chacón et al., 2001; Paddock et al., 2008; Tucker et al., 2004). Furthermore, calcium binding by C2B has can induce C2B binding of multiple membranes simultaneously, thus bringing two membranes into close proximity for efficient fusion (Araç et al., 2006).

Both the C2A and C2B domains of Syt1 bind calcium, interact with lipids, and participate in facilitating evoked release (Bykhovskaia, 2021; Lee et al., 2013; Mackler et al., 2002; Paddock

et al., 2008; Yoshihara et al., 2010). However, in the complete absence of Syt1, there is a robust increase in a calcium-sensitive and slower asynchronous phase of SV fusion that is not observed in control conditions (Bacaj et al., 2013; Geppert et al., 1994; Yoshihara et al., 2010; Yoshihara & Littleton, 2002). In *Drosophila Syt1* mutants where individual residues of each C2 domain have been altered in various combinations, current data indicate calcium binding to the C2B domain primarily drives synchronous fusion, while C2A calcium binding contributes a lesser role to synchronous release, but has a key function in suppressing asynchronous release (Guan et al., 2017; Mackler et al., 2002; Yoshihara et al., 2010; Yoshihara & Littleton, 2002). The slower asynchronous phase of neurotransmission that is enhanced in the absence of Syt1 has been seen across multiple systems, suggesting Syt1 is likely to compete with a second calcium sensor that primarily drives asynchronous SV fusion (Geppert et al., 1994; Goda & Stevens, 1994; Maximov & Südhof, 2005; Yoshihara & Littleton, 2002). In mammals, another protein of the Syt family, Synaptotagmin 7 (Syt7), has been shown to regulate this slower form of calcium-triggered release at some synapses (Bacaj et al., 2013), while other work suggests asynchronous release is likely to require a different calcium sensor (Turecek & Regehr, 2019). Although the asynchronous sensor has yet to be fully identified, these studies support the role of Syt1 as the primary calcium sensor that drives synchronous SV release and restricts the slower asynchronous pathway.

In addition to its role in evoked fusion, studies have also found a role for Syt1 in regulating spontaneous neurotransmitter release. In both cultured mammalian cortical/hippocampal neurons and *Drosophila Syt1* knockouts, a moderate two- to five-fold increase in spontaneous fusion is observed, measured as an increase in mini frequency (Bacaj et al., 2013; DiAntonio & Schwarz, 1994; Littleton et al., 1993, 1994; Mackler et al., 2002; Yoshihara & Littleton, 2002; Zhou et al., 2017). One proposed mechanism of Syt1 as a spontaneous fusion clamp involves calcium-free Syt1 (apo-Syt1), wherein apo-Syt1 functions as a fusion clamp until it binds calcium, which then triggers its role in driving evoked fusion. Liposome fusion assays have supported this model, showing that apo-Syt1 inhibits fusion, but when given calcium to bind, the protein promotes fusion (Chicka et al., 2008; Chicka & Chapman, 2009). Additionally, a C2B polylysine motif of Syt1 has been shown to facilitate a calcium-independent stage of SV docking/priming (Loewen et al., 2006), which may also contribute to the role of Syt1 in promoting fusion events.

Complexin

Similar to Syt1, Cpx is an important regulatory protein for SV fusion. Although *Cpx* mutants have been generated and analyzed in mice, *Drosophila* and *C. elegans*, key features of how the protein functions and how its properties are regulated are poorly understood. Cpx was originally identified by its binding affinity for the SNARE complex. The protein contains an N-terminal accessory helix, a conserved central SNARE-binding helix and an unstructured C-terminus that is predicted to interact with membranes to localize it to release sites, though the C-terminus may have other regulatory functions as well (Bera et al., 2022; Chen et al., 2002; McMahon et al., 1995). Fusion assays *in vitro* demonstrate that Cpx inhibits SNARE assembly and subsequent SNARE-mediated fusion (Giraudo et al., 2006; Malsam et al., 2020; Schaub et al., 2006). Mutations in Cpx in various model systems reveal a decrease in evoked release, supporting a role in facilitating SV fusion (Huntwork & Littleton, 2007; Reim et al., 2001). In particular, *Drosophila* mutants of *Cpx* exhibit a 50% decrease in synchronous evoked release (**Figure 1A, B**) and an increase in asynchronous release, similar but less severe compared to *Syt1* mutants (Huntwork & Littleton, 2007; Jorquera et al., 2012). The role of Cpx as an asychronous SV fusion clamp is also observed in mammals (Chang et al., 2015; X. Yang et al., 2010). Other studies in *Drosophila* indicate Cpx also tethers SVs to presynaptic AZs by interacting with a prominent AZ scaffold protein, Bruchpilot (Brp) (Scholz et al., 2019). Furthermore, *Cpx* mutants display a >50-fold increase in spontaneous fusion (**Figure 1C, D**), leading to synaptic overgrowth at NMJs (**Figure 1E, F**) (Buhl et al., 2013; Cho et al., 2015; Huntwork & Littleton, 2007). These studies suggest that Cpx facilitates tethering of SVs to release sites while also interacting with SNAREs to inhibit spontaneous fusion and facilitate evoked release at invertebrate synapses. The role of Cpx as a fusion clamp inhibiting spontaneous release seems less promiment in mammals, as Syt1appears to play more of this role at most synapses.

Although Cpx proteins across species share many similarities in sequence and structure, mammalian knockouts of *Cpx* generally do not exhibit a signficant increase in spontaneous fusion events, unlike their invertebrate counterparts (Chang et al., 2015; López-Murcia et al., 2019; Reim et al., 2001; Xue et al., 2007). However, *in vitro* studies with cultured mammalian neurons of *Cpx* knockdowns exhibit a moderate 3-fold increase of spontanous fusion (Maximov et al., 2009; X. Yang et al., 2010), and interestingly, mammalian Cpx is able to function as a fusion clamp when expressed at *Drosophila* NMJs (Buhl et al., 2013; Cho et al., 2010), indicating an evolutionarily-

conserved clamping ability for the protein. Although it is possible that mammalian *Cpx* knockouts may have compensatory effects that suppress the spontaneous *Cpx* phenotype (X. Yang et al., 2013), one model that may explain why mammalian synapses do not exhibit elevated spontaneous fusion when Cpx is absent involves a difference in basal calcium levels observed in different model systems. For instance, if invertebrate presynaptic terminals maintain a higher baseline calcium level than mammalian terminals and spontaneous fusion is calcium-sensitive, then a knockout of the clamping protein Cpx will have a larger effect on fusion events in invertebrate synapses. Although studies of this model are still ongoing, work in cultured cortical neurons has shown some interesting results. When *Cpx* is knocked down in cultured cortical neurons that are treated with BAPTA, a calcium chelator, neurons that normally exhibit an increase of spontaneous fusion now show >80% decrease in spontaneous release, suggesting that SV spontaneous release is regulated by calcium (X. Yang et al., 2010). Similar calcium-dependence of spontaneous fusion is also seen in Syt1-deficient cultured neurons subjected to BAPTA (Zhou et al., 2017). Ultimately, these data support that a higher basal calcium level in *Drosophila* and *C. elegans* neurons could account for differences in Cpx clamping phenotypes between model systems and may play a role in regulating the calcium-sensitivity of release. Together, with a more prominent role for Syt1 in clamping spontaneous fusion at mammalian synapses, the balance of the Cpx/Syt1 clamping functions may have also shifted more in favor of Syt1 during vertebrate evolution.

Interactions between Synaptotagmin 1, Complexin, and SNAREs

When considering the calcium-sensitivity of both spontaneous and evoked release, it is critical to understand how proteins like Cpx and Syt1 biochemically interact with SNAREs, calcium, and each other to regulate SV fusion. As previously mentioned, the Syt1 C2 domains serve as important calcium-sensitive domains that interact with synaptic membranes to facilitate evoked release, while Cpx has a dual regulatory role: facilitating evoked release and inhibiting spontaneous fusion. Studies in mammalian and invertebrate systems support a genetic separation of the activating and inhibiting functions of Cpx, although both functions require SNARE complex binding (Cho et al., 2010, 2014; Iyer et al., 2013; Malsam et al., 2020; Xue et al., 2007, 2010). One model for Cpx-SNARE binding is the “zig-zag” model, in which the central helix of Cpx is secluded within a partially-zippered SNARE complex, while the N-terminal accessory helix of Cpx sits at a 45° angle and interacts with an adjacent partially-zippered SNARE complex, thus

forming a clamping ring around the SV (Kümmel et al., 2011). A different model for Cpx-SNARE binding suggests direct competition between Syb and Cpx for t-SNARE binding, with the accessory helix of Cpx competing for binding Syx1 and SNAP-25 in the partially-assembled SNARE complex, consequently preventing full SNARE complex assembly (Giraudo et al., 2009; Lu et al., 2010; Zdanowicz et al., 2017). A variation of this model suggests interactions between the accessory helix of Cpx and Syb, in which Cpx clamps fusion by binding to the Syb C-terminus to prevent full SNARE zippering (Bykhovskaia et al., 2013; Vasin et al., 2016). A final model has recently been proposed in which the Cpx accessory helix binds Syb and one helix of SNAP-25 to displace Syx1 binding from the assembling SNARE complex (Malsam et al., 2020). Mutations in *Cpx* that disrupt the formation of the zig-zag SNARE interactions and Syb/SNAP-25 binding have mild effects on spontaneous fusion clamping, but do not disrupt the role of Cpx in evoked release (Cho et al., 2014; Malsam et al., 2020). Similarly, mutations that disrupt Cpx/Syb competition binding only mildly affect Cpx clamping function (Brady et al., 2021), suggesting other mechanisms, or a combination of binding states, are likely to regulate Cpx-mediated fusion events.

Looking into Syt1 interactions with SNAREs, a recent *Drosophila* study identified key SNARE-binding residues of the Syt1 C2B domain that, when disrupted, abolish synchronous fusion and subsequently increase asynchronous and spontaneous release (Guan et al., 2017). The ability of C2 domains to bind SNAREs and interact with lipid membranes in both a calcium-dependent and -independent manner helps Syt1 bring SV and plasma membranes together and facilitate full SNARE zippering (Bykhovskaia, 2021; Chapman & Davis, 1998; Guan et al., 2017; Loewen et al., 2006). Additionally, the interactions of Syt1 with SNAREs, lipids, and calcium may act to displace Cpx binding from SNAREs, which may also support SNARE zippering to overcome the energy barrier for SV fusion (Tang et al., 2006). In support of this displacement model, SNARE-dependent liposome fusion assays show that Cpx arrests release in a hemifusion step, while the addition of Syt1 and calcium alleviates this arrest and permits full fusion (Schaub et al., 2006). Conversely, other *in vitro* data suggests Syb mediates a conformational switch that changes Cpx from a clamping role to fusion-promoting role, with this switch in Cpx position allowing Syt1 to trigger fusion (Krishnakumar et al., 2011). While the exact interaction between Cpx and Syt1 is still unclear, structural studies have found evidence that Syt1 and Cpx can simultaneously bind the surface of the SNARE complex, where both Syt1 and Cpx form a split, but continuous, α-helix as part of a tripartite complex (Zhou et al., 2017). Mutations of the tripartite interface in cultured

cortical neurons results in reduced evoked release, suggesting the SNARE-Cpx-Syt1 tripartite interface regulates calcium-dependent fusion.

Although the exact biochemical interactions of Syt1 and Cpx are still being elucidated, *in vivo* genetic analysis of these proteins reveal functional interactions (Xue et al., 2010). *Drosophila* knockouts of either *Syt1* or *Cpx* produce similar changes to synchronous, asynchronous, and spontaneous SV fusion, though *Syt1* mutants demonstrate a more severe deficit in evoked fusion while *Cpx* mutants have a larger spontaneous fusion deficit (Jorquera et al., 2012; Yoshihara & Littleton, 2002). Furthermore, both mutants exhibit reduced calcium-sensitivity for evoked release and a slower speed of evoked SV fusion, with some evoked release deficits in *Cpx* mutants partially rescued by elevating extracellular calcium levels (Jorquera et al., 2012; Littleton et al., 1994; Yoshihara & Littleton, 2002). One model suggests Cpx may prevent premature Syt1-dependent SNARE zippering and SV fusion as a mechanism for clamping. In *Drosophila*, the elevated spontaneous release observed in *Cpx* mutants is suppressed in *Cpx, Syt1* double mutants, suggesting Syt1 may constitutively activate SV fusion in a calcium-independent way in the absence of Cpx (Jorquera et al., 2012). From these biochemical and genetic studies, it is clear that both Syt1 and Cpx function as key regulators of SNARE zippering and SV fusion, acting in concert to control release properties and fusion kinetics at synapses.

1.4 Complexin function and regulation across species

Altered Cpx expression with effects on synaptic transmission has been suggested to contribute to symptoms of several psychiatric and neurological disorders, including schizophrenia, Alzheimer's disease, Huntington's disease, traumatic brain injury, fetal alcohol syndrome, and addiction (Brose, 2008a, 2008b), demonstrating the importance of understanding how Cpx function and expression is regulated in the brain. Moreover, studies of *Cpx* genes in humans have identified several single nucleotide polymorphisms in *Cpx2* associated with cognitive deficits in schizophrenic patients (Begemann et al., 2010), while individuals with genetic variants of *Cpx1* (nonsense mutation of amino acid C105 or E108, or amino acid substitution L128M) exhibit severe myoclonic epilepsy, intellectual disability, and cortical atrophy (Karaca et al., 2015; Redler et al., 2017; Verhage & Sørensen, 2020). Importantly, all three *Cpx1* mutations are found in the Cpx C-terminus. Although Cpx function has been examined in multiple model systems, the role of the unstructured C-terminus of Cpx is still unclear. Given the critical role Cpx plays in SV fusion and

the clinical features associated with human loss-of-function Cpx variants, it is imperative to understand how the C-terminal domain of Cpx contributes to synaptic transmission.

Across species, Cpx proteins can generally be divided into two groups: those that have a membrane-tethering CAAX box prenylation motif at the C-terminus and those that lack this motif. In mammals, four *Cpx* genes exist, giving rise to Cpx1 and 2 which lack the motif (non-CAAX variants) and Cpx3 and 4 which contain the motif (CAAX variants). Cpx1 and 2 are widely expressed both within and outside of the nervous system, while Cpx3 and 4 exhibit more restricted expression patterns in the brain, where they are enriched in some sensory neurons (Brose, 2008b; Reim et al., 2005; Zanazzi & Matthews, 2010). In *Drosophila*, a similar division is seen, although only a single *Cpx* locus exists. To create two Cpx proteins with differing C-termini, *Drosophila Cpx* undergoes alternative splicing of the C-terminal exon 7, creating Cpx7A with a CAAX box motif and Cpx7B as a non-CAAX isoform (Buhl et al., 2013). These C-terminal differences suggest preservation of Cpx diversity is important for its function as a regulator of synaptic transmission across a range of species. Interestingly, *Drosophila* Cpx7A also undergoes RNA editing, producing further variants of the Cpx7A isoform. These editing variants will be discussed in greater detail below.

Membrane interactions of the Complexin C-terminus

Compared to the highly-conserved SNARE-binding central helix of Cpx which has ~75-90% sequence identity between mouse, *Drosophila*, and *C. elegans*, sequence alignment of the unstructured C-terminal domain reveals only ~20-30% conservation (Lottermoser & Dittman, 2023; Wragg et al., 2017; X. Yang et al., 2015). Though the C-terminal domain is variable in protein sequence across species, comparisons of many metazoan Cpx homologs, like those of sea anemone, ctenophore, and human, demonstrate that two subfamilies of Cpx exist, those containing or lacking a CAAX motif at the C-terminus (Buhl et al., 2013; Lottermoser & Dittman, 2023; Reim et al., 2005; X. Yang et al., 2015). Moreover, ancestral homologs of Cpx from unicellular organisms such as choanoflagellates, generally contain a CAAX motif, suggesting membrane-tethering of Cpx through prenylation is likely to be evolutionarily required for precise function of the CAAX subfamily (X. Yang et al., 2015). As such, this CAAX box characteristic can be seen in a more closely-related cnidarian Cpx homolog, which can even functionally restore evoked fusion in double knockout mouse *Cpx1/2* cultured neurons (X. Yang et al., 2015). Interestingly, a

C-terminal amphipathic helix found in all bilaterian Cpx is lacking in ancestral Cpx homologs, implying the amphipathic nature of the C-terminus of Cpx appeared later in synaptic evolution and may contribute to neuron-specific functions and localizations of the protein (Wragg et al., 2017). In addition, a section of acidic residues is maintained upstream from the C-terminal amphipathic motif in bilaterian Cpx that may interact with polybasic residues on the C2B Syt1 surface (Malsam et al., 2012; Tokumaru et al., 2008).

Although bilaterian Cpx proteins share many structural similarities, discrepancies arise when comparing Cpx function at mammalian and invertebrate synapses. In the mammalian field of Cpx research, a consensus has been reached that non-CAAX Cpx1 and 2 generally facilitate SV release, while Cpx3 and 4, the CAAX box variants, serve both faciliatory and inhibitory roles, similar to the observed Cpx function at invertebrate synapses (Chang et al., 2015; Cho et al., 2010; Hobson et al., 2011; Huntwork & Littleton, 2007; Martin et al., 2011; Mortensen et al., 2016; Reim et al., 2001; Vaithianathan et al., 2013, 2015; Xue et al., 2009). As previously discussed, these observed differences between model systems may be due to intrinsic cellular differences, such as basal calcium levels or co-evolution of other important fusion proteins, as well as differing lipid compositions that may alter membrane interactions of the Cpx C-terminus in various synapses. Even though slight functional discrepancies have been observed in various model synapses, it is clear that conserved CAAX and non-CAAX subfamilies of Cpx are required for distinct populations of neurons to regulate SV release.

Two subgroups of Complexin: prenylated and non-prenylated

Membrane-tethering of Cpx via the CAAX motif requires protein prenylation, also known as lipidation. Prenylation is a post-translational modification that includes an irreversible covalent attachment of either a farnesyl or geranylgeranyl group to help facilitate protein localization onto cellular membranes. In mice, farnesylation of Cpx3 and 4 is required for synaptic localization of the proteins (Reim et al., 2005), while chimera protein experiments in cultured mouse neurons demonstrate that a fused N-terminal half of Cpx1 to the CAAX-containing C-terminal domain of Cpx3 fails to inhibit spontaneous fusion, while the reverse chimera functionally appears like full-length Cpx1 and inhibits spontaneous fusion (Kaeser-Woo et al., 2012). In *Drosophila*, both Cpx7A and Cpx7B localize to the presynaptic terminal of NMJs, however, Cpx7A is the dominant isoform with 1000-fold higher mRNA expression in the nervous system than Cpx7B (**Figure 2A**)

(Buhl et al., 2013). Genetic rescues of a *Cpx* knockout with either isoform demonstrate that CAAX-containing Cpx7A is a more effective clamping spontaneous fusion (**Figure 2B**), while Cpx7B is an extremely strong facilitator of evoked release (**Figure 2C**). In addition, mutations to Cpx7A prenylation abolishes its clamping abilities at the NMJ and disrupts Cpx-mediated SV tethering to AZs (Buhl et al., 2013; Cho et al., 2010; Iyer et al., 2013; Scholz et al., 2019). Interestingly, rescue of the *Cpx* knockout with mouse Cpx4 (CAAX variant) produces similar results to that of Cpx7A, whereas rescue with mouse Cpx1 (non-CAAX variant) appears to function similarly to Cpx7B (Buhl et al., 2013).

These data support a model (**Figure 2D**) wherein prenylation of Cpx7A increases its local concentration on SVs, allowing it to bind many assembling SNARE complexes during SV docking and priming, where it can act as an effective fusion clamp. On the other hand, non-CAAX Cpx7B may be more soluble, and therefore, less present at fusion sites, thus reducing its clamping abilities. A more soluble Cpx clamping protein may also allow Syt1 to facilitate evoked fusion more readily, as it is not competing with Cpx for SNARE binding (Buhl et al., 2013).

However, other studies have suggested that mutations to Cpx7A prenylation do not make the protein more soluble, but instead results in enhanced AZ localization of the protein (Iyer et al., 2013; Robinson et al., 2018). Additionally, suppression of Cpx7A prenylation through a post-translational nitric oxide (NO) modification results in a more effective Cpx clamp, rather than abolishing this inhibitory function, although this may be due to the NO modification enhancing Cpx binding to other proteins, like SNAREs, which may further augment Cpx function (Robinson et al., 2018). These discrepancies highlight the uncertainties in the functional importance of the C-terminus and post-translational modifications to Cpx function. Together, data from mammalian and invertebrate fields indicate distinct functions exist for CAAX and non-CAAX Cpx at synapses, though their exact roles are still unclear.

Complexin is recruited to synaptic vesicles by its curvature-sensitive amphipathic helix

While the presence of a CAAX motif in Cpx provides one mode of lipid interactions, the C-terminal amphipathic helix present in both CAAX and non-CAAX proteins can also bind lipids. One of the first experiments to probe Cpx membrane interactions used *in vitro* liposome binding to study human Cpx1, a non-CAAX Cpx, finding that a conserved amphipathic helical domain near the Cpx C-terminus is required for interactions with small liposomes (~50 nm in diameter)

that resembled the size of SVs (~40 nm in diameter) (Seiler et al., 2009). More recently, *C. elegans* Cpx-1 (non-CAAX Cpx homolog) and mammalian Cpx1 C-termini were found to be curvature-sensitive, wherein a smaller liposome leads to higher Cpx lipid binding (Gong et al., 2016; Snead et al., 2014; Zdanowicz et al., 2017). Biochemical assays, like CD spectroscopy and NMR, further provide support for model in which the C-terminus of Cpx is largely unstructured in solution, but becomes partially helical when binding curved membranes (Grasso et al., 2023; Snead et al., 2014). Additionally, the amphipathic C-terminus of mammalian Cpx2 (last 21 residues) can remodel lipids to convert flat membranes into highly-curved structures in which some C-terminal peptides can bind the lipid bilayer, oligomerize into a pore-forming structure, and stabilize an open state for the fusion pore (Courtney et al., 2022). Together, these data suggest the C-terminal amphipathic region of both mammalian and invertebrate Cpx can bind to and sculpt lipid membranes like those found in SVs, providing a mechanism for membrane interactions that may recruit Cpx to SVs to enhance its presence as sites of SNARE assembly.

Further *in vivo* studies sought to determine if Cpx is recruited to SVs through its amphipathic C-terminus, as previously hypothesized. *C. elegans* Cpx-1 that lacks a CAAX motif can colocalize with SVs and is functional when driven to SVs using foreign tethers, but loses function when driven to the presynaptic plasma membrane (Wragg et al., 2013). When the C-terminus of Cpx-1 is deleted, Cpx-1 mobility is increased, as C-terminal interactions that aided in Cpx retention in the bouton are no longer present (Wragg et al., 2015). Additionally, overexpression of the truncated Cpx-1 that lacked its C-terminus does not rescue inhibitory clamping in *Cpx-1* mutants and only partially rescues faciliatory abilities, but fusion of the same truncated Cpx-1 to Rab3, a SV protein, greatly rescues Cpx function (Wragg et al., 2013). Interestingly, when the amphipathic helical conformation is destabilized, Cpx-1 inhibition is reduced, even though the protein retains its C-terminus (Snead et al., 2014; Wragg et al., 2013), suggesting a conformational switch in Cpx structure is required for some aspect of Cpx function. In support of amphipathicity playing a role in Cpx function, chromaffin cell granule secretion assays where the helix of mammalian Cpx2 is replaced with a similar helix from SNAP-25 found that the inhibitory function of Cpx2 is largely preserved, while lack of any amphipathic helix fails to rescue release in *Cpx2* knockout cells (Makke et al., 2018). Overall, these studies support that amphipathicity of the Cpx C-terminus, along with the membrane-tethering CAAX motif, function in concert to localize Cpx to SVs to promote its function in the regulation of SV fusion.

Phosphorylation of the Complexin C-terminus alters function

One characteristic of the amphipathic helix is the grouping of hydrophobic and polar residues on opposite sides to create a hydrophobic face that interacts with lipid surfaces and an hydrophilic aqueous face that remains exposed to the cytosol where it can interact with other proteins and regulatory molecules (Giménez-Andrés et al., 2018). Similar to the Cpx C-terminus, amphipathic lipid packing sensor (ALPS) motifs share these amphipathic properties in which they can selectively bind to highly-curved membranes and are found in other membrane-interacting proteins involved in vesicular trafficking pathways (Antonny, 2011; Bigay et al., 2005; Doucet et al., 2015; Mesmin et al., 2007; Vanni et al., 2013). Interestingly, ALPS motifs can be regulated by phosphorylation, leading to changes in their membrane binding or protein interactions (Cabrera et al., 2010; Karanasios et al., 2010), suggesting the amphipathic helix of Cpx may share similar biochemical properties and be subject to phosphorylation that modify its membrane interactions.

Several studies of mammalian and invertebrate Cpxs indicate phosphorylation occurs at the Cpx C-terminal domain. Mammalian Cpx1 and 2 (non-CAAX) can be phosphorylated at C-terminal domain residue S115 by protein kinase CK2 (CK2), leading to higher affinities to native and recombinant SNARE complexes (Shata et al., 2007), while sequence analysis of Cpx3 and 4 (CAAX Cpx) suggests additional potential CK2 phosphorylation sites (Reim et al., 2005). Interestingly, the phospho-competent S115 residue of Cpx1 and 2 sits at the beginning of the amphipathic region and mutations to this site *in vitro* impair the fusogenic function of the C-terminus (Malsam et al., 2009). In *Drosophila*, protein kinase A (PKA) phosphorylates amphipathic helix residue S126 of the non-CAAX Cpx7B protein *in vitro.* At the NMJ, activity-dependent phosphorylation of S126, induced by a high-frequency stimulation, can selectively and transiently enhance spontaneous release (**Figure 3**) (Cho et al., 2015). Furthermore, this enhanced spontaneous release is required for activity-dependent synaptic growth at the NMJ. Mutation of the S126 site to a phospho-mimetic S126D residue (containing a negative charge that mimics the charge of phosphorylated amino acids) severely impairs Cpx7B inhibitory function and abolishes activity-dependent plasticity (Cho et al., 2015). These findings demonstrate that phosphorylation of the Cpx C-terminus can regulate Cpx-mediated fusion. These data also support a role for spontaneous neurotransmitter release in functional and structural synaptic plasticity. However, it is still unknown if the predominant *Drosophila* Cpx7A splice isoform containing the CAAX motif is similarly regulated by phosphorylation, or if Cpx7A plays a role in synaptic plasticity at NMJs.

1.5 RNA editing as a genetic mechanism for protein diversity

In addition to alternative splicing of exon 7, *Drosophila* Cpx is subject to RNA editing by ADAR (adenosine deaminase acting on RNA), the major RNA editing enzyme in mammals and the only known RNA editing enzyme in *Drosophila* (Palladino et al., 2000b). Pre-mRNA editing by ADAR provides an evolutionarily-conserved post-transcriptional mechanism to increase protein diversity by modifying specific nucleotides of both coding and noncoding RNA sequences (Bhalla et al., 2004; Jepson & Reenan, 2008). These RNA edited sequences have functional implications for the cell by affecting RNA sequence and structure which can create or eliminate splicing sites, modify protein sequences, or alter mRNA stability and localization, as well as altering other RNA-mediated processes (Bhalla et al., 2004; Buhl et al., 2013; Deng et al., 2020; Hanrahan et al., 1999; Hoopengardner et al., 2003; Nishikura, 2010; Palladino et al., 2000a, 2000b; Rueter et al., 1999).

ADAR catalyzes the deamination of an adenosine-to-inosine (A-to-I) by binding to an imperfect double-stranded RNA structure formed between the pre-mRNA region containing the editing site (the adenosine of interest) and the editing site complementary sequence (ECS) that is frequently found in a downstream intronic region (Higuchi et al., 1993; Nishikura, 2010). The inosine modification is then interpreted as a guanosine during translation, which can result in altered protein sequences. In the case of Cpx, RNA editing occurs in exon 7A. As Cpx7B lacks this exon, only the Cpx7A splice isoform is subject to RNA editing. Cpx7A editing occurs at three base positions in the amphipathic region of the C-terminus, creating coding changes at two amino acid residues: I125 and N130 (Buhl et al., 2013; Hoopengardner et al., 2003). Single base editing at I125 converts this residue to a methionine (M), while combinatorial editing at two bases of N130 can create a serine (S), aspartate (D), or glycine (G) change (Buhl et al., 2013; Sapiro et al., 2019). Notably, N130 editing produces a phospho-competent (N130S) and phospho-mimetic (N130D) edit variant of Cpx7A, providing a potential regulatory site for Cpx7A function that may fine-tune presynaptic output.

Regulated RNA editing contributes to neuronal health

Most known ADAR targets in vertebrates and invertebrates are predominantly expressed in the nervous system where ADAR editing activity is predicted to alter neuronal structure and function, though ADAR activity is also detected in other non-neuronal tissues (Maldonado et al.,

2013; Paul & Bass, 1998; Paupard et al., 1999). The first characterization of A-to-I editing in mRNA was discovered in mouse transcripts encoding the ionotropic glutamate receptor subunit GluR-B. Editing of a key amino acid located within the channel pore-loop domain of the GluR-B subunit from glutamine (Q) to arginine (R) alters protein function so that a channel incorporating this edited subunit becomes impermeable to calcium (Higuchi et al., 1993; Sommer et al., 1991). This change in calcium permeability is important for proper neuronal development, as developing cells require calcium signaling to grow and strengthen synapses, but after this developmental window, prolonged calcium permeability can become neurotoxic to the cell (Brusa et al., 1995; Konur & Ghosh, 2005; Seeburg et al., 1998; Verkhratsky, 2007). Another editing site within GluR subunits alters arginine (R) to glycine (G) which affects the desensitization recovery rate of GluR channels (Lomeli et al., 1994). In addition to GluR subunits, vertebrate and invertebrate RNA editing has been observed in other synaptic proteins involved in neurotransmission including mammalian serotonin receptors (Burns et al., 1997; Niswender et al., 1999), *Drosophila* voltage-gated sodium (*Para*), calcium (*Cac*), and potassium (*Shab*) ion channels, and proteins like Syt1, Unc-13, Tomosyn (Tom), and Cpx7A (Buhl et al., 2013; Hanrahan et al., 1999, 2000; Hoopengardner et al., 2003; Ingleby et al., 2009; Palladino et al., 2000b; Sapiro et al., 2019; Smith et al., 1998).

ADARs themselves are also targets of regulated auto-editing across multiple model systems. ADAR auto-editing can be modulated by internal spatial (brain region and cell type) and temporal (development, cellular activity, or circadian periods) factors, in addition to regulation by environmental stimuli like temperature (Ansell et al., 2021; Duan et al., 2017; Keegan et al., 2005; Licht & Jantsch, 2016; Palladino et al., 2000a; Rieder et al., 2015; Sanjana et al., 2012). Notably, *Drosophila* ADAR auto-editing occurs at a site near its catalytic pocket which makes the edited form of ADAR less active and may serve as a negative feedback loop in some neuronal processes (Keegan et al., 2005; Savva et al., 2012). Overall, auto-regulatory RNA editing may alter ADAR activity, providing an avenue for temporal and spatial regulation of editing activity within cells and may contribute to environmental adaptation.

Although the functional consequence of ADAR-mediated RNA editing of the Cpx7A C-terminus is unknown, disrupted editing in both mammalian and invertebrate model systems can have detrimental effects (Brusa et al., 1995; Palladino et al., 2000b; Tonkin et al., 2002). Inactivation of mammalian ADAR1 is embryonic lethal due to widespread apoptosis (Hartner et

al., 2004; Q. Wang et al., 2000, 2004), while loss of ADAR2 in mice results in epileptic seizures and premature death, largely due to excessive calcium influx from unedited GluR subunits (Brusa et al., 1995; Higuchi et al., 2000). However, *Adar2* knockout mice can be functionally rescued by expressing a constitutively-edited form of the GluR-B subunit (calcium-impermeable R variant) (Higuchi et al., 2000). Under-editing of this same Q/R site in humans has been implicated in motor neuron death observed in sporadic amyotrophic lateral sclerosis (ALS) patients (Kawahara et al., 2004) and is a possible contributor to aggressive tumor cell growth (Ishiuchi et al., 2002; Maas et al., 2001).

In *Drosophila*, *Adar* null mutants are viable but display seizure-like tremors, uncoordinated movements, temperature-sensitive paralysis, lack of courtship behaviors, and age-dependent neurodegeneration (Palladino et al., 2000b). As ADAR is a target of auto-editing near its catalytic site, expression of only the unedited isoform of *Drosophila* ADAR in *Adar* null embryos is lethal due to excessive ADAR-mediated editing activity (Keegan et al., 2005). These neurological and behavioral phenotypes are consistent with a role for ADAR in modifying nervous system function by editing known synaptic targets, like the ion channels *Para* and *Cac*. As such, both mammalian and *Drosophila* models of fragile X syndrome (FXS), the most common form of heritable intellectual disability, have altered levels of ADAR-mediated editing of synaptic proteins which may contribute to FXS pathogenesis (Bhogal et al., 2011; Filippini et al., 2017), suggesting proper modulation of ADAR activity is critical for synaptic function.

At the synaptic level, analysis of *Drosophila Adar* mutants indicates loss of ADAR increases quantal size (amplitude of mini events) and reduces quantal content (fewer vesicles released per action potential, calculated as the evoked amplitude divided by mini amplitude), but does not alter mini frequency. Furthermore, *Adar* mutants display an increase in synaptic growth, abnormal synaptic ultrastructure, and altered calcium-dependence of SV release (Bhogal et al., 2011; Maldonado et al., 2013). Since the calcium-binding Syt1 C2B domain is a predicted target of RNA editing, it is possible that Syt1 edit variants, or similarly edited neurotransmission regulators like Cpx7A, may modulate calcium-dependent SV release properties (Hoopengardner et al., 2003; Maldonado et al., 2013). Similarly, study of the mammalian calcium-dependent activator protein for secretion 1 (CAPS1), which facilitates docking and priming of SVs and dense core vesicles, demonstrates that maintenance of the CAPS1 unedited versus edited isoform ratio

is important for SV organization, recycling, and release (Ulbricht et al., 2017), supporting a role for RNA editing in regulating neurotransmission.

While different RNA editing targets exist between mammalian and *Drosophila* synapses, the editing function of ADAR is evolutionarily-conserved. Expression of human ADAR2 in *Drosophila Adar* nulls can restore RNA editing of transcripts in these animals and rescue associated locomotion defects and age-dependent neurodegeneration (Keegan et al., 2011). This suggests that proper modulation of ADAR editing activity is important for establishing neuronal properties across multiple model systems, whereas altered editing patterns can have deleterious effects.

Taken together, ADAR-mediated RNA editing provides an evolutionarily-conserved mechanism to create synaptic protein diversity that is important for development and maintenance of neurotransmission properties across a range of neural systems. This RNA editing process can be regulated by cellular activity, environmental stimuli, and by ADAR auto-editing, providing a mechanism by which RNA editing can control neurotransmission and synaptic plasticity. Chapter 2 will discuss insights regarding how ADAR-mediated protein diversity of Cpx7A contributes to neurotransmission regulation at *Drosophila* NMJs.

References

Andreae, L. C., & Burrone, J. (2018). The role of spontaneous neurotransmission in synapse and circuit development. *Journal of Neuroscience Research*, *96*(3), 354–359. https://doi.org/10.1002/jnr.24154

Ansell, B. R. E., Thomas, S. N., Bonelli, R., Munro, J. E., Freytag, S., & Bahlo, M. (2021). A survey of RNA editing at single-cell resolution links interneurons to schizophrenia and autism. *RNA*, *27*(12), 1482–1496. https://doi.org/10.1261/rna.078804.121

Antonny, B. (2011). Mechanisms of Membrane Curvature Sensing. *Annual Review of Biochemistry*, *80*(1), 101–123. https://doi.org/10.1146/annurev-biochem-052809-155121

Araç, D., Chen, X., Khant, H. A., Ubach, J., Ludtke, S. J., Kikkawa, M., Johnson, A. E., Chiu, W., Südhof, T. C., & Rizo, J. (2006). Close membrane-membrane proximity induced by Ca2+-dependent multivalent binding of synaptotagmin-1 to phospholipids. *Nature Structural & Molecular Biology*, *13*(3), 209–217. https://doi.org/10.1038/nsmb1056

Atluri, P. P., & Regehr, W. G. (1998). Delayed Release of Neurotransmitter from Cerebellar Granule Cells. *The Journal of Neuroscience*, *18*(20), 8214–8227. https://doi.org/10.1523/JNEUROSCI.18-20-08214.1998

Augustin, I., Rosenmund, C., Südhof, T. C., & Brose, N. (1999). Munc13-1 is essential for fusion competence of glutamatergic synaptic vesicles. *Nature*, *400*(6743), 457–461. https://doi.org/10.1038/22768

Babcock, M., Macleod, G. T., Leither, J., & Pallanck, L. (2004). Genetic Analysis of Soluble *N* -Ethylmaleimide-Sensitive Factor Attachment Protein Function in *Drosophila* Reveals Positive and Negative Secretory Roles. *The Journal of Neuroscience*, *24*(16), 3964–3973. https://doi.org/10.1523/JNEUROSCI.5259-03.2004

Bacaj, T., Wu, D., Yang, X., Morishita, W., Zhou, P., Xu, W., Malenka, R. C., & Südhof, T. C. (2013). Synaptotagmin-1 and Synaptotagmin-7 Trigger Synchronous and Asynchronous Phases of Neurotransmitter Release. *Neuron*, *80*(4), 947–959. https://doi.org/10.1016/j.neuron.2013.10.026

Banerjee, S., Vernon, S., Jiao, W., Choi, B. J., Ruchti, E., Asadzadeh, J., Burri, O., Stowers, R. S., & McCabe, B. D. (2021). Miniature neurotransmission is required to maintain Drosophila synaptic structures during ageing. *Nature Communications*, *12*(1), 4399. https://doi.org/10.1038/s41467-021-24490-1

Begemann, M., Grube, S., Papiol, S., Malzahn, D., Krampe, H., Ribbe, K., Friedrichs, H., Radyushkin, K. A., El-Kordi, A., Benseler, F., Hannke, K., Sperling, S., Schwerdtfeger, D., Thanhäuser, I., Gerchen, M. F., Ghorbani, M., Gutwinski, S., Hilmes, C., Leppert, R., … Ehrenreich, H. (2010). Modification of Cognitive Performance in Schizophrenia by Complexin 2 Gene Polymorphisms. *Archives of General Psychiatry*, *67*(9), 879. https://doi.org/10.1001/archgenpsychiatry.2010.107

Bera, M., Ramakrishnan, S., Coleman, J., Krishnakumar, S. S., & Rothman, J. E. (2022). Molecular determinants of complexin clamping and activation function. *ELife*, *11*, e71938. https://doi.org/10.7554/eLife.71938

Betz, A., Okamoto, M., Benseler, F., & Brose, N. (1997). Direct Interaction of the Rat unc-13 Homologue Munc13-1 with the N Terminus of Syntaxin. *Journal of Biological Chemistry*, *272*(4), 2520–2526. https://doi.org/10.1074/jbc.272.4.2520

Betz, A., Thakur, P., Junge, H. J., Ashery, U., Rhee, J.-S., Scheuss, V., Rosenmund, C., Rettig, J., & Brose, N. (2001). Functional Interaction of the Active Zone Proteins Munc13-1 and

RIM1 in Synaptic Vesicle Priming. *Neuron*, *30*(1), 183–196. https://doi.org/10.1016/S0896-6273(01)00272-0

Bhalla, T., Rosenthal, J. J. C., Holmgren, M., & Reenan, R. (2004). Control of human potassium channel inactivation by editing of a small mRNA hairpin. *Nature Structural & Molecular Biology*, *11*(10), 950–956. https://doi.org/10.1038/nsmb825

Bhogal, B., Jepson, J. E., Savva, Y. A., Pepper, A. S.-R., Reenan, R. A., & Jongens, T. A. (2011). Modulation of dADAR-dependent RNA editing by the Drosophila fragile X mental retardation protein. *Nature Neuroscience*, *14*(12), 1517–1524. https://doi.org/10.1038/nn.2950

Bigay, J., Casella, J.-F., Drin, G., Mesmin, B., & Antonny, B. (2005). ArfGAP1 responds to membrane curvature through the folding of a lipid packing sensor motif. *The EMBO Journal*, *24*(13), 2244–2253. https://doi.org/10.1038/sj.emboj.7600714

Bowen, M. E., Weninger, K., Brunger, A. T., & Chu, S. (2004). Single Molecule Observation of Liposome-Bilayer Fusion Thermally Induced by Soluble N-Ethyl Maleimide Sensitive-Factor Attachment Protein Receptors (SNAREs). *Biophysical Journal*, *87*(5), 3569–3584. https://doi.org/10.1529/biophysj.104.048637

Bowers, M. R., & Reist, N. E. (2020). The C2A domain of synaptotagmin is an essential component of the calcium sensor for synaptic transmission. *PLOS ONE*, *15*(2), e0228348. https://doi.org/10.1371/journal.pone.0228348

Brady, J., Vasin, A., & Bykhovskaia, M. (2021). The Accessory Helix of Complexin Stabilizes a Partially Unzippered State of the SNARE Complex and Mediates the Complexin Clamping Function *In Vivo*. *Eneuro*, *8*(2), ENEURO.0526-20.2021. https://doi.org/10.1523/ENEURO.0526-20.2021

Brenner, S. (1974). The genetics of Caenorhabditis elegans. *Genetics*, *77*(1), 71-94. https://doi.org/10.1093/genetics/77.1.71

Brose, N. (2008a). Altered Complexin Expression in Psychiatric and Neurological Disorders: Cause or Consequence? *Molecules and Cells*, *25*(1), 7–19.

Brose, N. (2008b). For Better or for Worse: Complexins Regulate SNARE Function and Vesicle Fusion. *Traffic*, *9*(9), 1403–1413. https://doi.org/10.1111/j.1600-0854.2008.00758.x

Brose, N., Petrenko, A., Sudhof, T., & Jahn, R. (1992). Synaptotagmin: A calcium sensor on the synaptic vesicle surface. *Science*, *256*(5059), 1021–1025. https://doi.org/10.1126/science.1589771

Brunger, A. T. (2006). Structure and function of SNARE and SNARE-interacting proteins. *Quarterly Reviews of Biophysics*, *38*(01), 1. https://doi.org/10.1017/S0033583505004051

Brusa, R., Zimmermann, F., Koh, D. S., Feldmeyer, D., Gass, P., Seeburg, P. H., & Sprengel, R. (1995). Early-onset epilepsy and postnatal lethality associated with an editing-deficient GluR-B allele in mice. *Science*, *270*(5242), 1677-1680.10.1126/science.270.5242.1677

Buhl, L. K., Jorquera, R. A., Akbergenova, Y., Huntwork-Rodriguez, S., Volfson, D., & Littleton, J. T. (2013). Differential regulation of evoked and spontaneous neurotransmitter release by C-terminal modifications of complexin. *Molecular and Cellular Neuroscience*, *52*, 161–172. https://doi.org/10.1016/j.mcn.2012.11.009

Burns, C. M., Chu, H., Rueter, S. M., Hutchinson, L. K., Canton, H., Sanders-Bush, E., & Emeson, R. B. (1997). Regulation of serotonin-2C receptor G-protein coupling by RNA editing. *Nature*, *387*(6630), 303–308. https://doi.org/10.1038/387303a0

Bykhovskaia, M. (2021). SNARE complex alters the interactions of the Ca2+ sensor synaptotagmin 1 with lipid bilayers. *Biophysical Journal*, *120*(4), 642–661. https://doi.org/10.1016/j.bpj.2020.12.025

Bykhovskaia, M., Jagota, A., Gonzalez, A., Vasin, A., & Littleton, J. T. (2013). Interaction of the Complexin Accessory Helix with the C-Terminus of the SNARE Complex: Molecular-Dynamics Model of the Fusion Clamp. *Biophysical Journal*, *105*(3), 679–690. https://doi.org/10.1016/j.bpj.2013.06.018

Cabrera, M., Langemeyer, L., Mari, M., Rethmeier, R., Orban, I., Perz, A., Bröcker, C., Griffith, J., Klose, D., Steinhoff, H.-J., Reggiori, F., Engelbrecht-Vandré, S., & Ungermann, C. (2010). Phosphorylation of a membrane curvature–sensing motif switches function of the HOPS subunit Vps41 in membrane tethering. *Journal of Cell Biology*, *191*(4), 845–859. https://doi.org/10.1083/jcb.201004092

Calakos, N., Bennett, M. K., Peterson, K. E., & Scheller, R. H. (1994). Protein-protein interactions contributing to the specificity of intracellular vesicular trafficking. *Science*, *263*(5150), 1146-1149. https://doi.org/10.1126/science.8108733

Camacho, M., Basu, J., Trimbuch, T., Chang, S., Pulido-Lozano, C., Chang, S.-S., Duluvova, I., Abo-Rady, M., Rizo, J., & Rosenmund, C. (2017). Heterodimerization of Munc13 C2A domain with RIM regulates synaptic vesicle docking and priming. *Nature Communications*, *8*(1), 15293. https://doi.org/10.1038/ncomms15293

Chanaday, N. L., Cousin, M. A., Milosevic, I., Watanabe, S., & Morgan, J. R. (2019). The Synaptic Vesicle Cycle Revisited: New Insights into the Modes and Mechanisms. *The Journal of Neuroscience*, *39*(42), 8209–8216. https://doi.org/10.1523/JNEUROSCI.1158-19.2019

Chang, S., Reim, K., Pedersen, M., Neher, E., Brose, N., & Taschenberger, H. (2015). Complexin Stabilizes Newly Primed Synaptic Vesicles and Prevents Their Premature Fusion at the Mouse Calyx of Held Synapse. *Journal of Neuroscience*, *35*(21), 8272–8290. https://doi.org/10.1523/JNEUROSCI.4841-14.2015

Chapman, E. R., & Davis, A. F. (1998). Direct Interaction of a Ca2+-binding Loop of Synaptotagmin with Lipid Bilayers. *Journal of Biological Chemistry*, *273*(22), 13995–14001. https://doi.org/10.1074/jbc.273.22.13995

Chen, X., Tomchick, D. R., Kovrigin, E., Arac, D., Machius, M., Südhof, T. C., & Rizo, J. (2002). Three-Dimensional Structure of the Complexin/SNARE Complex. *Neuron*, *33*(3), 397–409. https://doi.org/10.1016/S0896-6273(02)00583-4

Chicka, M. C., & Chapman, E. R. (2009). Concurrent Binding of Complexin and Synaptotagmin to Liposome-Embedded SNARE Complexes. *Biochemistry*, *48*(4), 657–659. https://doi.org/10.1021/bi801962d

Chicka, M. C., Hui, E., Liu, H., & Chapman, E. R. (2008). Synaptotagmin arrests the SNARE complex before triggering fast, efficient membrane fusion in response to Ca2+. *Nature Structural & Molecular Biology*, *15*(8), 827–835. https://doi.org/10.1038/nsmb.1463

Cho, R. W., Buhl, L. K., Volfson, D., Tran, A., Li, F., Akbergenova, Y., & Littleton, J. T. (2015). Phosphorylation of Complexin by PKA Regulates Activity-Dependent Spontaneous Neurotransmitter Release and Structural Synaptic Plasticity. *Neuron*, *88*(4), 749–761. https://doi.org/10.1016/j.neuron.2015.10.011

Cho, R. W., Kummel, D., Li, F., Baguley, S. W., Coleman, J., Rothman, J. E., & Littleton, J. T. (2014). Genetic analysis of the Complexin trans-clamping model for cross-linking

SNARE complexes in vivo. *Proceedings of the National Academy of Sciences*, *111*(28), 10317–10322. https://doi.org/10.1073/pnas.1409311111

Cho, R. W., Song, Y., & Littleton, J. T. (2010). Comparative analysis of Drosophila and mammalian complexins as fusion clamps and facilitators of neurotransmitter release. *Molecular and Cellular Neuroscience*, *45*(4), 389–397. https://doi.org/10.1016/j.mcn.2010.07.012

Choi, B. J., Imlach, W. L., Jiao, W., Wolfram, V., Wu, Y., Grbic, M., Cela, C., Baines, R. A., Nitabach, M. N., & McCabe, B. D. (2014). Miniature Neurotransmission Regulates Drosophila Synaptic Structural Maturation. *Neuron*, *82*(3), 618–634. https://doi.org/10.1016/j.neuron.2014.03.012

Courtney, K. C., Wu, L., Mandal, T., Swift, M., Zhang, Z., Alaghemandi, M., Wu, Z., Bradberry, M. M., Deo, C., Lavis, L. D., Volkmann, N., Hanein, D., Cui, Q., Bao, H., & Chapman, E. R. (2022). The complexin C-terminal amphipathic helix stabilizes the fusion pore open state by sculpting membranes. *Nature Structural & Molecular Biology*. https://doi.org/10.1038/s41594-021-00716-0

Davis, A. F., Bai, J., Fasshauer, D., Wolowick, M. J., Lewis, J. L., & Chapman, E. R. (1999). Kinetics of Synaptotagmin Responses to Ca2+ and Assembly with the Core SNARE Complex onto Membranes. *Neuron*, *24*(2), 363–376.

Dawidowski, D., & Cafiso, D. S. (2016). Munc18-1 and the Syntaxin-1 N Terminus Regulate Open-Closed States in a t-SNARE Complex. *Structure*, *24*(3), 392–400. https://doi.org/10.1016/j.str.2016.01.005

Deng, P., Khan, A., Jacobson, D., Sambrani, N., McGurk, L., Li, X., Jayasree, A., Hejatko, J., Shohat-Ophir, G., O'Connell, M. A., Li, J. B., & Keegan, L. P. (2020). Adar RNA editing-dependent and -independent effects are required for brain and innate immune functions in Drosophila. *Nature Communications*, *11*(1), 1580. https://doi.org/10.1038/s41467-020-15435-1

DiAntonio, A., & Schwarz, T. L. (1994). The Effect on Synaptic Physiology of synaptotagmin Mutations in Drosophila. *Neuron*, *12*(4), 909–920. https://doi.org/10.1016/0896-6273(94)90342-5

Doucet, C. M., Esmery, N., de Saint-Jean, M., & Antonny, B. (2015). Membrane Curvature Sensing by Amphipathic Helices Is Modulated by the Surrounding Protein Backbone. *PLOS ONE*, *10*(9), e0137965. https://doi.org/10.1371/journal.pone.0137965

Duan, Y., Dou, S., Luo, S., Zhang, H., & Lu, J. (2017). Adaptation of A-to-I RNA editing in Drosophila. *PLOS Genetics*, *13*(3), e1006648. https://doi.org/10.1371/journal.pgen.1006648

Dulubova, I. (1999). A conformational switch in syntaxin during exocytosis: Role of munc18. *The EMBO Journal*, *18*(16), 4372–4382. https://doi.org/10.1093/emboj/18.16.4372

Dulubova, I., Lou, X., Lu, J., Huryeva, I., Alam, A., Schneggenburger, R., Südhof, T. C., & Rizo, J. (2005). A Munc13/RIM/Rab3 tripartite complex: From priming to plasticity? *The EMBO Journal*, *24*(16), 2839–2850. https://doi.org/10.1038/sj.emboj.7600753

Fasshauer, D., Otto, H., Eliason, W. K., Jahn, R., & Brünger, A. T. (1997). Structural Changes Are Associated with Soluble N-Ethylmaleimide-sensitive Fusion Protein Attachment Protein Receptor Complex Formation. *Journal of Biological Chemistry*, *272*(44), 28036–28041. https://doi.org/10.1074/jbc.272.44.28036

Fasshauer, D., Sutton, R. B., Brunger, A. T., & Jahn, R. (1998). Conserved structural features of the synaptic fusion complex: SNARE proteins reclassified as Q- and R-SNAREs.

Proceedings of the National Academy of Sciences, *95*(26), 15781–15786. https://doi.org/10.1073/pnas.95.26.15781

Fatt, P., & Katz, B. (1952). Spontaneous subthreshold activity at motor nerve endings. *The Journal of Physiology*, *117*(1), 109–128. https://doi.org/10.1113/jphysiol.1952.sp004735

Fernandez, I., Araç, D., Ubach, J., Gerber, S. H., Shin, O.-H., Gao, Y., Anderson, R. G. W., Südhof, T. C., & Rizo, J. (2001). Three-Dimensional Structure of the Synaptotagmin 1 C2B-Domain: Synaptotagmin 1 as a Phospholipid Binding Machine. *Neuron*, *32*(6), 1057–1069. https://doi.org/10.1016/S0896-6273(01)00548-7

Fernández-Chacón, R., Königstorfer, A., Gerber, S. H., García, J., Matos, M. F., Stevens, C. F., Brose, N., Rizo, J., Rosenmund, C., & Südhof, T. C. (2001). Synaptotagmin I functions as a calcium regulator of release probability. *Nature*, *410*(6824), 41–49. https://doi.org/10.1038/35065004

Fiebig, K. M., Rice, L. M., Pollock, E., & Brunger, A. T. (1999). Folding intermediates of SNARE complex assembly. *Nature Structural Molecular Biology*, *6*(2). https://doi.org/10.1038/5803

Filippini, A., Bonini, D., Lacoux, C., Pacini, L., Zingariello, M., Sancillo, L., Bosisio, D., Salvi, V., Mingardi, J., La Via, L., Zalfa, F., Bagni, C., & Barbon, A. (2017). Absence of the Fragile X Mental Retardation Protein results in defects of RNA editing of neuronal mRNAs in mouse. *RNA Biology*, *14*(11), 1580–1591. https://doi.org/10.1080/15476286.2017.1338232

Fujita, Y., Shirataki, H., Sakisaka, T., Asakura, T., Ohya, T., Kotani, H., Yokoyama, S., Nishioka, H., Matsuura, Y., Mizoguchi, A., Scheller, R. H., & Takai, Y. (1998). Tomosyn: A Syntaxin-1–Binding Protein that Forms a Novel Complex in the Neurotransmitter Release Process. *Neuron*, *20*(5), 905–915. https://doi.org/10.1016/S0896-6273(00)80472-9

Gan, Q., & Watanabe, S. (2018). Synaptic Vesicle Endocytosis in Different Model Systems. *Frontiers in Cellular Neuroscience*, *12*, 171. https://doi.org/10.3389/fncel.2018.00171

Genç, Ö., Kochubey, O., Toonen, R. F., Verhage, M., & Schneggenburger, R. (2014). Munc18-1 is a dynamically regulated PKC target during short-term enhancement of transmitter release. *ELife*, *3*, e01715. https://doi.org/10.7554/eLife.01715

Geppert, M., Goda, Y., Hammer, R. E., Li, C., Rosahl, T. W., Stevens, C. F., & Südhof, T. C. (1994). Synaptotagmin I: A major Ca2+ sensor for transmitter release at a central synapse. *Cell*, *79*(4), 717–727. https://doi.org/10.1016/0092-8674(94)90556-8

Geppert, M., Goda, Y., Stevens, C. F., & Südhof, T. C. (1997). The small GTP-binding protein Rab3A regulates a late step in synaptic vesicle fusion. *Nature*, *387*(6635), 810–814. https://doi.org/10.1038/42954

Ghelani, T., & Sigrist, S. J. (2018). Coupling the Structural and Functional Assembly of Synaptic Release Sites. *Frontiers in Neuroanatomy*, *12*, 81. https://doi.org/10.3389/fnana.2018.00081

Giménez-Andrés, M., Čopič, A., & Antonny, B. (2018). The Many Faces of Amphipathic Helices. *Biomolecules*, *8*(3), 45. https://doi.org/10.3390/biom8030045

Giraudo, C. G., Eng, W. S., Melia, T. J., & Rothman, J. E. (2006). A Clamping Mechanism Involved in SNARE-Dependent Exocytosis. *Science*, *313*(5787), 676–680. https://doi.org/10.1126/science.1129450

Giraudo, C. G., Garcia-Diaz, A., Eng, W. S., Chen, Y., Hendrickson, W. A., Melia, T. J., & Rothman, J. E. (2009). Alternative Zippering as an On-Off Switch for SNARE-Mediated Fusion. *Science*, *323*(5913), 512–516. https://doi.org/10.1126/science.1166500

Goda, Y., & Stevens, C. F. (1994). Two components of transmitter release at a central synapse. *Proceedings of the National Academy of Sciences*, *91*(26), 12942–12946. https://doi.org/10.1073/pnas.91.26.12942

Gong, J., Lai, Y., Li, X., Wang, M., Leitz, J., Hu, Y., Zhang, Y., Choi, U. B., Cipriano, D., Pfuetzner, R. A., Südhof, T. C., Yang, X., Brunger, A. T., & Diao, J. (2016). C-terminal domain of mammalian complexin-1 localizes to highly curved membranes. *Proceedings of the National Academy of Sciences*, *113*(47). https://doi.org/10.1073/pnas.1609917113

Graf, E. R., Daniels, R. W., Burgess, R. W., Schwarz, T. L., & DiAntonio, A. (2009). Rab3 Dynamically Controls Protein Composition at Active Zones. *Neuron*, *64*(5), 663–677. https://doi.org/10.1016/j.neuron.2009.11.002

Graf, E. R., Valakh, V., Wright, C. M., Wu, C., Liu, Z., Zhang, Y. Q., & DiAntonio, A. (2012). RIM Promotes Calcium Channel Accumulation at Active Zones of the *Drosophila* Neuromuscular Junction. *The Journal of Neuroscience*, *32*(47), 16586–16596. https://doi.org/10.1523/JNEUROSCI.0965-12.2012

Grasso, E. M., Terakawa, M. S., Lai, A. L., Xue Xie, Y., Ramlall, T. F., Freed, J. H., & Eliezer, D. (2023). Membrane Binding Induces Distinct Structural Signatures in the Mouse Complexin-1C-Terminal Domain. *Journal of Molecular Biology*, *435*(1), 167710. https://doi.org/10.1016/j.jmb.2022.167710

Guan, Z., Bykhovskaia, M., Jorquera, R. A., Sutton, R. B., Akbergenova, Y., & Littleton, J. T. (2017). A synaptotagmin suppressor screen indicates SNARE binding controls the timing and Ca2+ cooperativity of vesicle fusion. *ELife*, *6*, e28409. https://doi.org/10.7554/eLife.28409

Han, X., Wang, C.-T., Bai, J., Chapman, E. R., & Jackson, M. B. (2004). Transmembrane Segments of Syntaxin Line the Fusion Pore of Ca ^{2} +-Triggered Exocytosis. *Science*, *304*(5668), 289–292. https://doi.org/10.1126/science.1095801

Han, Y., Kaeser, P. S., Südhof, T. C., & Schneggenburger, R. (2011). RIM Determines Ca2+ Channel Density and Vesicle Docking at the Presynaptic Active Zone. *Neuron*, *69*(2), 304–316. https://doi.org/10.1016/j.neuron.2010.12.014

Hanrahan, C. J., Palladino, M. J., Bonneau, L. J., & Reenan, R. A. (1999). RNA Editing of a Drosophila Sodium Channel Gene. *Annals of the New York Academy of Sciences*, *868*(1 MOLECULAR AND), 51–66. https://doi.org/10.1111/j.1749-6632.1999.tb11273.x

Hanrahan, C. J., Palladino, M. J., Ganetzky, B., & Reenan, R. A. (2000). RNA Editing of the Drosophila *para* Na+ Channel Transcript: Evolutionary Conservation and Developmental Regulation. *Genetics*, *155*(3), 1149–1160. https://doi.org/10.1093/genetics/155.3.1149

Harris, K. P., & Littleton, J. T. (2015). Transmission, Development, and Plasticity of Synapses. *Genetics*, *201*(2), 345–375. https://doi.org/10.1534/genetics.115.176529

Hartner, J. C., Schmittwolf, C., Kispert, A., Müller, A. M., Higuchi, M., & Seeburg, P. H. (2004). Liver Disintegration in the Mouse Embryo Caused by Deficiency in the RNA-editing Enzyme ADAR1. *Journal of Biological Chemistry*, *279*(6), 4894–4902. https://doi.org/10.1074/jbc.M311347200

Hata, Y., Slaughter, C. A., & Südhof, T. C. (1993). Synaptic vesicle fusion complex contains unc-18 homologue bound to syntaxin. *Nature*, *366*(6453), 347–351. https://doi.org/10.1038/366347a0

Hatsuzawa, K., Lang, T., Fasshauer, D., Bruns, D., & Jahn, R. (2003). The R-SNARE Motif of Tomosyn Forms SNARE Core Complexes with Syntaxin 1 and SNAP-25 and Down-regulates Exocytosis. *Journal of Biological Chemistry*, *278*(33), 31159–31166. https://doi.org/10.1074/jbc.M305500200

Higuchi, M., Maas, S., Single, F. N., Hartner, J., Rozov, A., Burnashev, N., Feldmeyer, D., Sprengel, R., & Seeburg, P. H. (2000). Point mutation in an AMPA receptor gene rescues lethality in mice deficient in the RNA-editing enzyme ADAR2. *Nature*, *406*(6791), 78–81. https://doi.org/10.1038/35017558

Higuchi, M., Single, F. N., Kohler, M., Sommer, B., Sprengel, R., & Seeburg, P. H. (1993). RNA Editing of AMPA Receptor Subunit GluR-B: A Base-Paired Intron-Exon Structure Determines Position and Efficiency. *Cell*, *75*(7), 1361–1370. https://doi.org/10.1016/0092-8674(93)90622-W

Hobson, R. J., Liu, Q., Watanabe, S., & Jorgensen, E. M. (2011). Complexin Maintains Vesicles in the Primed State in C. elegans. *Current Biology*, *21*(2), 106–113. https://doi.org/10.1016/j.cub.2010.12.015

Hoopengardner, B., Bhalla, T., Staber, C., & Reenan, R. (2003). Nervous System Targets of RNA Editing Identified by Comparative Genomics. *Science*, *301*(5634), 832–836. https://doi.org/10.1126/science.1086763

Hosono, R., Hekimi, S., Kamiya, Y., Sassa, T., Murakami, S., Nishiwaki, K., ... & Kodaira, K. I. (1992). The unc-18 gene encodes a novel protein affecting the kinetics of acetylcholine metabolism in the nematode Caenorhabditis elegans. *Journal of neurochemistry*, *58*(4), 1517-1525. https://doi.org/10.1111/j.1471- 4159.1992.tb11373.x

Hua, Y., & Scheller, R. H. (2001). Three SNARE complexes cooperate to mediate membrane fusion. *Proceedings of the National Academy of Sciences*, *98*(14), 8065–8070. https://doi.org/10.1073/pnas.131214798

Huntwork, S., & Littleton, J. T. (2007). A complexin fusion clamp regulates spontaneous neurotransmitter release and synaptic growth. *Nature Neuroscience*, *10*(10), 1235–1237. https://doi.org/10.1038/nn1980

Ingleby, L., Maloney, R., Jepson, J., Horn, R., & Reenan, R. (2009). Regulated RNA Editing and Functional Epistasis in Shaker Potassium Channels. *Journal of General Physiology*, *133*(1), 17–27. https://doi.org/10.1085/jgp.200810133

Ishiuchi, S., Tsuzuki, K., Yoshida, Y., Yamada, N., Hagimura, N., Okado, H., Miwa, A., Kurihara, H., Nakazato, Y., Tamura, M., Sasaki, T., & Ozawa, S. (2002). Blockage of Ca2+-permeable AMPA receptors suppresses migration and induces apoptosis in human glioblastoma cells. *Nature Medicine*, *8*(9), 971–978. https://doi.org/10.1038/nm746

Israelachvili, J. N., Mitchell, D. J., & Ninham, B. W. (1977). Theory of self-assembly of lipid bilayers and vesicles. *Biochimica et Biophysica Acta (BBA) - Biomembranes*, *470*(2), 185–201. https://doi.org/10.1016/0005-2736(77)90099-2

Iyer, J., Wahlmark, C. J., Kuser-Ahnert, G. A., & Kawasaki, F. (2013). Molecular mechanisms of COMPLEXIN fusion clamp function in synaptic exocytosis revealed in a new Drosophila mutant. *Molecular and Cellular Neuroscience*, *56*, 244–254. https://doi.org/10.1016/j.mcn.2013.06.002

Jepson, J. E. C., & Reenan, R. A. (2008). RNA editing in regulating gene expression in the brain. *Biochimica et Biophysica Acta (BBA) - Gene Regulatory Mechanisms*, *1779*(8), 459–470. https://doi.org/10.1016/j.bbagrm.2007.11.009

Jorquera, R. A., Huntwork-Rodriguez, S., Akbergenova, Y., Cho, R. W., & Littleton, J. T. (2012). Complexin Controls Spontaneous and Evoked Neurotransmitter Release by Regulating the Timing and Properties of Synaptotagmin Activity. *Journal of Neuroscience*, *32*(50), 18234–18245. https://doi.org/10.1523/JNEUROSCI.3212-12.2012

Kaeser-Woo, Y. J., Yang, X., & Südhof, T. C. (2012). C-Terminal Complexin Sequence Is Selectively Required for Clamping and Priming But Not for Ca^{2+} Triggering of Synaptic Exocytosis. *The Journal of Neuroscience*, *32*(8), 2877–2885. https://doi.org/10.1523/JNEUROSCI.3360-11.2012

Karaca, E., Harel, T., Pehlivan, D., Jhangiani, S. N., Gambin, T., Coban Akdemir, Z., Gonzaga-Jauregui, C., Erdin, S., Bayram, Y., Campbell, I. M., Hunter, J. V., Atik, M. M., Van Esch, H., Yuan, B., Wiszniewski, W., Isikay, S., Yesil, G., Yuregir, O. O., Tug Bozdogan, S., … Lupski, J. R. (2015). Genes that Affect Brain Structure and Function Identified by Rare Variant Analyses of Mendelian Neurologic Disease. *Neuron*, *88*(3), 499–513. https://doi.org/10.1016/j.neuron.2015.09.048

Karanasios, E., Han, G.-S., Xu, Z., Carman, G. M., & Siniossoglou, S. (2010). A phosphorylation-regulated amphipathic helix controls the membrane translocation and function of the yeast phosphatidate phosphatase. *Proceedings of the National Academy of Sciences*, *107*(41), 17539–17544. https://doi.org/10.1073/pnas.1007974107

Katz, B., & Miledi, R. (1969). Spontaneous and evoked activity of motor nerve endings in calcium Ringer. *The Journal of Physiology*, *203*(3), 689–706. https://doi.org/10.1113/jphysiol.1969.sp008887

Kavalali, E. T. (2015). The mechanisms and functions of spontaneous neurotransmitter release. *Nature Reviews Neuroscience*, *16*(1), 5–16. https://doi.org/10.1038/nrn3875

Kawahara, Y., Ito, K., Sun, H., Aizawa, H., Kanazawa, I., & Kwak, S. (2004). RNA editing and death of motor neurons. *Nature*, *427*(6977), 801–801. https://doi.org/10.1038/427801a

Kawasaki, F., & Ordway, R. W. (1999). The *Drosophila* NSF Protein, dNSF1, Plays a Similar Role at Neuromuscular and Some Central Synapses. *Journal of Neurophysiology*, *82*(1), 123–130. https://doi.org/10.1152/jn.1999.82.1.123

Keegan, L. P., Brindle, J., Gallo, A., Leroy, A., Reenan, R. A., & O'Connell, M. A. (2005). Tuning of RNA editing by ADAR is required in Drosophila. *The EMBO Journal*, *24*(12), 2183–2193. https://doi.org/10.1038/sj.emboj.7600691

Keegan, L. P., McGurk, L., Palavicini, J. P., Brindle, J., Paro, S., Li, X., Rosenthal, J. J. C., & O'Connell, M. A. (2011). Functional conservation in human and Drosophila of Metazoan ADAR2 involved in RNA editing: Loss of ADAR1 in insects. *Nucleic Acids Research*, *39*(16), 7249–7262. https://doi.org/10.1093/nar/gkr423

Konur, S., & Ghosh, A. (2005). Calcium Signaling and the Control of Dendritic Development. *Neuron*, *46*(3), 401–405. https://doi.org/10.1016/j.neuron.2005.04.022

Koushika, S. P., Richmond, J. E., Hadwiger, G., Weimer, R. M., Jorgensen, E. M., & Nonet, M. L. (2001). A post-docking role for active zone protein Rim. *Nature Neuroscience*, *4*(10), 997–1005. https://doi.org/10.1038/nn732

Krishnakumar, S. S., Radoff, D. T., Kümmel, D., Giraudo, C. G., Li, F., Khandan, L., Baguley, S. W., Coleman, J., Reinisch, K. M., Pincet, F., & Rothman, J. E. (2011). A conformational switch in complexin is required for synaptotagmin to trigger synaptic fusion. *Nature Structural & Molecular Biology*, *18*(8), 934–940. https://doi.org/10.1038/nsmb.2103

Kümmel, D., Krishnakumar, S. S., Radoff, D. T., Li, F., Giraudo, C. G., Pincet, F., Rothman, J. E., & Reinisch, K. M. (2011). Complexin cross-links prefusion SNAREs into a zigzag array. *Nature Structural & Molecular Biology*, *18*(8), 927–933. https://doi.org/10.1038/nsmb.2101

Lai, Y., Choi, U. B., Leitz, J., Rhee, H. J., Lee, C., Altas, B., Zhao, M., Pfuetzner, R. A., Wang, A. L., Brose, N., Rhee, J., & Brunger, A. T. (2017). Molecular Mechanisms of Synaptic Vesicle Priming by Munc13 and Munc18. *Neuron*, *95*(3), 591-607.e10. https://doi.org/10.1016/j.neuron.2017.07.004

Laidlaw, K. M., Livingstone, R., Al-Tobi, M., Bryant, N. J., & Gould, G. W. (2017). SNARE phosphorylation: a control mechanism for insulin-stimulated glucose transport and other regulated exocytic events. *Biochemical Society Transactions*, *45*(6), 1271-1277. https://doi.org/10.1042/BST20170202

Lao, G., Scheuss, V., Gerwin, C. M., Su, Q., Mochida, S., Rettig, J., & Sheng, Z.-H. (2000). Syntaphilin: A Syntaxin-1 Clamp that Controls SNARE Assembly. *Neuron*, *25*(1), 191–201. https://doi.org/10.1016/S0896-6273(00)80882-X

Lee, J., Guan, Z., Akbergenova, Y., & Littleton, J. T. (2013). Genetic Analysis of Synaptotagmin C2 Domain Specificity in Regulating Spontaneous and Evoked Neurotransmitter Release. *The Journal of Neuroscience*, *33*(1), 187–200. https://doi.org/10.1523/JNEUROSCI.3214-12.2013

Lerman, J. C., Robblee, J., Fairman, R., & Hughson, F. M. (2000). Structural Analysis of the Neuronal SNARE Protein Syntaxin-1A ‡. *Biochemistry*, *39*(29), 8470–8479. https://doi.org/10.1021/bi0003994

Li, F., Sundaram, V. K., Gatta, A. T., Coleman, J., Krishnakumar, S. S., Pincet, F., & Rothman, J. E. (2020). *Vesicle capture by discrete self-assembled clusters of membrane-bound Munc13* [Preprint]. Biochemistry. https://doi.org/10.1101/2020.08.17.254821

Licht, K., & Jantsch, M. F. (2016). Rapid and dynamic transcriptome regulation by RNA editing and RNA modifications. *Journal of Cell Biology*, *213*(1), 15–22. https://doi.org/10.1083/jcb.201511041

Littleton, J. T., Chapman, E. R., Kreber, R., Garment, M. B., Carlson, S. D., & Ganetzky, B. (1998). Temperature-Sensitive Paralytic Mutations Demonstrate that Synaptic Exocytosis Requires SNARE Complex Assembly and Disassembly. *Neuron*, *21*(2), 401–413. https://doi.org/10.1016/S0896-6273(00)80549-8

Littleton, J. T., Stern, M., Perin, M., & Bellen, H. J. (1994). Calcium dependence of neurotransmitter release and rate of spontaneous vesicle fusions are altered in Drosophila synaptotagmin mutants. *Proceedings of the National Academy of Sciences*, *91*(23), 10888–10892. https://doi.org/10.1073/pnas.91.23.10888

Littleton, J. T., Stern, M., Schulze, K., Perin, M., & Bellen, H. J. (1993). Mutational analysis of Drosophila synaptotagmin demonstrates its essential role in Ca2+-activated neurotransmitter release. *Cell*, *74*(6), 1125–1134. https://doi.org/10.1016/0092-8674(93)90733-7

Liu, X., Seven, A. B., Camacho, M., Esser, V., Xu, J., Trimbuch, T., Quade, B., Su, L., Ma, C., Rosenmund, C., & Rizo, J. (2016). Functional synergy between the Munc13 C-terminal C1 and C2 domains. *ELife*, *5*, e13696. https://doi.org/10.7554/eLife.13696

Loewen, C. A., Lee, S.-M., Shin, Y.-K., & Reist, N. E. (2006). C $_2$ B Polylysine Motif of Synaptotagmin Facilitates a Ca $^{2+}$ -independent Stage of Synaptic Vesicle Priming In

Vivo. *Molecular Biology of the Cell*, *17*(12), 5211–5226. https://doi.org/10.1091/mbc.e06-07-0622

Lomeli, H., Mosbacher, J., Melcher, T., Höger, T., Geiger, J. R. P., Kuner, T., Monyer, H., Higuchi, M., Bach, A., & Seeburg, P. H. (1994). Control of Kinetic Properties of AMPA Receptor Channels by Nuclear RNA Editing. *Science*, *266*(5191), 1709–1713. https://doi.org/10.1126/science.7992055

López-Murcia, F. J., Reim, K., Jahn, O., Taschenberger, H., & Brose, N. (2019). Acute Complexin Knockout Abates Spontaneous and Evoked Transmitter Release. *Cell Reports*, *26*(10), 2521-2530.e5. https://doi.org/10.1016/j.celrep.2019.02.030

Lottermoser, J. A., & Dittman, J. S. (2023). Complexin Membrane Interactions: Implications for Synapse Evolution and Function. *Journal of Molecular Biology*, 167774. https://doi.org/10.1016/j.jmb.2022.167774

Lu, B., Song, S., & Shin, Y.-K. (2010). Accessory α-Helix of Complexin I Can Displace VAMP2 Locally in the Complexin–SNARE Quaternary Complex. *Journal of Molecular Biology*, *396*(3), 602–609. https://doi.org/10.1016/j.jmb.2009.12.020

Ma, C., Li, W., Xu, Y., & Rizo, J. (2011). Munc13 mediates the transition from the closed syntaxin–Munc18 complex to the SNARE complex. *Nature Structural & Molecular Biology*, *18*(5), 542–549. https://doi.org/10.1038/nsmb.2047

Maas, S., Patt, S., Schrey, M., & Rich, A. (2001). Underediting of glutamate receptor GluR-B mRNA in malignant gliomas. *Proceedings of the National Academy of Sciences*, *98*(25), 14687–14692. https://doi.org/10.1073/pnas.251531398

Mackler, J. M., Drummond, J. A., Loewen, C. A., Robinson, I. M., & Reist, N. E. (2002). The C2B Ca2+-binding motif of synaptotagmin is required for synaptic transmission in vivo. *Nature*, *418*(6895), 340–344. https://doi.org/10.1038/nature00846

Makke, M., Mantero Martinez, M., Gaya, S., Schwarz, Y., Frisch, W., Silva-Bermudez, L., Jung, M., Mohrmann, R., Dhara, M., & Bruns, D. (2018). A mechanism for exocytotic arrest by the Complexin C-terminus. *ELife*, *7*, e38981. https://doi.org/10.7554/eLife.38981

Maldonado, C., Alicea, D., Gonzalez, M., Bykhovskaia, M., & Marie, B. (2013). Adar is essential for optimal presynaptic function. *Molecular and Cellular Neuroscience*, *52*, 173–180. https://doi.org/10.1016/j.mcn.2012.10.009

Malsam, J., Bärfuss, S., Trimbuch, T., Zarebidaki, F., Sonnen, A. F.-P., Wild, K., Scheutzow, A., Rohland, L., Mayer, M. P., Sinning, I., Briggs, J. A. G., Rosenmund, C., & Söllner, T. H. (2020). Complexin Suppresses Spontaneous Exocytosis by Capturing the Membrane-Proximal Regions of VAMP2 and SNAP25. *Cell Reports*, *32*(3), 107926. https://doi.org/10.1016/j.celrep.2020.107926

Malsam, J., Parisotto, D., Bharat, T. A., Scheutzow, A., Krause, J. M., Briggs, J. A., & Söllner, T. H. (2012). Complexin arrests a pool of docked vesicles for fast Ca2+-dependent release. *The EMBO journal*, *31*(15), 3270-3281. https://doi.org/10.1038/emboj.2012.164

Malsam, J., Seiler, F., Schollmeier, Y., Rusu, P., Krause, J. M., & Söllner, T. H. (2009). The carboxy-terminal domain of complexin I stimulates liposome fusion. *Proceedings of the National Academy of Sciences*, *106*(6), 2001–2006. https://doi.org/10.1073/pnas.0812813106

Martin, J. A., Hu, Z., Fenz, K. M., Fernandez, J., & Dittman, J. S. (2011). Complexin Has Opposite Effects on Two Modes of Synaptic Vesicle Fusion. *Current Biology*, *21*(2), 97–105. https://doi.org/10.1016/j.cub.2010.12.014

Masuda, E. S., Huang, B. C., Fisher, J. M., Luo, Y., & Scheller, R. H. (1998). Tomosyn binds t-SNARE proteins via a VAMP-like coiled coil. *Neuron*, *21*(3), 479-480. https://doi.org/10.1016/S0896-6273(00)80559-0

Maximov, A., & Südhof, T. C. (2005). Autonomous Function of Synaptotagmin 1 in Triggering Synchronous Release Independent of Asynchronous Release. *Neuron*, *48*(4), 547–554. https://doi.org/10.1016/j.neuron.2005.09.006

Maximov, A., Tang, J., Yang, X., Pang, Z. P., & Südhof, T. C. (2009). Complexin Controls the Force Transfer from SNARE Complexes to Membranes in Fusion. *Science*, *323*(5913), 516–521. https://doi.org/10.1126/science.1166505

Maycox, P. R., Deckwerth, T., Hell, J. W., & Jahn, R. (1988). Glutamate uptake by brain synaptic vesicles. Energy dependence of transport and functional reconstitution in proteoliposomes. *Journal of Biological Chemistry*, *263*(30), 15423–15428. https://doi.org/10.1016/S0021-9258(19)37605-7

McEwen, J. M., Madison, J. M., Dybbs, M., & Kaplan, J. M. (2006). Antagonistic Regulation of Synaptic Vesicle Priming by Tomosyn and UNC-13. *Neuron*, *51*(3), 303–315. https://doi.org/10.1016/j.neuron.2006.06.025

McKinney, R. A., Capogna, M., Dürr, R., Gähwiler, B. H., & Thompson, and S. M. (1999). Miniature synaptic events maintain dendritic spines via AMPA receptor activation. *Nature Neuroscience*, *2*(1), 44–49. https://doi.org/10.1038/4548

McMahon, H. T., Missler, M., Li, C., & Südhof, T. C. (1995). Complexins: Cytosolic proteins that regulate SNAP receptor function. *Cell*, *83*(1), 111–119. https://doi.org/10.1016/0092-8674(95)90239-2

McNew, J. A., Weber, T., Parlati, F., Johnston, R. J., Melia, T. J., Söllner, T. H., & Rothman, J. E. (2000). Close Is Not Enough: SNARE-dependent Membrane Fusion Requires an Active Mechanism that Transduces Force to Membrane Anchors. *The Journal of Cell Biology*, *150*.

Meijer, M., Dörr, B., Lammertse, H. C., Blithikioti, C., van Weering, J. R., Toonen, R. F., ... & Verhage, M. (2018). Tyrosine phosphorylation of Munc18-1 inhibits synaptic transmission by preventing SNARE assembly. *The EMBO journal*, *37*(2), 300-320. https://doi.org/10.15252/embj.201796484

Mesmin, B., Drin, G., Levi, S., Rawet, M., Cassel, D., Bigay, J., & Antonny, B. (2007). Two Lipid-Packing Sensor Motifs Contribute to the Sensitivity of ArfGAP1 to Membrane Curvature. *Biochemistry*, *46*(7), 1779–1790. https://doi.org/10.1021/bi062288w

Michelassi, F., Liu, H., Hu, Z., & Dittman, J. S. (2017). A C1-C2 Module in Munc13 Inhibits Calcium-Dependent Neurotransmitter Release. *Neuron*, *95*(3), 577-590.e5. https://doi.org/10.1016/j.neuron.2017.07.015

Miledi, R., & Thies, R. (1971). Tetanic and post-tetanic rise in frequency of miniature end-plate potentials in low-calcium solutions. *The Journal of Physiology*, *212*(1), 245–257. https://doi.org/10.1113/jphysiol.1971.sp009320

Misura, K. M. S., Scheller, R. H., & Weis, W. I. (2001). Self-association of the H3 Region of Syntaxin 1A. *Journal of Biological Chemistry*, *276*(16), 13273–13282. https://doi.org/10.1074/jbc.M009636200

Montecucco, C., Schiavo, G., & Pantano, S. (2005). SNARE complexes and neuroexocytosis: How many, how close? *Trends in Biochemical Sciences*, *30*(7), 367–372. https://doi.org/10.1016/j.tibs.2005.05.002

Mortensen, L. S., Park, S. J. H., Ke, J., Cooper, B. H., Zhang, L., Imig, C., Löwel, S., Reim, K., Brose, N., Demb, J. B., Rhee, J.-S., & Singer, J. H. (2016). Complexin 3 Increases the Fidelity of Signaling in a Retinal Circuit by Regulating Exocytosis at Ribbon Synapses. *Cell Reports*, *15*(10), 2239–2250. https://doi.org/10.1016/j.celrep.2016.05.012

Nalefski, E. A., Wisner, M. A., Chen, J. Z., Sprang, S. R., Fukuda, M., Mikoshiba, K., & Falke, J. J. (2001). C2 Domains from Different Ca $^{2+}$ Signaling Pathways Display Functional and Mechanistic Diversity. *Biochemistry*, *40*(10), 3089–3100. https://doi.org/10.1021/bi001968a

Newman, Z. L., Bakshinskaya, D., Schultz, R., Kenny, S. J., Moon, S., Aghi, K., Stanley, C., Marnani, N., Li, R., Bleier, J., Xu, K., & Isacoff, E. Y. (2022). Determinants of synapse diversity revealed by super-resolution quantal transmission and active zone imaging. *Nature Communications*, *13*(1), 229. https://doi.org/10.1038/s41467-021-27815-2

Newman, Z. L., Hoagland, A., Aghi, K., Worden, K., Levy, S. L., Son, J. H., Lee, L. P., & Isacoff, E. Y. (2017). Input-Specific Plasticity and Homeostasis at the Drosophila Larval Neuromuscular Junction. *Neuron*, *93*(6), 1388-1404.e10. https://doi.org/10.1016/j.neuron.2017.02.028

Nicholson, K. L., Munson, M., Miller, R. B., Filip, T. J., Fairman, R., & Hughson, F. M. (1998). Regulation of SNARE complex assembly by an N-terminal domain of the t-SNARE Sso1p. *Nature Structural Biology*, *5*(9), 793–802. https://doi.org/10.1038/1834

Nishikura, K. (2010). Functions and Regulation of RNA Editing by ADAR Deaminases. *Annual Review of Biochemistry*, *79*(1), 321–349. https://doi.org/10.1146/annurev-biochem-060208-105251

Niswender, C. M., Copeland, S. C., Herrick-Davis, K., Emeson, R. B., & Sanders-Bush, E. (1999). RNA Editing of the Human Serotonin 5-Hydroxytryptamine 2C Receptor Silences Constitutive Activity. *Journal of Biological Chemistry*, *274*(14), 9472–9478. https://doi.org/10.1074/jbc.274.14.9472

Nonet, M. L., Staunton, J. E., Kilgard, M. P., Fergestad, T., Hartwieg, E., Horvitz, H. R., Jorgensen, E. M., & Meyer, B. J. (1997). *Caenorhabditis elegans rab-3* Mutant Synapses Exhibit Impaired Function and Are Partially Depleted of Vesicles. *The Journal of Neuroscience*, *17*(21), 8061–8073. https://doi.org/10.1523/JNEUROSCI.17-21-08061.1997

Novick, P., Field, C., & Schekman, R. (1980). Identification of 23 complementation groups required for post-translational events in the yeast secretory pathway. *Cell*, *21*(1), 205–215. https://doi.org/10.1016/0092-8674(80)90128-2

Novick, P., & Schekman, R. (1979). Secretion and cell-surface growth are blocked in a temperature-sensitive mutant of *Saccharomyces cerevisiae*. *Proceedings of the National Academy of Sciences*, *76*(4), 1858–1862. https://doi.org/10.1073/pnas.76.4.1858

Paddock, B. E., Striegel, A. R., Hui, E., Chapman, E. R., & Reist, N. E. (2008). Ca $^{2+}$ -Dependent, Phospholipid-Binding Residues of Synaptotagmin Are Critical for Excitation–Secretion Coupling *In Vivo*. *The Journal of Neuroscience*, *28*(30), 7458–7466. https://doi.org/10.1523/JNEUROSCI.0197-08.2008

Palladino, M. J., Keegan, L. P., O'Connell, M. A., & Reenan, R. A. (2000a). DADAR, a Drosophila double-stranded RNA-specific adenosine deaminase is highly developmentally regulated and is itself a target for RNA editing. *RNA*, *6*(7), 1004–1018. https://doi.org/10.1017/S1355838200000248

Palladino, M. J., Keegan, L. P., O'Connell, M. A., & Reenan, R. A. (2000b). A-to-I Pre-mRNA Editing in Drosophila Is Primarily Involved in Adult Nervous System Function and Integrity. *Cell*, *102*(4), 437–449. https://doi.org/10.1016/S0092-8674(00)00049-0

Paul, M.S. and Bass, B.L. (1998). Inosine exists in mRNA at tissue-specific levels and is most abundant in brain mRNA. *EMBO J.* 17, 1120–1127. https://doi.org/10.1093/emboj/17.4.1120

Paupard, M.-C., O'Connell, M. A., Gerber, A. P., & Zukin, R. S. (1999). Patterns of developmental expression of the RNA editing enzyme rADAR2. *Neuroscience*, *95*(3), 869–879. https://doi.org/10.1016/S0306-4522(99)00431-5

Perin, M. S., Brose, N., Jahn, R., & Südhof, T. C. (1991). Domain structure of synaptotagmin (p65). *Journal of Biological Chemistry*, *266*(1), 623–629. https://doi.org/10.1016/S0021-9258(18)52480-7

Pevsner, J., Hsu, S.-C., Braun, J. E. A., Calakos, N., Ting, A. E., Bennett, M. K., & Scheller, R. H. (1994). Specificity and regulation of a synaptic vesicle docking complex. *Neuron*, *13*(2), 353–361. https://doi.org/10.1016/0896-6273(94)90352-2

Pobbati, A. V., Razeto, A., Böddener, M., Becker, S., & Fasshauer, D. (2004). Structural Basis for the Inhibitory Role of Tomosyn in Exocytosis. *Journal of Biological Chemistry*, *279*(45), 47192–47200. https://doi.org/10.1074/jbc.M408767200

Pobbati, A. V., Stein, A., & Fasshauer, D. (2006). N- to C-Terminal SNARE Complex Assembly Promotes Rapid Membrane Fusion. *Science*, *313*(5787), 673–676. https://doi.org/10.1126/science.1129486

Quade, B., Camacho, M., Zhao, X., Orlando, M., Trimbuch, T., Xu, J., Li, W., Nicastro, D., Rosenmund, C., & Rizo, J. (2019). Membrane bridging by Munc13-1 is crucial for neurotransmitter release. *ELife*, *8*, e42806. https://doi.org/10.7554/eLife.42806

Reddy-Alla, S., Böhme, M. A., Reynolds, E., Beis, C., Grasskamp, A. T., Mampell, M. M., Maglione, M., Jusyte, M., Rey, U., Babikir, H., McCarthy, A. W., Quentin, C., Matkovic, T., Bergeron, D. D., Mushtaq, Z., Göttfert, F., Owald, D., Mielke, T., Hell, S. W., … Walter, A. M. (2017). Stable Positioning of Unc13 Restricts Synaptic Vesicle Fusion to Defined Release Sites to Promote Synchronous Neurotransmission. *Neuron*, *95*(6), 1350-1364.e12. https://doi.org/10.1016/j.neuron.2017.08.016

Redler, S., Strom, T. M., Wieland, T., Cremer, K., Engels, H., Distelmaier, F., Schaper, J., Küchler, A., Lemke, J. R., Jeschke, S., Schreyer, N., Sticht, H., Koch, M., Lüdecke, H.-J., & Wieczorek, D. (2017). Variants in CPLX1 in two families with autosomal-recessive severe infantile myoclonic epilepsy and ID. *European Journal of Human Genetics*, *25*(7), 889–893. https://doi.org/10.1038/ejhg.2017.52

Reim, K., Mansour, M., Varoqueaux, F., McMahon, H. T., Südhof, T. C., Brose, N., & Rosenmund, C. (2001). Complexins Regulate a Late Step in Ca2+-Dependent Neurotransmitter Release. *Cell*, *104*(1), 71–81. https://doi.org/10.1016/S0092-8674(01)00192-1

Reim, K., Wegmeyer, H., Brandstätter, J. H., Xue, M., Rosenmund, C., Dresbach, T., Hofmann, K., & Brose, N. (2005). Structurally and functionally unique complexins at retinal ribbon synapses. *Journal of Cell Biology*, *169*(4), 669–680. https://doi.org/10.1083/jcb.200502115

Rieder, L. E., Savva, Y. A., Reyna, M. A., Chang, Y.-J., Dorsky, J. S., Rezaei, A., & Reenan, R. A. (2015). Dynamic response of RNA editing to temperature in Drosophila. *BMC Biology*, *13*(1), 1–16. https://doi.org/10.1186/s12915-014-0111-3

Rizo, J., & Rosenmund, C. (2008). Synaptic vesicle fusion. *Nature Structural & Molecular Biology*, *15*(7), 665–674. https://doi.org/10.1038/nsmb.1450

Rizo, J., & Südhof, T. C. (2002). Snares and munc18 in synaptic vesicle fusion. *Nature Reviews Neuroscience*, *3*(8), 641–653. https://doi.org/10.1038/nrn898

Robinson, S. W., Bourgognon, J.-M., Spiers, J. G., Breda, C., Campesan, S., Butcher, A., Mallucci, G. R., Dinsdale, D., Morone, N., Mistry, R., Smith, T. M., Guerra-Martin, M., Challiss, R. A. J., Giorgini, F., & Steinert, J. R. (2018). Nitric oxide-mediated posttranslational modifications control neurotransmitter release by modulating complexin farnesylation and enhancing its clamping ability. *PLOS Biology*, *16*(4), e2003611. https://doi.org/10.1371/journal.pbio.2003611

Rothman, J. E., Krishnakumar, S. S., Grushin, K., & Pincet, F. (2017). Hypothesis—Buttressed rings assemble, clamp, and release SNAREpins for synaptic transmission. *FEBS Letters*, *591*(21), 3459–3480. https://doi.org/10.1002/1873-3468.12874

Rueter, S. M., Dawson, T. R., & Emeson, R. B. (1999). Regulation of alternative splicing by RNA editing. *Nature*, *399*(6731), 75–80. https://doi.org/10.1038/19992

Sabatini, B. L., & Regehr, W. G. (1996). Timing of neurotransmission at fast synapses in the mammalian brain. *Nature*, *384*(6605), 170–172. https://doi.org/10.1038/384170a0

Sanjana, N. E., Levanon, E. Y., Hueske, E. A., Ambrose, J. M., & Li, J. B. (2012). Activity-Dependent A-to-I RNA Editing in Rat Cortical Neurons. *Genetics*, *192*(1), 281–287. https://doi.org/10.1534/genetics.112.141200

Sapiro, A. L., Shmueli, A., Henry, G. L., Li, Q., Shalit, T., Yaron, O., Paas, Y., Billy Li, J., & Shohat-Ophir, G. (2019). Illuminating spatial A-to-I RNA editing signatures within the *Drosophila* brain. *Proceedings of the National Academy of Sciences*, *116*(6), 2318–2327. https://doi.org/10.1073/pnas.1811768116

Sauvola, C. W., Akbergenova, Y., Cunningham, K. L., Aponte-Santiago, N. A., & Littleton, J. T. (2021). The decoy SNARE Tomosyn sets tonic versus phasic release properties and is required for homeostatic synaptic plasticity. *ELife*, *10*, e72841. https://doi.org/10.7554/eLife.72841

Sauvola, C. W., & Littleton, J. T. (2021). SNARE Regulatory Proteins in Synaptic Vesicle Fusion and Recycling. *Frontiers in Molecular Neuroscience*, *14*, 733138. https://doi.org/10.3389/fnmol.2021.733138

Savva, Y. A., Jepson, J. E. C., Sahin, A., Sugden, A. U., Dorsky, J. S., Alpert, L., Lawrence, C., & Reenan, R. A. (2012). Auto-regulatory RNA editing fine-tunes mRNA re-coding and complex behaviour in Drosophila. *Nature Communications*, *3*(1), 790. https://doi.org/10.1038/ncomms1789

Scales, S., Hesser, B., Masuda, E., & Scheller, R. H. (2002). Amisyn, a Novel Syntaxin-binding Protein That May Regulate SNARE Complex Assembly. *Journal of Biological Chemistry*, *277*(31), i–ii. https://doi.org/10.1016/S0021-9258(19)66212-5

Schaub, J. R., Lu, X., Doneske, B., Shin, Y.-K., & McNew, J. A. (2006). Hemifusion arrest by complexin is relieved by Ca2+–synaptotagmin I. *Nature Structural & Molecular Biology*, *13*(8), 748–750. https://doi.org/10.1038/nsmb1124

Schlüter, O. M., Basu, J., Südhof, T. C., & Rosenmund, C. (2006). Rab3 Superprimes Synaptic Vesicles for Release: Implications for Short-Term Synaptic Plasticity. *The Journal of Neuroscience*, *26*(4), 1239–1246. https://doi.org/10.1523/JNEUROSCI.3553-05.2006

Scholz, N., Ehmann, N., Sachidanandan, D., Imig, C., Cooper, B. H., Jahn, O., Reim, K., Brose, N., Meyer, J., Lamberty, M., Altrichter, S., Bormann, A., Hallermann, S., Pauli, M.,

Heckmann, M., Stigloher, C., Langenhan, T., & Kittel, R. J. (2019). Complexin cooperates with Bruchpilot to tether synaptic vesicles to the active zone cytomatrix. *Journal of Cell Biology*, *218*(3), 1011–1026. https://doi.org/10.1083/jcb.201806155

Seeburg, P. H., Higuchi, M., & Sprengel, R. (1998). RNA editing of brain glutamate receptor channels: Mechanism and physiology. *Brain Research Reviews*, *26*(2–3), 217–229. https://doi.org/10.1016/S0165-0173(97)00062-3

Seiler, F., Malsam, J., Krause, J. M., & Söllner, T. H. (2009). A role of complexin-lipid interactions in membrane fusion. *FEBS Letters*, *583*(14), 2343–2348. https://doi.org/10.1016/j.febslet.2009.06.025

Shata, A., Saisu, H., Odani, S., & Abe, T. (2007). Phosphorylated synaphin/complexin found in the brain exhibits enhanced SNARE complex binding. *Biochemical and Biophysical Research Communications*, *354*(3), 808–813. https://doi.org/10.1016/j.bbrc.2007.01.064

Shen, J., Tareste, D. C., Paumet, F., Rothman, J. E., & Melia, T. J. (2007). Selective Activation of Cognate SNAREpins by Sec1/Munc18 Proteins. *Cell*, *128*(1), 183–195. https://doi.org/10.1016/j.cell.2006.12.016

Shi, L., Shen, Q.-T., Kiel, A., Wang, J., Wang, H.-W., Melia, T. J., Rothman, J. E., & Pincet, F. (2012). SNARE Proteins: One to Fuse and Three to Keep the Nascent Fusion Pore Open. *Science*, *335*(6074), 1355–1359. https://doi.org/10.1126/science.1214984

Shin, O.-H., Lu, J., Rhee, J.-S., Tomchick, D. R., Pang, Z. P., Wojcik, S. M., Camacho-Perez, M., Brose, N., Machius, M., Rizo, J., Rosenmund, C., & Südhof, T. C. (2010). Munc13 C2B domain is an activity-dependent Ca2+ regulator of synaptic exocytosis. *Nature Structural & Molecular Biology*, *17*(3), 280–288. https://doi.org/10.1038/nsmb.1758

Smith, L. A., Peixoto, A. A., & Hall, J. C. (1998). RNA Editing in the Drosophila Dmcaia Calcium-Channel α1 Subunit Transcript. *Journal of Neurogenetics*, *12*(4), 227–240. https://doi.org/10.3109/01677069809108560

Snead, D., Wragg, R. T., Dittman, J. S., & Eliezer, D. (2014). Membrane curvature sensing by the C-terminal domain of complexin. *Nature Communications*, *5*(1), 4955. https://doi.org/10.1038/ncomms5955

Söllner, T., Bennett, M. K., Whiteheart, S. W., Scheller, R. H., & Rothman, J. E. (1993). A protein assembly-disassembly pathway in vitro that may correspond to sequential steps of synaptic vesicle docking, activation, and fusion. *Cell*, *75*(3), 409–418. https://doi.org/10.1016/0092-8674(93)90376-2

Söllner, T., Whiteheart, S. W., Brunner, M., Erdjument-Bromage, H., Geromanos, S., Tempst, P., & Rothman, J. E. (1993). SNAP receptors implicated in vesicle targeting and fusion. *Nature*, *362*(6418), 318–324. https://doi.org/10.1038/362318a0

Sommer, B., Köhler, M., Sprengel, R., & Seeburg, P. H. (1991). RNA editing in brain controls a determinant of ion flow in glutamate-gated channels. *Cell*, *67*(1), 11–19. https://doi.org/10.1016/0092-8674(91)90568-J

Soykan, T., Maritzen, T., & Haucke, V. (2016). Modes and mechanisms of synaptic vesicle recycling. *Current Opinion in Neurobiology*, *39*, 17–23. https://doi.org/10.1016/j.conb.2016.03.005

Stadler, H., & Tsukita, S. (1984). Synaptic vesicles contain an ATP-dependent proton pump and show ‘knob-like’ protrusions on their surface. *The EMBO journal*, *3*(13), 3333-3337. https://doi.org/10.1002/j.1460-2075.1984.tb02300.x

Stenmark, H., & Olkkonen, V. M. (2001). The rab gtpase family. *Genome biology*, *2*(5), 1-7. https://doi.org/10.1186/gb-2001-2-5-reviews3007

Südhof, T. C. (2013a). A molecular machine for neurotransmitter release: Synaptotagmin and beyond. *Nature Medicine*, *19*(10), 1227–1231. https://doi.org/10.1038/nm.3338
Südhof, T. C. (2013b). Neurotransmitter Release: The Last Millisecond in the Life of a Synaptic Vesicle. *Neuron*, *80*(3), 675–690. https://doi.org/10.1016/j.neuron.2013.10.022
Südhof, T. C., & Rothman, J. E. (2009). Membrane Fusion: Grappling with SNARE and SM Proteins. *Science*, *323*(5913), 474–477. https://doi.org/10.1126/science.1161748
Sutton, M. A., Wall, N. R., Aakalu, G. N., & Schuman, E. M. (2004). Regulation of Dendritic Protein Synthesis by Miniature Synaptic Events. *Science*, *304*(5679), 1979–1983. https://doi.org/10.1126/science.1096202
Sutton, R. B., Fasshauer, D., Jahn, R., & Brunger, A. T. (1998). Crystal structure of a SNARE complex involved in synaptic exocytosis at 2.4 Å resolution. *Nature*, *395*(6700), 347–353. https://doi.org/10.1038/26412
Tang, J., Maximov, A., Shin, O.-H., Dai, H., Rizo, J., & Südhof, T. C. (2006). A Complexin/Synaptotagmin 1 Switch Controls Fast Synaptic Vesicle Exocytosis. *Cell*, *126*(6), 1175–1187. https://doi.org/10.1016/j.cell.2006.08.030
Tokumaru, H., Shimizu-Okabe, C., & Abe, T. (2008). Direct interaction of SNARE complex binding protein synaphin/complexin with calcium sensor synaptotagmin 1. *Brain Cell Biology*, *36*(5–6), 173–189. https://doi.org/10.1007/s11068-008-9032-9
Tolar, L. A., & Pallanck, L. (1998). NSF Function in Neurotransmitter Release Involves Rearrangement of the SNARE Complex Downstream of Synaptic Vesicle Docking. *The Journal of Neuroscience*, *18*(24), 10250–10256. https://doi.org/10.1523/JNEUROSCI.18-24-10250.1998
Tonkin, L. A., Saccomanno, L., Morse, D. P., Brodigan, T., Krause, M., & Bass, B. L. (2002). RNA editing by ADARs is important for normal behavior in Caenorhabditis elegans. *The EMBO Journal*, *21*(22), 6025–6035. https://doi.org/10.1093/emboj/cdf607
Tucker, W. C., Weber, T., & Chapman, E. R. (2004). Reconstitution of Ca^{2+} -Regulated Membrane Fusion by Synaptotagmin and SNAREs. *Science*, *304*(5669), 435–438. https://doi.org/10.1126/science.1097196
Turecek, J., & Regehr, W. G. (2019). Neuronal Regulation of Fast Synaptotagmin Isoforms Controls the Relative Contributions of Synchronous and Asynchronous Release. *Neuron*, *101*(5), 938-949.e4. https://doi.org/10.1016/j.neuron.2019.01.013
Ubach, J., Lao, Y., Fernandez, I., Arac, D., Südhof, T. C., & Rizo, J. (2001). The C_2 B Domain of Synaptotagmin I Is a Ca^{2+} -Binding Module. *Biochemistry*, *40*(20), 5854–5860. https://doi.org/10.1021/bi010340c
Ubach, J., Zhang, X., Shao, X., Südhof, T. C., & Rizo, J. (1998). Ca2+ binding to synaptotagmin: how many Ca2+ ions bind to the tip of a C2-domain?. *The EMBO journal*, *17*(14), 3921-3930. https://doi.org/10.1093/emboj/17.14.3921
Ulbricht, R. J., Sun, S. J., DelBove, C. E., Kitko, K. E., Rehman, S. C., Wang, M. Y., Lazarenko, R. M., Zhang, Q., & Emeson, R. B. (2017). *RNA editing of CAPS1 regulates synaptic vesicle organization, release and retrieval* [Preprint]. Biochemistry. https://doi.org/10.1101/178202
Vaithianathan, T., Henry, D., Akmentin, W., & Matthews, G. (2015). Functional Roles of Complexin in Neurotransmitter Release at Ribbon Synapses of Mouse Retinal Bipolar Neurons. *The Journal of Neuroscience*, *35*(9), 4065–4070. https://doi.org/10.1523/JNEUROSCI.2703-14.2015

Vaithianathan, T., Zanazzi, G., Henry, D., Akmentin, W., & Matthews, G. (2013). Stabilization of Spontaneous Neurotransmitter Release at Ribbon Synapses by Ribbon-Specific Subtypes of Complexin. *The Journal of Neuroscience*, *33*(19), 8216–8226. https://doi.org/10.1523/JNEUROSCI.1280-12.2013

Vanni, S., Vamparys, L., Gautier, R., Drin, G., Etchebest, C., Fuchs, P. F. J., & Antonny, B. (2013). Amphipathic Lipid Packing Sensor Motifs: Probing Bilayer Defects with Hydrophobic Residues. *Biophysical Journal*, *104*(3), 575–584. https://doi.org/10.1016/j.bpj.2012.11.3837

Vasin, A., Volfson, D., Littleton, J. T., & Bykhovskaia, M. (2016). Interaction of the Complexin Accessory Helix with Synaptobrevin Regulates Spontaneous Fusion. *Biophysical Journal*, *111*(9), 1954–1964. https://doi.org/10.1016/j.bpj.2016.09.017

Verhage, M., Maia, A. S., Plomp, J. J., Brussaard, A. B., Heeroma, J. H., Vermeer, H., Toonen, R. F., Hammer, R. E., van den, T. K., Berg, Missler, M., Geuze, H. J., & Südhof, T. C. (2000). Synaptic Assembly of the Brain in the Absence of Neurotransmitter Secretion. *Science*, *287*(5454), 864–869. https://doi.org/10.1126/science.287.5454.864

Verhage, M., & Sørensen, J. B. (2020). SNAREopathies: Diversity in Mechanisms and Symptoms. *Neuron*, *107*(1), 22–37. https://doi.org/10.1016/j.neuron.2020.05.036

Verkhratsky, A. (2007). *Calcium and cell death. Calcium signalling and disease: Molecular pathology of calcium* (E. Carafoli, Ed.). Springer.

Wang, Q., Khillan, J., Gadue, P., & Nishikura, K. (2000). Requirement of the RNA Editing Deaminase ADAR1 Gene for Embryonic Erythropoiesis. *Science*, *290*(5497), 1765–1768. https://doi.org/10.1126/science.290.5497.1765

Wang, Q., Miyakoda, M., Yang, W., Khillan, J., Stachura, D. L., Weiss, M. J., & Nishikura, K. (2004). Stress-induced Apoptosis Associated with Null Mutation of ADAR1 RNA Editing Deaminase Gene. *Journal of Biological Chemistry*, *279*(6), 4952–4961. https://doi.org/10.1074/jbc.M310162200

Wang, S., Choi, U. B., Gong, J., Yang, X., Li, Y., Wang, A. L., Yang, X., Brunger, A. T., & Ma, C. (2017). Conformational change of syntaxin linker region induced by Munc13s initiates SNARE complex formation in synaptic exocytosis. *The EMBO Journal*, *36*(6), 816–829. https://doi.org/10.15252/embj.201695775

Wang, X., Gong, J., Zhu, L., Wang, S., Yang, X., Xu, Y., Yang, X., & Ma, C. (2020). Munc13 activates the Munc18-1/syntaxin-1 complex and enables Munc18-1 to prime SNARE assembly. *The EMBO Journal*, *39*(16). https://doi.org/10.15252/embj.2019103631

Wang, Y., Okamoto, M., Schmitz, F., Hofmann, K., & Südhof, T. C. (1997). Rim is a putative Rab3 effector in regulating synaptic-vesicle fusion. *Nature*, *388*(6642), 593–598. https://doi.org/10.1038/41580

Weber, T., Zemelman, B. V., McNew, J. A., Westermann, B., Gmachl, M., Parlati, F., Söllner, T. H., & Rothman, J. E. (1998). SNAREpins: Minimal Machinery for Membrane Fusion. *Cell*, *92*(6), 759–772. https://doi.org/10.1016/S0092-8674(00)81404-X

Weimbs, T., Low, S. H., Chapin, S. J., Mostov, K. E., Bucher, P., & Hofmann, K. (1997). A conserved domain is present in different families of vesicular fusion proteins: A new superfamily. *Proceedings of the National Academy of Sciences*, *94*(7), 3046–3051. https://doi.org/10.1073/pnas.94.7.3046

Weimer, R. M., Richmond, J. E., Davis, W. S., Hadwiger, G., Nonet, M. L., & Jorgensen, E. M. (2003). Defects in synaptic vesicle docking in unc-18 mutants. *Nature Neuroscience*, *6*(10), 1023–1030. https://doi.org/10.1038/nn1118

Weninger, K., Bowen, M. E., Chu, S., & Brunger, A. T. (2003). Single-molecule studies of SNARE complex assembly reveal parallel and antiparallel configurations. *Proceedings of the National Academy of Sciences*, *100*(25), 14800–14805. https://doi.org/10.1073/pnas.2036428100

Whyte, J. R. C., & Munro, S. (2002). Vesicle tethering complexes in membrane traffic. *Journal of Cell Science*, *115*(13), 2627–2637. https://doi.org/10.1242/jcs.115.13.2627

Wragg, R. T., Gouzer, G., Bai, J., Arianna, G., Ryan, T. A., & Dittman, J. S. (2015). Synaptic Activity Regulates the Abundance and Binding of Complexin. *Biophysical Journal*, *108*(6), 1318–1329. https://doi.org/10.1016/j.bpj.2014.12.057

Wragg, R. T., Parisotto, D. A., Li, Z., Terakawa, M. S., Snead, D., Basu, I., Weinstein, H., Eliezer, D., & Dittman, J. S. (2017). Evolutionary Divergence of the C-terminal Domain of Complexin Accounts for Functional Disparities between Vertebrate and Invertebrate Complexins. *Frontiers in Molecular Neuroscience*, *10*, 146. https://doi.org/10.3389/fnmol.2017.00146

Wragg, R. T., Snead, D., Dong, Y., Ramlall, T. F., Menon, I., Bai, J., Eliezer, D., & Dittman, J. S. (2013). Synaptic Vesicles Position Complexin to Block Spontaneous Fusion. *Neuron*, *77*(2), 323–334. https://doi.org/10.1016/j.neuron.2012.11.005

Xiao, W., Poirier, M. A., Bennett, M. K., & Shin, Y.-K. (2001). The neuronal t-SNARE complex is a parallel four-helix bundle. *Nature Structural Molecular Biology*, *8*(4), 308–311. https://doi.org/10.1038/86174

Xue, M., Craig, T. K., Xu, J., Chao, H.-T., Rizo, J., & Rosenmund, C. (2010). Binding of the complexin N terminus to the SNARE complex potentiates synaptic-vesicle fusogenicity. *Nature Structural & Molecular Biology*, *17*(5), 568–575. https://doi.org/10.1038/nsmb.1791

Xue, M., Lin, Y. Q., Pan, H., Reim, K., Deng, H., Bellen, H. J., & Rosenmund, C. (2009). Tilting the Balance between Facilitatory and Inhibitory Functions of Mammalian and Drosophila Complexins Orchestrates Synaptic Vesicle Exocytosis. *Neuron*, *64*(3), 367–380. https://doi.org/10.1016/j.neuron.2009.09.043

Xue, M., Reim, K., Chen, X., Chao, H.-T., Deng, H., Rizo, J., Brose, N., & Rosenmund, C. (2007). Distinct domains of complexin I differentially regulate neurotransmitter release. *Nature Structural & Molecular Biology*, *14*(10), 949–958. https://doi.org/10.1038/nsmb1292

Yang, B., Steegmaier, M., Gonzalez, L. C., & Scheller, R. H. (2000). Nsec1 Binds a Closed Conformation of Syntaxin1a. *Journal of Cell Biology*, *148*(2), 247–252. https://doi.org/10.1083/jcb.148.2.247

Yang, X., Cao, P., & Südhof, T. C. (2013). Deconstructing complexin function in activating and clamping Ca^{2+}-triggered exocytosis by comparing knockout and knockdown phenotypes. *Proceedings of the National Academy of Sciences*, *110*(51), 20777–20782. https://doi.org/10.1073/pnas.1321367110

Yang, X., Kaeser-Woo, Y. J., Pang, Z. P., Xu, W., & Südhof, T. C. (2010). Complexin Clamps Asynchronous Release by Blocking a Secondary Ca2+ Sensor via Its Accessory α Helix. *Neuron*, *68*(5), 907–920. https://doi.org/10.1016/j.neuron.2010.11.001

Yang, X., Pei, J., Kaeser-Woo, Y. J., Bacaj, T., Grishin, N. V., & Südhof, T. C. (2015). Evolutionary conservation of complexins: From choanoflagellates to mice. *EMBO Reports*, *16*(10), 1308–1317. https://doi.org/10.15252/embr.201540305

Yoshihara, M., Guan, Z., & Littleton, J. T. (2010). Differential regulation of synchronous versus asynchronous neurotransmitter release by the C2 domains of synaptotagmin 1. *Proceedings of the National Academy of Sciences*, *107*(33), 14869–14874. https://doi.org/10.1073/pnas.1000606107

Yoshihara, M., & Littleton, J. T. (2002). Synaptotagmin I Functions as a Calcium Sensor to Synchronize Neurotransmitter Release. *Neuron*, *36*(5), 897–908. https://doi.org/10.1016/S0896-6273(02)01065-6

Yu, I.-M., & Hughson, F. M. (2010). Tethering Factors as Organizers of Intracellular Vesicular Traffic. *Annual Review of Cell and Developmental Biology*, *26*(1), 137–156. https://doi.org/10.1146/annurev.cellbio.042308.113327

Zanazzi, G., & Matthews, G. (2010). Enrichment and differential targeting of complexins 3 and 4 in ribbon-containing sensory neurons during zebrafish development. *Neural Development*, *5*(1), 24. https://doi.org/10.1186/1749-8104-5-24

Zdanowicz, R., Kreutzberger, A., Liang, B., Kiessling, V., Tamm, L. K., & Cafiso, D. S. (2017). Complexin Binding to Membranes and Acceptor t-SNAREs Explains Its Clamping Effect on Fusion. *Biophysical Journal*, *113*(6), 1235–1250. https://doi.org/10.1016/j.bpj.2017.04.002

Zhai, R. G., & Bellen, H. J. (2004). The Architecture of the Active Zone in the Presynaptic Nerve Terminal. *Physiology*, *19*(5), 262–270. https://doi.org/10.1152/physiol.00014.2004

Zhang, Y., & Hughson, F. M. (2021). Chaperoning SNARE Folding and Assembly. *Annual Review of Biochemistry*, *90*(1), 581–603. https://doi.org/10.1146/annurev-biochem-081820-103615

Zhou, Q., Lai, Y., Bacaj, T., Zhao, M., Lyubimov, A. Y., Uervirojnangkoorn, M., Zeldin, O. B., Brewster, A. S., Sauter, N. K., Cohen, A. E., Soltis, S. M., Alonso-Mori, R., Chollet, M., Lemke, H. T., Pfuetzner, R. A., Choi, U. B., Weis, W. I., Diao, J., Südhof, T. C., & Brunger, A. T. (2015). Architecture of the synaptotagmin–SNARE machinery for neuronal exocytosis. *Nature*, *525*(7567), 62–67. https://doi.org/10.1038/nature14975

Zhou, Q., Zhou, P., Wang, A. L., Wu, D., Zhao, M., Südhof, T. C., & Brunger, A. T. (2017). The primed SNARE–complexin–synaptotagmin complex for neuronal exocytosis. *Nature*, *548*(7668), 420–425. https://doi.org/10.1038/nature23484

Zikich, D., Mezer, A., Varoqueaux, F., Sheinin, A., Junge, H. J., Nachliel, E., Melamed, R., Brose, N., Gutman, M., & Ashery, U. (2008). Vesicle Priming and Recruitment by ubMunc13-2 Are Differentially Regulated by Calcium and Calmodulin. *The Journal of Neuroscience*, *28*(8), 1949–1960. https://doi.org/10.1523/JNEUROSCI.5096-07.2008

Figures

Figure 1. Cpx is enriched at presynaptic terminals of *Drosophila* larval NMJs, where it regulates neurotransmission and synaptic growth. (**A**) Representative evoked response in 2.0 mM external calcium saline. (**B**) Quantification of evoked response amplitude shows the role of Cpx is facilitating calcium-dependent fusion. (**C**) *Cpx* null animals show increased spontaneous fusion events at muscle 6 NMJs. (**D**) Loss of Cpx leads to a significant difference in spontaneous release rate, demonstrating the Cpx "clamp" function. (**E**) Immunostaining of control and *cpx* null larvae with presynaptic active zone marker Bruchpilot (Brp, nc82, magenta) and neuronal membrane marker horseradish peroxidase (HRP) in green. *Cpx* null animals show increased synaptic growth, quantified as an increase in active zone number (**F**). Adapted from Buhl et al., 2013 and Huntwork & Littleton, 2007.

Figure 2. Functional differences between *Drosophila* Cpx7A and Cpx7B splice variants. (**A**) Log-scale quantitative RT-PCR results demonstrating that the Cpx7A transcript is predominantly expressed over the Cpx7B transcript in adult flies and 3rd instar larvae. (**B**) Spontaneous fusion analysis of Cpx variants on a semi-logarithmic plot and (**C**) evoked amplitude analysis in 0.2 mM external calcium saline. Abbreviations: Dm – *Drosophila melanogaster*, m – mammalian (mouse). Rescue of *cpx* null animals with Cpx proteins containing a prenylation motif (DmCpx7A and mCpxIV) are better at "clamping" spontaneous SV fusion, while Cpx proteins lacking this motif (DmCpx7B and mCpxI) are better facilitators of evoked release. (**D**) Model of the differential effects of Cpx7A and Cpx7B on SV fusion. Top-down view of a single SV fusing shows SNARE complexes (orange) arranged in circular manner. Cpx (purple) is denoted with a black line to represent Cpx7A prenylation. This prenylation of Cpx7A may increase its local concentration at fusion sites, allowing for Cpx7A to efficiently bind SNARE complexes and clamp fusion. Cpx7B lacks the prenylation motif and has reduced membrane-tethering capabilities which may lower Cpx7B local concentration at fusion sites, thus making it less effective at clamping. Adapted from Buhl et al., 2013.

Figure 3. Phosphorylation of Cpx7B regulates synaptic plasticity. Model of proposed retrograde Synaptotagmin 4 (Syt4)-dependent signaling pathway that is activated by strong stimulation. Postsynaptic calcium elevation following stimulation drives release of a retrograde

signal that activates the presynaptic PKA pathway. PKA is hypothesized to phosphorylate Cpx7B, altering its clamping properties. In addition, PKA may phosphorylate additional targets to facilitate structural growth. Adapted from Cho et al., 2015.

Figure 1

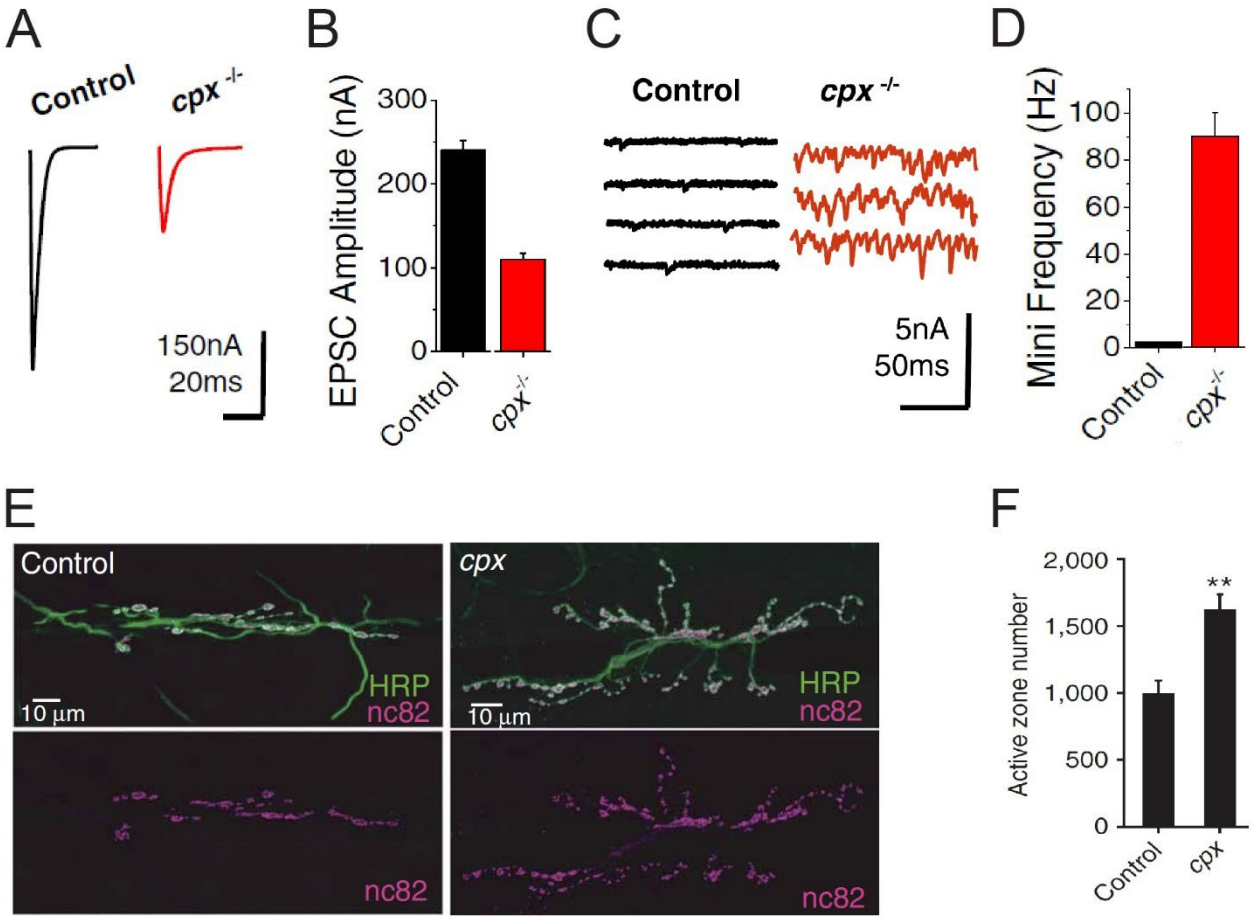
A
Control
cpx -/-
150nA
20ms
B
EPSC Amplitude (nA)
300
200
100
0
Control
cpx -/-
C
Control
cpx -/-
5nA
50ms
D
Mini Frequency (Hz)
100
80
60
40
20
0
Control
cpx -/-
E
Control
cpx
HRP
nc82
10 µm
nc82
F
Active zone number
2,000
1,500
1,000
500
0
**
Control
cpx

Figure 2

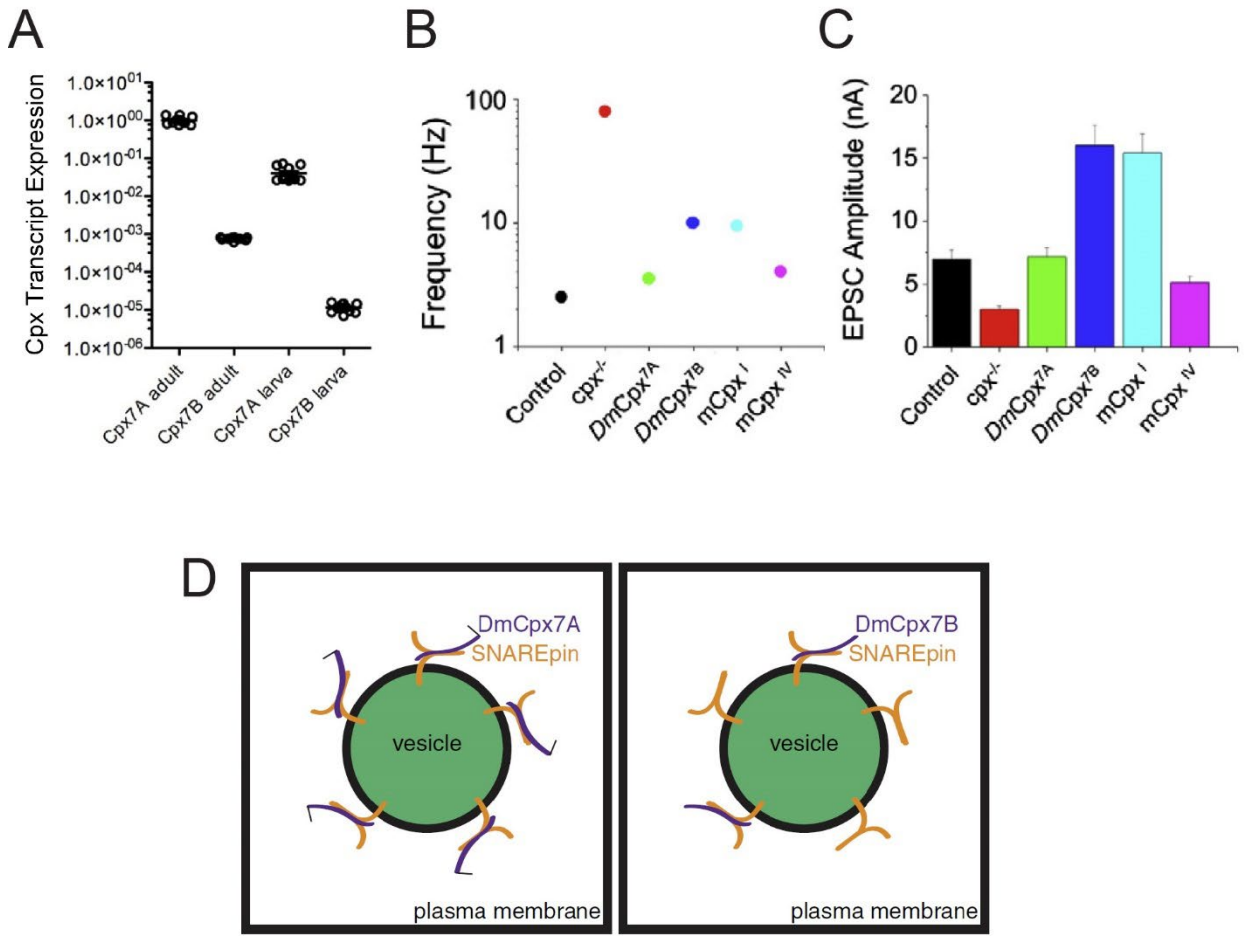
A
Cpx Transcript Expression
1.0×10^01
1.0×10^00
1.0×10^-01
1.0×10^-02
1.0×10^-03
1.0×10^-04
1.0×10^-05
1.0×10^-06
Cpx7A adult
Cpx7B adult
Cpx7A larva
Cpx7B larva
B
Frequency (Hz)
100
10
1
Control
cpx-/-
DmCpx7A
DmCpx7B
mCpx I
mCpx IV
C
EPSC Amplitude (nA)
20
15
10
5
0
Control
cpx-/-
DmCpx7A
DmCpx7B
mCpx I
mCpx IV
D
DmCpx7A
SNAREpin
vesicle
plasma membrane
DmCpx7B
SNAREpin
vesicle
plasma membrane

Figure 3

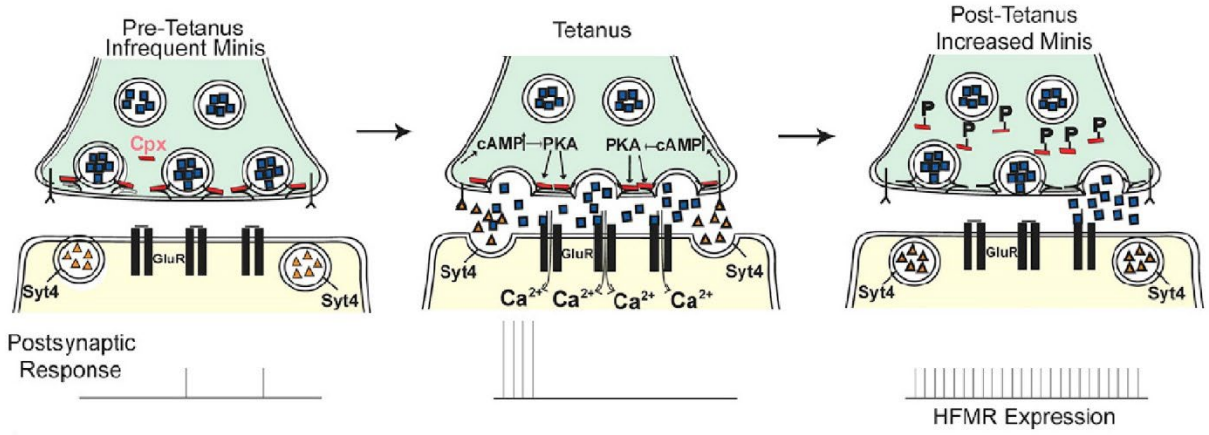
Pre-Tetanus
Infrequent Minis
Cpx
GluR
Syt4
Syt4
Tetanus
cAMP
PKA
PKA
cAMP
Syt4
GluR
Syt4
Ca2+
Ca2+
Ca2+
Ca2+
Post-Tetanus
Increased Minis
P
P
P
P
P
P
GluR
Syt4
Syt4
Postsynaptic
Response
HFMR Expression

Chapter 2

Stochastic RNA editing of the Complexin C-terminus within single neurons regulates neurotransmitter release in *Drosophila*

Elizabeth A. Brija[1], Zhuo Guan[1,2], Suresh K. Jetti[1,2], and J. Troy Littleton[1,2]

[1]The Picower Institute for Learning and Memory, Department of Brain and Cognitive Sciences,
[2]Department of Biology, Massachusetts Institute of Technology, Cambridge, MA 02139

Author Contributions: E.A.B performed most of the experiments described in this chapter. Z.G. performed and analyzed two-electrode voltage-clamp electrophysiology. S.K.J. provided unpublished RNAseq data, which was analyzed by E.A.B. for RNA editing. J.T.L. supervised the project. E.A.B. and J.T.L. designed experiments and wrote the manuscript.

2.1 Introduction

Neuronal communication is initiated by Ca^{2+}-evoked fusion of synaptic vesicles (SVs) in response to action potentials (Katz and Miledi, 1967). Single SVs can also fuse spontaneously to generate events known as "minis". The SNARE-binding protein Complexin (Cpx) and the Ca^{2+} sensor Synaptotagmin 1 (Syt1) play key roles in determining whether SVs fuse spontaneously or through the evoked pathway (Quiñones-Frías and Littleton, 2021; Sauvola and Littleton, 2021; Rizo, 2022). In particular, Cpx arrests zippering of the SNARE complex fusion machinery at the SV/plasma membrane interface to maintain SVs in a fusion-ready state and allow Ca^{2+}-bound Syt1 to rapidly trigger release (Jorquera et al., 2012; Bykhovskaia et al., 2013; Malsam et al., 2020; Bera et al., 2022). Invertebrate Cpxs also act as "fusion clamps" to reduce spontaneous release in the absence of Ca^{2+} (Huntwork and Littleton, 2007; Hobson et al., 2011; Martin et al., 2011; Cho et al., 2014). Indeed, alterations in spontaneous release rate through changes in Cpx activity can regulate structural and functional synaptic plasticity (Huntwork and Littleton, 2007; Choi et al., 2014; Cho et al., 2015; Mahoney et al., 2016; Robinson et al., 2018; Banerjee et al., 2021; Astacio et al., 2022). The Cpx C-terminus has emerged as a key site for such regulatory control, as it encodes a conserved amphipathic helix that functions as a membrane curvature sensor to localize Cpx to SVs and concentrate its activity at release sites (Lottermoser and Dittman, 2023).

In *Drosophila,* a single *cpx* gene produces two isoforms with different C-termini due to alternative splicing of exon 7 (Buhl et al., 2013). The Cpx7A isoform has a conserved membrane-tethering prenylation CAAX box, while Cpx7B lacks this motif (Cho et al., 2010). Prior studies demonstrated Cpx7B is regulated by PKA phosphorylation of a C-terminal serine (S126) within this alternatively spliced region. PKA phosphorylation of Cpx7B reduces its clamping function at neuromuscular junctions (NMJs), leading to elevated spontaneous release that triggers activity-induced structural plasticity (Cho et al. 2015). The Cpx7A isoform lacks this serine and instead undergoes RNA editing by ADAR (adenosine deaminase acting on RNA) to generate multiple Cpx7A proteins with unique C-terminal sequences. A-to-I editing recodes pre-spliced mRNAs by deaminating target adenosines in double-stranded RNA structures induced from exon-intron complementary pairing, causing the resulting inosine base to be read as guanosine by the translation machinery (Nishikura, 2016). RNA editing of Cpx7A can change an asparagine (N130) to a glycine (N130G), aspartate (N130D), or serine (N130S) at a site near the phosphorylated S126 residue in Cpx7B (Hoopengardner et al., 2003; Buhl et al., 2013). Given Cpx7A is expressed at

higher levels and is the dominant isoform in the *Drosophila* nervous system (Buhl et al., 2013), RNA editing at this site represents an attractive mechanism for regulating spontaneous release and structural plasticity across a larger population of neurons.

Here we used CRISPR and transgenic rescue to assay the role of Cpx splicing and RNA editing in neurotransmitter release. Although Cpx7A is expressed at higher levels, the two isoforms are largely redundant in their ability to support baseline synaptic transmission. In addition, analysis of single-cell RNAseq data from individual motoneurons reveals multiple Cpx7A RNA editing variants can be simultaneously expressed, indicating RNA editing does not act in an "all-or-none" fashion as previously hypothesized. The most prominent edit variant ($Cpx7A^{I125M,N130S}$) can be phosphorylated by casein kinase 2 (CK2). Transgenic rescue of *cpx* null mutants with $Cpx7A^{I125M,N130S}$ demonstrates RNA editing alters the protein's subcellular localization and reduces its ability to clamp spontaneous SV fusion, leading to synaptic overgrowth. Rescue with both $Cpx7A^{I125M,N130S}$ and unedited Cpx7A indicates the N130S variant acts in a dominant fashion, consistent with a model where Cpxs engage multiple assembling SNARE complexes during SV fusion (Radhakrishnan et al., 2021). Such a mechanism would allow edited and unedited Cpx proteins to assert independent effects in a combinatorial fashion to control SV fusion dynamics. Together, these data indicate stochastic RNA editing of the Cpx7A C-terminus can set distinct spontaneous release rates in individual *Drosophila* neurons to control presynaptic output.

2.2 Materials and Methods

Drosophila stocks

Flies were cultured on standard medium and maintained at 25 °C. Late 3rd instar larvae were used for imaging and electrophysiological experiments. Western blots were performed on adult brain extracts. Males were used for experiments unless otherwise noted. Experiments were performed in a w^{1118} (Bloomington *Drosophila* Stock Center #3605) genetic background unless otherwise noted.

Transgenic constructs

QuikChange Lightning (Agilent) was used for site-directed mutagenesis on unedited Cpx7A to generate specified *Cpx* edit variants that were subcloned into modified pValum construct, as previously described (Cho et al., 2015). The resulting constructs were injected into a yv;;attP 3rd

chromosome docking strain by BestGene Inc. (Chino Hills, CA, USA). UAS lines were recombined into the cpx^{SH1} null mutant background and $elav^{C155}$-GAL4 (BDSC #8765) was used for pan-neuronal expression of transgenes.

Generation of CRISPR-modified Cpx strains

Two endogenous *Cpx* truncation lines were generated ($cpx^{\Delta 7A}$ and $cpx^{\Delta 7B}$) using a CRISPR genome engineering approach. Four guide RNAs (gRNAs) flanking the splice acceptor site of exon 7A or 7B were selected using the CRISPR Optimal Target Finder (Gratz et al., 2014). gRNAs were cloned into the pCFD5 expression vector (Addgene #73914) (Port and Bullock, 2016) and donor constructs were generated to encode a floxed P3>DsRed reporter cassette (Addgene #51434) in the reverse orientation flanked with one kb homology arms upstream and downstream of the splice acceptor site of either exon 7A or 7B by Gibson assembly protocol using NEBuilder HighFidelity DNA Assembly Cloning Kit (E5520). An early stop codon was inserted between homology arms for each respective exon construct, with several amino acid coding sequences maintained to preserve proper exon splicing. gRNA binding sites of donor template were mutated using silent mutations that did not alter amino acid sequence. Template and gRNA plasmids were co-injected into *vasa*-Cas9 embryos (BDSC #56552) by BestGene Inc (Chino Hills, CA, USA) and Ds>Red positive transformants were selected by BestGene Inc (Chino Hills, CA, USA). The modified locus with stop codons inserted into exon 7A or 7B were confirmed by sequencing.

Locomotion analysis

Adult geotaxis was measured in adult male flies aged 2-3 days as previously described (Ali et al., 2011). Briefly, eight cohorts of ten adult males (80 total flies) per genotype were separated after eclosion and allowed to recover from CO_2 for 24 hours on standard fly medium. After 24 hours, each cohort was moved to a chamber made from two clear plastic vials taped together, with a line drawn around the lower vial 8 cm from the bottom. Each cohort was allowed to acclimate in the chamber for five minutes before assays began. Negative geotaxis was measured as percent of the cohort that crossed the 8 cm line within ten seconds after being tapped to the bottom of the chamber. Each cohort was subjected to ten rounds of negative geotaxis assay, with a one-minute rest period between each. The percent of flies that crossed the 8 cm line after each round was averaged to produce a pass rate per cohort.

Larval crawling was assayed in 3rd instar larvae of both sexes, as previously described (Nichols et al., 2012; Kashima et al., 2017). Larvae were briefly washed in room-temperature water before placing onto the center of a 5 cm petri dish containing 2% agarose, with five animals from a single genotype placed together (n = 10 larvae per genotype). The petri dish was placed over a grid and velocity was measured as average distance (in mm) traveled during the first 30 seconds following placement.

Immunohistochemistry

Larvae were dissected in hemolymph-like HL3.1 solution (in mM: 70 NaCl, 5 KCl, 4 $MgCl_2$, 10 NaHCO3, 5 trehalose, 115 sucrose, 5 HEPES, pH 7.18) and fixed in 4% paraformaldehyde for 18 minutes. Larvae were washed three times for five minutes with PBST (PBS containing 0.1% Triton X-100), followed by a thirty-minute incubation in block solution (5% NGS in PBST). Fresh block solution and primary antibodies were then added. Samples were incubated overnight at 4°C and washed with two short washes and three extended 20 minutes washed in PBST. PBST was replaced with block solution and fluorophore-conjugated secondary antibodies were added. Samples were incubated at room temperature for two hours. Finally, larvae were rewashed with PBST and mounted in Vectashield (Vector Laboratories, Burlingame, CA). Antibodies used for this study include: mouse anti-Brp, 1:500 (NC82; Developmental Studies Hybridoma Bank (DSHB), Iowa City, IA)); rabbit anti-Cpx, 1:5000 (Huntwork and Littleton, 2007); goat anti-rabbit Alexa Fluor 488, 1:500 (A-11008; ThermoFisher Scientific, Waltham, MA, USA); goat anti-mouse Alexa Fluor 546, 1:500 (A-11030; ThermoFisher); DyLight 649 conjugated anti-HRP, 1:500 (#123-605-021; Jackson Immuno Research, West Grove, PA, USA).

Confocal imaging and imaging data analysis

Imaging was performed on a Zeiss Pascal confocal microscope (Carl Zeiss Microscopy, Jena, Germany) using a 63X 1.3 NA oil-immersion objective (Carl Zeiss Microscopy). Images were processed with the Zen (Zeiss) software. A 3D image stack was acquired for each NMJ imaged (muscle 4 Ib NMJ of abdominal segment A3) and merged into a single plane for 2D analysis using FIJI image analysis software (Schindelin et al., 2012). No more than two NMJs were analyzed per larva. Anti-HRP labeling was used to identify neuronal anatomy (axons and NMJs) and quantify synaptic bouton number and NMJ area. Brp puncta quantification was used to measure AZ

number. Muscle 4 area was used to normalize quantifications for muscle surface area. For Cpx fluorescence quantification, the HRP-positive area was used to outline NMJs and axons. Total Cpx fluorescent intensity was measured in the outlined area, with background fluorescence of mean pixel intensity of non-HRP areas subtracted. For NMJ/axon ratios, background subtracted mean NMJ Cpx fluorescence was compared to background subtracted mean axon Cpx fluorescence within the same image.

Two-electrode voltage-clamp electrophysiology

Postsynaptic currents were recorded from 3rd instar muscle 6 at segment A3 using two-electrode voltage clamp with a -80 mV holding potential. Experiments were performed in room temperature HL3.1 saline solution (in mM, 70 NaCl, 5 KCl, 10 NaHCO3, 4 MgCl2, 5 trehalose, 115 sucrose, 5 HEPES, pH 7.2). Final [Ca^{2+}] was adjusted to 2 mM unless otherwise noted. Motor axon bundles were cut and suctioned into a glass electrode and action potentials were stimulated at 0.5 Hz (unless indicated) using a programmable stimulator (Master8, AMPI; Jerusalem, Israel). Data acquisition and analysis was performed using Axoscope 10.0 and Clampfit 10.0 software (Molecular Devices, Sunnyvale, CA, USA) and inward currents were labeled on a reverse axis for clarity.

Western blot analysis

Western blotting of adult head lysates (three heads per sample with one head loaded per lane) was performed using standard laboratory procedures with mouse anti-Tubulin (T5168; Sigma) at 1:10000 (UAS rescue experiments) or 1:1000000 (CRISPR experiments) and rabbit anti-Cpx at 1:5000. IRDye 680LT-conjugated goat anti-mouse, 1:5000 (926–68020; LICOR) and IRDye 800CW conjugated goat anti-rabbit, 1:5000 (926-32211; LICOR) were used as secondary antibodies. Blocking was performed in a solution containing four parts TBS (10 mM Tris Base pH 7.5, 150 mM NaCl) to one part Blocking Buffer (Rockland) for one hour. Antibody incubations were performed in a solution containing four parts TBST (1X TBS with 1% Tween-20) to one part Blocking Buffer. A LI-COR Odyssey Imaging System (LI-COR Biosciences, Lincoln, MA, USA) was used for visualization and analysis was performed using FIJI image analysis software. Relative Cpx expression was calculated by normalizing to Tubulin intensity.

Purification of Complexin for in vitro phosphorylation assays

QuikChange Lightning (Agilent) was used for site-directed mutagenesis of unedited Cpx7A to generate Cpx7A^{I125M,N130S} (termed N130S). Recombinant Cpx fused with GST was expressed in E. coli (BL21) and purified using glutathione sepharose 4B (Fisher Scientific). Peak fractions were concentrated and further purified by gel filtration as previously described (Cho et al., 2015). *In vitro* kinase assays were performed using purified recombinant Cpx proteins and the catalytic subunit of CK2 (C70-10G, SignalChem). Briefly, 10 mg of purified GST-fusion protein (unedited Cpx$^{I125,\ N130}$ or edited Cpx^{I125M,N130S}) was used per reaction and incubated with 2,500 units of recombinant kinase and [^{32}P]ATP (Perkin Elmer). Reaction products were separated by SDS-PAGE and gels were stained with Bio-Safe Coomassie Blue (Bio-Rad), dried, and exposed to autoradiography film at room temperature. Mean integrated density of each band was quantified using FIJI and relative density of phospho-Cpx (pCpx) was calculated by normalizing to input band intensity determined by Coomassie staining.

RNAseq analysis of RNA editing

RNAseq data from 105 single MN1-Ib and 101 single MNISN-Is 3rd instar larval motoneurons obtained using isoform Patchseq protocols (Jetti et al., 2023) were analyzed using the Integrative Genomics Viewer (IGV) (Robinson et al., 2011). To create single-cell Cpx RNA editing expression profiles, single RNA reads were analyzed for Cpx and included in the analysis if all three C-terminal Cpx7A edited bases were represented on a continuous single read. The percent of each Cpx7A edit variant was determined by the number of edited variant reads divided by total RNA reads for each cell, creating an RNA editing profile for each neuron. To compare single base editing across different genes, the edit percent at each base of interest was analyzed and compared to known edits in other genes within the same neurons. Neurons were excluded if each base of interest did not contain ten or more reads for all edits of interest.

Experimental design and statistical analysis

Statistical analysis and plot generation was performed using GraphPad Prism (San Diego, CA, USA). Appropriate sample size was determined using a normality test. Statistical significance for comparisons of two groups was determined by a Student's t-test. For comparisons of three or more groups of data, a one-way ANOVA followed by Tukey's Multiple Comparisons test was used to

determine significance. For **Figure 3B** and **6B**, cpx^{SH1} was excluded from one-way ANOVA as sample mean fell outside of normal data distribution due to the extreme elevation of mini frequency in the null background. For comparisons of two factors with three or more groups of data, as described in **Figure 4A, G**, a two-way ANOVA was used. The mean of each distribution is plotted in figures with individual datapoints also shown. Figure legends report mean ± SEM, and *n*. Asterisks indicate the following *p*-values: *, $p<0.05$; **, $p<0.01$; ***, $p<0.001$; ****, $p<0.0001$, with ns = not significant. For **Figure 4C-D**, a line of best-fit was generated with 95% confidence intervals displayed.

Statistical comparison of western blot in Figure 2A: Control (2.058 ± 0.1262, $n = 6$ lanes with one adult head per lane); $cpx^{\Delta 7A}$ (0.2739 ± 0.04859, $n = 6$ lanes with one adult head per lane, $p < 0.0001$ to control, $p < 0.0001$ to $cpx^{\Delta 7B}$, $p = 0.4891$ to cpx^{SH1}); $cpx^{\Delta 7B}$ (1.843 ± 0.2206, $n = 6$ lanes with one adult head per lane, $p = 0.6336$ to control, $p < 0.0001$ to cpx^{SH1}); cpx^{SH1} (0.02579 ± 0.00759, $n = 7$ lanes with one adult head per lane, $p < 0.0001$ to control).

Statistical comparison of Cpx fluorescence in Figure 2C: Control (75.61 ± 8.392, $n = 15$ NMJs); cpx^{SH1} (0.843 ± 0.158, $n = 15$, $p < 0.0001$ to control); $cpx^{\Delta 7A}$ (11.21 ± 1.776, $n = 18$, $p < 0.0001$ to control, $p < 0.0001$ to $cpx^{\Delta 7B}$, $p = 0.735$ to cpx^{SH1}); $cpx^{\Delta 7B}$ (87.48 ± 11.96, $n = 16$, $p = 0.6648$ to control, $p < 0.0001$ to cpx^{SH1}).

Statistical comparisons of adult climbing behavior in Figure 2D: Control (50.38 ± 8.309% pass rate, $n = 8$ cohorts of ten flies); $cpx^{\Delta 7A}$ (0 ± 0% pass rate, $n = 8$ cohorts of ten flies, $p < 0.0001$ to control); $cpx^{\Delta 7B}$ (79 ± 5.467% pass rate, $n = 8$ cohorts of ten flies, $p = 0.0055$ to control, $p < 0.0001$ to $cpx^{\Delta 7A}$).

Statistical comparison of larval crawling behavior in Figure 2E: Control (0.6667 ± 0.03333 mm/sec, $n = 10$ larvae); cpx^{SH1} (0.03333 ± 0.01843 mm/sec, $n = 10$ larvae, $p < 0.0001$ to control); $cpx^{\Delta 7A}$ (0.05 ± 0.02833 mm/sec, $n = 10$ larvae, $p < 0.0001$ to control, $p = 0.0066$ to $cpx^{\Delta 7B}$, $p = 0.9975$ to cpx^{SH1}); $cpx^{\Delta 7B}$ (0.3583 ± 0.05833 mm/sec, $n = 10$ larvae, $p = 0.0066$ to control, $p = 0.0039$ to cpx^{SH1}).

Statistical comparison of AZ number in Figure 2F. Control (0.00449 ± 0.00021 AZ per μm^2, $n = 15$ NMJs); cpx^{SH1} (0.00739 ± 0.00029 AZ per μm^2, $n = 15$ NMJs, $p < 0.0001$ to control); $cpx^{\Delta 7A}$ (0.00522 ± 0.0003 AZ per μm^2, $n = 17$ NMJs, $p = 0.2782$ to control, $p > 0.9999$ to $cpx^{\Delta 7B}$, $p <$

0.0001 to cpx^{SH1}); $cpx^{\Delta 7B}$ (0.00524 ± 0.00032 AZ per μm^2, n = 16 NMJs, p = 0.2758 to control, p < 0.0001 to cpx^{SH1}).

Statistical comparison of bouton number in Figure 2G. Control (0.000377 ± 0.00002355 bouton per μm^2, n = 15 NMJs); cpx^{SH1} (0.000648 ± 0.00005418 bouton per μm^2, n = 15 NMJs, p < 0.0001 to control); $cpx^{\Delta 7A}$ (0.000439 ± 0.00002827 bouton per μm^2, n = 17 NMJs, p = 0.6134 to control, p = 0.9935 to $cpx^{\Delta 7B}$, p = 0.0007 to cpx^{SH1}); $cpx^{\Delta 7B}$ (0.000426 ± 0.00003257 bouton per μm^2, n = 16 NMJs, p = 0.7769 to control, p = 0.0003 to cpx^{SH1}).

Statistical comparisons of mini frequency in Figure 3B: Control (1.646 ± 0.07273 Hz, n = 14 NMJs); cpx^{SH1} (91.66 ± 2.704 Hz, n = 14 NMJs); $cpx^{\Delta 7A}$ (3.311 ± 0.2155 Hz, n = 14 NMJs, p < 0.0001 to control); $cpx^{\Delta 7B}$ (1.431 ± 0.07724 Hz, n = 14 NMJs, p = 0.5208 to control, p < 0.0001 to $cpx^{\Delta 7A}$).

Statistical comparisons of evoked peak amplitude in Figure 3D: Control (232.7 ± 13.6 nA, n = 14 NMJs); cpx^{SH1} (67.8 ± 9.1 nA, n = 14 NMJs, p < 0.0001 to control); $cpx^{\Delta 7A}$ (125.5 ± 14.5 nA, n = 15 NMJs, p < 0.0001 to control, p = 0.0273 to cpx^{SH1}); $cpx^{\Delta 7B}$ (175.8 ± 16.5 nA, n = 16 NMJs, p = 0.0269 to control, p < 0.0001 to cpx^{SH1}, p = 0.0554 to $cpx^{\Delta 7A}$).

Statistical comparisons of evoked release charge area in Figure 3E: Control (2575.9 ± 129.0 nA×ms, n = 14 NMJs); cpx^{SH1} (1088.95 ± 144.3 nA×ms, n = 14 NMJs, p < 0.0001 to control); $cpx^{\Delta 7A}$ (1164.7 ± 132.5 nA×ms, n = 15 NMJs, p < 0.0001 to control, p = 0.9860 to cpx^{SH1}); $cpx^{\Delta 7B}$ (1986.8 ± 192.8 nA×ms, n = 16 NMJs, p = 0.0433 to control, p = 0.0007 to cpx^{SH1}, p = 0.0017 to $cpx^{\Delta 7A}$).

Statistical comparisons of evoked half-width in Figure 3I: Control (10.4 ± 0.4 ms, n = 14 NMJs); cpx^{SH1} (12.6 ± 0.4 ms, n = 14 NMJs, p = 0.0001 to control); $cpx^{\Delta 7A}$ (8.7 ± 0.4 ms, n = 15 NMJs, p = 0.0069 to control, p < 0.0001 to cpx^{SH1}); $cpx^{\Delta 7B}$ (10.4 ± 0.3 ms, n = 16 NMJs, p = 0.9999 to control, p = 0.0001 to cpx^{SH1}, p = 0.0040 to $cpx^{\Delta 7A}$).

Statistical comparisons of Cpx edit variant expression in Figure 4A: Unedited Ib (53.08 ± 2.496 edit % per cell, n = 95 cells); unedited Is (52.75 ± 2.592 edits per cell, n = 86 cells); I125M Ib (31.73 ± 2.395 edit % per cell, n = 95 cells, p < 0.0001 to unedited Ib); I125M Is (30.27 ± 2.408 edit % cell, n = 86 cells, p < 0.0001 to unedited Is); N130D Ib (0 ± 0 edit % per cell, n = 95 cells, p > 0.9999 to N130S Ib, p = 0.9986 to N130S Is, p > 0.9999 to N130G Ib, p > 0.9999 to N130G Is, p > 0.9999 to I125M, N130D Ib, p > 0.9999 to I125M, N130D Is, p = 0.0001 to I125M, N130S Ib, p = 0.0002 to I125M, N130S Is, p = 0.8706 to I125M, N130G Ib, p = 0.7014 to I125M, N130G

Is); N130D Is (0.109 ± 0.109 edit % per cell, n = 86 cells, p > 0.9999 to N130S Ib, p = 0.9994 to N130S Is, p > 0.9999 to N130G Ib, p > 0.9999 to N130G Is, p > 0.9999 to I125M, N130D Ib, p > 0.9999 to I125M, N130D Is, p = 0.0003 to I125M, N130S Ib, p = 0.0004 to I125M, N130S Is, p = 0.9134 to I125M, N130G Ib, p = 0.7729 to I125M, N130G Is); N130S Ib (1.470 ± 0.509 edit % per cell, n = 95 cells, p > 0.9999 to N130G Ib, p > 0.9999 to N130G Is, p > 0.9999 to I125M, N130D Ib, p > 0.9999 to I125M, N130D Is, p = 0.0035 to I125M, N130S Ib, p = 0.0046 to I125M, N130S Is, p = 0.999 to I125M, N130G Ib, p = 0.9873 to I125M, N130G Is); N130S Is (2.339 ± 0.685 edit % per cell, n = 86 cells, p = 0.9997 to N130G Ib, p > 0.9999 to N130G Is, p = 0.9995 to I125M, N130D Ib, p = 0.9995 to I125M, N130D Is, p = 0.0276 to I125M, N130S Ib, p = 0.0324 to I125M, N130S Is, p > 0.9999 to I125M, N130G Ib, p = 0.9998 to I125M, N130G Is); N130G Ib (0.316 ± 0.139 edit % per cell, n = 95 cells, p > 0.9999 to I125M, N130D Ib, p > 0.9999 to I125M, N130D Is, p = 0.0002 to I125M, N130S Ib, p = 0.0004 to I125M, N130S Is, p = 0.9336 to I125M, N130G Ib, p = 0.8057 to I125M, N130G Is); N130G Is (0.464 ± 0.186 edit % per cell, n = 86 cells, p > 0.9999 to I125M, N130D Ib, p > 0.9999 to I125M, N130D Is, p = 0.0006 to I125M, N130S Ib, p = 0.0008 to I125M, N130S Is, p = 0.963 to I125M, N130G Ib, p = 0.87 to I125M, N130G Is); I125M, N130D Ib (0.209 ± 0.117 edit % cell, n = 95 cells, p = 0.0002 to I125M, N130S Ib, p = 0.0003 to I125M, N130S Is, p = 0.9153 to I125M, N130G Ib, p = 0.7726 to I125M, N130G Is); I125M, N130D Is (0.152 ± 0.079 edit % per cell, n = 86 cells, p = 0.0003 to I125M, N130S Ib, p = 0.0004 to I125M, N130S Is, p = 0.9211 to I125M, N130G Ib, p = 0.7864 to I125M, N130G Is); I125M, N130S Ib (9.496 ± 1.490 edit % per cell, n = 95 cells, p = 0.1674 to I125M, N130G Ib, p = 0.3992 to I125M, N130G Is); I125M, N130S Is (9.574 ± 1.340 edit % per cell, n = 86 cells, p = 0.1831 to I125M, N130G Ib, p = 0.4163 to I125M, N130G Is); I125M, N130G Ib (3.691 ± 1.100 edit % per cell, n = 95 cells); I125M, N130G Is (4.346 ± 0.834 edits per cell, n = 86 cells). p > 0.9999 for all Ib to Is comparisons between same edit variant. p < 0.0001 for all comparisons between different edit variants unless otherwise noted.

Statistics for Cpx I125M Ib editing percent in Figure 4C: 44.91 ± 2.435 I125M editing % per cell, 1.628 ADAR TPM ± 0.189 per cell, n = 95 cells.

Statistics for Cpx I125M Is editing percent in Figure 4D: 44.55 ± 2.582 I125M editing % per cell, 2.203 ± 0.217 per cell, n = 86 cells.

Statistical comparisons of editing of various synaptic genes in Figure 4E: Syn N15D Ib (6.061 ± 6.061 editing % per cell, n = 9 cells); Syn N15D Is (0.925 ± 0.680 editing % per cell, n = 11 cells,

$p = 0.741$ to Syn N15D Ib); Syn R19G Ib (0 ± 0 editing % per cell, $n = 9$ cells); Syn R19G Is (0 ± 0 editing % per cell, $n = 11$ cells); Syn R20G Ib (34.57 ± 9.346 editing % per cell, $n = 9$ cells); Syn R20G Is (54.53 ± 11.56 editing % per cell, $n = 11$ cells, $p = 0.610$ to Syn R20G Ib); Cpx I125M Ib (40.67 ± 7.155 editing % per cell, $n = 9$ cells); Cpx I125M Is (39.64 ± 7.388 editing % per cell, $n = 11$ cells, $p = 0.922$ to Cpx I125M Ib); SyxIA M244V Ib (8.804 ± 3.799 editing % per cell, $n = 9$ cells); Syx1A M244V Is (5.418 ± 3.808 editing % per cell, $n = 11$ cells, $p = 0.790$ to Syx1A Ib).

Statistical comparisons of phosphorylation assay in 4G: Unedited, CK2 present (0.216 ± 0.088, $n = 4$ lanes with one *in vitro* reaction per lane, $p = 0.9554$ to unedited CK2 absent, $p = 0.0007$ to I125M, N130S CK2 present, $p = 0.9513$ to I125M, N130S CK2 absent); unedited, CK2 absent (0.0327 ± 0.007, $n = 4$ lanes with one *in vitro* reaction per lane, $p = 0.0003$ to I125M, N130S CK2 present, $p > 0.9999$ to I125M, N130S CK2 absent); I125M, N130S, CK2 present (2.187 ± 0.502, $n = 4$ lanes with one *in vitro* reaction per lane, $p = 0.0003$ to I125M, N130S CK2 absent); I125M, N130S, CK2 absent (0.027 ± 0.004, $n = 4$ lanes with one *in vitro* reaction per lane).

Statistical comparisons of western blot in Figure 5B: Control (0.1373 ± 0.0103, $n = 6$ lanes with one adult head per lane); cpx^{SH1} (0.02235 ± 0.0016, $n = 6$ lanes with one adult head per lane, $p = 0.5799$ to control); Unedited (1.523 ± 0.0515, $n = 6$ lanes with one adult head per lane, $p < 0.0001$ to control, $p < 0.0001$ to cpx^{SH1}); I125M, N130S (1.434 ± 0.0755, $n = 6$ lanes with one adult head per lane, $p < 0.0001$ to control, $p < 0.0001$ to cpx^{SH1}, $p = 0.774$ to unedited); I125M, N130D (1.557 ± 0.0805, $n = 6$ lanes with one adult head per lane, $p < 0.0001$ to control, $p < 0.0001$ to cpx^{SH1}, $p = 0.9914$ to unedited, $p = 0.5093$ to I125M, N130S).

Statistical comparisons of Cpx fluorescence in Figure 5D: Control (471.6 ± 43.64, $n = 15$ NMJs); cpx^{SH1} (13.74 ± 1.549, $n = 14$ NMJs, $p = 0.6567$ to control); Unedited (3221 ± 331.9, $n = 13$ NMJs, $p < 0.0001$ to control, $p < 0.0001$ to cpx^{SH1}); I125M, N130S (4144 ± 381.1, $n = 14$ NMJs, $p < 0.0001$ to control, $p < 0.0001$ to cpx^{SH1}, $p = 0.0754$ to unedited); I125M, N130D (3369 ± 244.7, $n = 12$ NMJs, $p < 0.0001$ to control, $p < 0.0001$ to cpx^{SH1}, $p = 0.9942$ to unedited, $p = 0.204$ to I125M, N130S).

Statistical comparisons of Cpx NMJ/axon fluorescence ratio in Figure 5F: Control (3.599 ± 0.312, $n = 13$ NMJs); Unedited (4.686 ± 0.313, $n = 10$ NMJs, $p = 0.0174$ to control); I125M, N130S (1.159 ± 0.09367, $n = 12$ NMJs, $p < 0.0001$ to control, $p < 0.0001$ to unedited); I125M, N130D

(2.035 ± 0.1903, n = 10 NMJs, p = 0.0003 to control, p < 0.0001 to unedited, p = 0.0821 to I125M, N130S).

Statistical comparisons of AZ number in Figure 5G: Control (0.006005 ± 0.000478 AZ per μm^2, n = 15 NMJs); *cpx*^{SH1} (0.01154 ± 0.000667 AZ per μm^2, n = 14 NMJs, p < 0.0001 to control); Unedited (0.009379 ± 0.000549 AZ per μm^2, n = 13 NMJs, p = 0.0013 to control, p = 0.092 to *cpx*^{SH1}); I125M, N130S (0.01067 ± 0.000566 AZ per μm^2, n = 14 NMJs, p < 0.0001 to control, p = 0.8301 to *cpx*^{SH1}, p = 0.5533 to unedited); I125M, N130D (0.007566 ± 0.000735 AZ per μm^2, n = 12 NMJs, p = 0.3658 to control, p = 0.0002 to *cpx*^{SH1}, p = 0.2518 to unedited, p = 0.0058 to I125M, N130S).

Statistical comparisons of bouton number in Figure 5H: Control (0.0005208 ± 0.00003491 bouton per μm^2, n = 15 NMJs); *cpx*^{SH1} (0.001149 ± 0.00007811 bouton per μm^2, n = 14 NMJs, p < 0.0001 to control); Unedited (0.0008424 ± 0.00003883 bouton per μm^2, n = 13 NMJs, p = 0.0001 to control, p = 0.0004 to *cpx*^{SH1}); I125M, N130S (0.000964 ± 0.00003329 bouton per μm^2, n = 14 NMJs, p < 0.0001 to control, p = 0.0638 to *cpx*^{SH1}, p = 0.4127 to unedited); I125M, N130D (0.0006363 ± 0.00004369 bouton per μm^2, n = 12 NMJs, p = 0.4709 to control, p < 0.0001 to *cpx*^{SH1}, p = 0.0451 to unedited, p = 0.0002 to I125M, N130S).

Statistical comparisons of mini frequency in Figure 6B: Control (3.78 ± 0.26 Hz, n = 17 NMJs); cpx^{SH1} (102.25 ± 2.08 Hz, n = 15 NMJs); Unedited (12.67 ± 1.96 Hz, n = 16 NMJs, p = 0.1121 to control); I125M, N130S (47.29 ± 5.07 Hz, n = 17 NMJs, p < 0.0001 to control, p < 0.0001 to unedited); I125M, N130D (3.88 ± 0.41 Hz, n = 18 NMJs, p > 0.9999 to control, p = 0.1107 to unedited, p < 0.0001 to I125M, N130S).

Statistical comparisons of evoked peak amplitude in Figure 6D: Control (298.13 ± 19.37 nA, n = 15 NMJs); *cpx*^{SH1} (96.40 ± 5.99 nA, n = 15 NMJs, p < 0.0001 to control); Unedited (172.36 ± 8.65 nA, n = 14 NMJs, p < 0.0001 to control, p = 0.0009 to *cpx*^{SH1}); I125M, N130S (212.23 ± 10.03 nA, n = 16 NMJs p < 0.0001 to control, p < 0.0001 to *cpx*^{SH1}, p = 0.1877 to unedited); I125M, N130D (221.05 ± 14.79 nA, n = 15 NMJs, p = 0.0005 to control, p < 0.0001 to *cpx*^{SH1}, p = 0.0709 to unedited, p = 0.9874 to I125M, N130S).

Statistical comparisons of evoked release charge area in Figure 6E: Control (2364.36 ± 184.8002 nA×ms, n = 15 NMJs); *cpx*^{SH1} (1264.597 ± 93.439 nA×ms, n = 15NMJs, p < 0.0001 to control); Unedited (1671.824 ± 127.3062 nA×ms, n = 14 NMJs, p = 0.0023 to control, p = 0.1687 to *cpx*^{SH1}); I125M, N130S (1841.926 ± 84.402 nA×ms, n = 16 NMJs p = 0.0294 to control, p = 0.0121 to

cpx^{SH1}, $p = 0.8717$ to unedited); I125M, N130D (1856.46 ± 113.832 nA×ms, $n = 15$ NMJs, $p = 0.0413$ to control, $p = 0.0111$ to *cpx*^{SH1}, $p = 0.8421$ to unedited, $p > 0.9999$ to I125M, N130S).

Statistical comparisons of evoked half-width in Figure 6F: Control (7.2622 ± 0.231 ms, $n = 15$ NMJs); *cpx*^{SH1} (10.257 ± 0.31576 ms, $n = 15$ NMJs, $p < 0.0001$ to control); Unedited (8.3626 ± 0.3471 ms, $n = 14$ NMJs, $p = 0.0505$ to control, $p < 0.0001$ to *cpx*^{SH1}); I125M, N130S (7.786 ± 0.2070 ms, $n = 16$ NMJs $p = 0.6449$ to control, $p < 0.0001$ to *cpx*^{SH1}, $p = 0.5734$ to unedited); I125M, N130D (7.8133 ± 0.2594 ms, $n = 15$ NMJs, $p = 0.6136$ to control, $p < 0.0001$ to *cpx*^{SH1}, $p = 0.6323$ to unedited, $p > 0.9999$ to I125M, N130S).

Statistical comparisons of mini frequency in Figure 6G: Unedited I125, N130 and N130S together (23.14 ± 4.51 Hz, n = 16 NMJs, p=0.0414 compared to unedited I125, N130 alone and p=0.0013 compared to Cpx7A^{I125M,N130S}. Student's t-test two-tailed comparison to mini frequency data from unedited Cpx7A or Cpx7A^{I125M,N130S} from 6B data above was used for this comparison.

Statistical comparisons of evoked peak amplitude in Figure 6H: Unedited I125, N130 and N130S together (212.23 ± 10.03 nA, $n = 16$ NMJs, p=0.0425 compared to unedited I125, N130 alone and p=0.4775 compared to Cpx7A^{I125M,N130S}. Student's t-test two-tailed comparison to evoked amplitude data from unedited Cpx7A or Cpx7A^{I125M,N130S} from 6D data above was used for this comparison.

2.3 Results

Alternative splicing and RNA editing of *Drosophila complexin* generate divergent C-terminal sequences within a conserved amphipathic helical domain

In contrast to four Cpx homologs in mammals, a single *cpx* gene is present in *Drosophila*. *Drosophila cpx* undergoes alternative splicing of exon 7 to generate two unique isoforms, Cpx7A and Cpx7B, that differ in their last ~20 amino acids (**Figure 1A, B**). Although the encoded exon 7 sequences are not similar at the amino acid level, the C-terminus of both splice isoforms is predicted to encode a membrane-binding amphipathic helix (**Figure 1B-D**) that is conserved across invertebrate and vertebrate Cpx homologs (Lottermoser and Dittman, 2023). Cpx7A is the more abundant isoform and contains a C-terminal CAAX box that undergoes prenylation (Buhl et al., 2013), a post-translational lipid attachment that helps localize this variant and mammalian CPX3 and CPX4 within synapses (Reim et al., 2005; Cho et al., 2010; Robinson et al., 2018). The less abundant Cpx7B lacks this prenylation motif, similar to mammalian CPX1 and CPX2. We

previously demonstrated the Cpx7B C-terminal domain can be phosphorylated by PKA at residue S126 in an activity-dependent manner, leading to a reduction in its clamping function that enhances spontaneous SV release and synaptic growth (Cho et al., 2015).

Given the regulatory role of Cpx7B phosphorylation, it is surprising the more abundant Cpx7A lacks this PKA phosphorylation site. Unlike Cpx7B, Cpx7A is subject to RNA editing via ADAR at three adenosine residues within the mRNA sequence of exon 7A (Hoopengardner et al., 2003; Buhl et al., 2013). One edit site generates a isoleucine (I) to methionine (M) conserved substitution at amino acid 125 that is not predicted to alter protein function, but induces mRNA conformational changes in exon-intron base pairing that facilitates editing of the two downstream adenosine residues (Buhl et al., 2013). At this downstream site, the unedited AAT codon encodes an asparagine (N) at amino acid 130. Editing of both residues (AAT to GGT) produces a glycine (N130G), while editing of only the 1st base (AAT to GAT) generates an aspartic acid (N130D) and editing of the 2nd base (AAT to AGT) produces a serine (N130S) (**Figure 1E**). Given RNA editing can generate a potentially phospho-competent Cpx7A^{N130S}, a phospho-mimetic Cpx7A^{N130D} and a phospho-incompetent Cpx7A^{N130G}, we assayed if RNA editing alters Cpx7A function. To begin this analysis, a structural comparison of Cpx7A and Cpx7B to their mammalian homologs was performed using AlphaFold (Jumper et al., 2021; Varadi et al., 2022). AlphaFold predictions indicate each Cpx homolog contains a conserved SNARE-binding central helix and a C-terminal helical domain (**Figure 1C**).

Given the C-terminal amphipathic helix allows Cpx to detect membrane curvature and bind SVs (Snead et al., 2014, 2017, Wragg et al., 2015, 2017; Gong et al., 2016), helical wheel models were generated with HELIQUEST (Gautier et al., 2008) to examine hydrophilic and hydrophobic faces of the helix in relation to the Cpx7A N130 editing site and the Cpx7B S126 PKA phosphorylation site (**Figure 1D**). Both splice isoforms have phospho-competent serine and/or threonine residues in similar positions on the hydrophilic face, including the Cpx7B S126 residue. Human and mouse CPXs also contain phospho-competent residues on this hydrophilic surface (**Figure 1D**), suggesting phosphorylation of this region may represent a conserved mechanism for modulating Cpx activity. The I125M edit resides on the hydrophobic face and does not alter the hydrophobic nature of this region (**Figure 1D, E**). In contrast, the Cpx7A N130S edit adds another phospho-competent residue to precisely match the paired S/T residues where Cpx7B S126 resides (**Figure 1E**). The N130D edit adds another negative charge to the hydrophilic face, generating a

helix with a negative charge at nearly every other amino acid on this surface. The N130G edit inserts a glycine residue that exactly matches glycine residues found at the same site in human and mouse CPX3, consistent with a functional impact for this editing event as well. We conclude that RNA editing alters the hydrophilic face of the Cpx7A C-terminal amphipathic helix to generate variants that more closely resemble Cpx7B or mammalian CPXs, suggesting RNA editing may alter the properties of the helix or its potential for phosphorylation.

Characterizing the functional significance of alternative splicing of Cpx exon 7

The role of alternative splicing on endogenous Cpx function is unknown. In *cpx* null mutants that lack both isoforms (cpx^{SH1}), spontaneous mini frequency is dramatically elevated (>50-fold), evoked release is decreased, and larval NMJ synaptic growth is enhanced (Huntwork and Littleton, 2007). Overexpression of either Cpx7A or Cpx7B in cpx^{SH1} partially rescues these phenotypes, with Cpx7A having more robust clamping properties and Cpx7B over-rescuing evoked release (Buhl et al., 2013). Although both variants support aspects of Cpx function when overexpressed, endogenous Cpx7A mRNA is 1000-fold more abundant than Cpx7B in *Drosophila* adults and larvae based on quantitative RT-PCR (Buhl et al., 2013). As such, Cpx7A is hypothesized to play a more critical role in synaptic transmission. To directly test the endogenous function of the two splicing isoforms, CRISPR mutants of 7A ($cpx^{\Delta 7A}$) or 7B ($cpx^{\Delta 7B}$) were generated by introducing an early stop codon at the beginning of exon 7A or 7B, respectively. Western analysis of adult head lysates with a Cpx antibody that recognizes both variants showed an 87% reduction in overall Cpx expression in $cpx^{\Delta 7A}$ ($p<0.0001$) and a milder 10% reduction in $cpx^{\Delta 7B}$ ($p=0.6336$), consistent with Cpx7A being the predominant isoform (**Figure 2A**). Immunostaining for Cpx at 3rd instar larval NMJs showed a similar effect (**Figure 2B, C**), with a >85% reduction in Cpx at synapses in $cpx^{\Delta 7A}$ mutants ($p<0.0001$) and no detectable decrease in $cpx^{\Delta 7B}$ mutants ($p=0.6648$).

To assay the functional requirement for the two splice variants *in vivo*, adult and larval motor behavior were examined in $cpx^{\Delta 7A}$ and $cpx^{\Delta 7B}$ and compared to control and cpx^{SH1} null mutants. Complete loss of Cpx in cpx^{SH1} severely disrupts behavior and reduces viability, with the few escaper adults that emerge from the pupal case displaying a profound loss of motor control and an inability to walk in a coordinated manner. Loss of the predominant Cpx7A isoform also strongly disrupted motor behavior, though not as severely as cpx^{SH1}. In contrast to cpx^{SH1} where

homozygous adults are rarely observed, $cpx^{\Delta 7A}$ could be maintained as a homozygous stock, indicating the remaining endogenous Cpx7B can improve viability and fertility compared to animals lacking both isoforms. However, in a negative geotaxis assay to quantify adult climbing behavior (**Figure 2D**), $cpx^{\Delta 7A}$ mutants showed a complete inability to climb. In contrast, $cpx^{\Delta 7B}$ adults were fully viable and did not display obvious motor defects. In addition, they were moderately hyperactive in climbing compared to controls (control: 50.4±8.3% pass rate, n=8 cohorts of ten flies; $cpx^{\Delta 7A}$: 0±0% pass rate, n=8 cohorts of ten flies, p<0.0001 to control; $cpx^{\Delta 7B}$: 79±5.5% pass rate, n=8 cohorts of ten flies, p=0.0055 to control, p<0.0001 to $cpx^{\Delta 7A}$). To examine larval locomotion, crawling velocity of 3rd instar larvae was assayed in a petri chamber in $cpx^{\Delta 7A}$ and $cpx^{\Delta 7B}$ mutants (**Figure 2E**). Similar to the severe defects observed in cpx^{SH1}, $cpx^{\Delta 7A}$ larvae displayed a dramatic reduction in crawling velocity (p<0.0001). In contrast, $cpx^{\Delta 7B}$ mutants showed a mild decrease in velocity (p=0.0066). Together, these data indicate Cpx7A has a more prominent role in supporting larval and adult behavior.

To examine synaptic morphology and neurotransmitter release in $cpx^{\Delta 7A}$ and $cpx^{\Delta 7B}$ mutants, the well-characterized 3rd instar larval glutamatergic NMJ preparation was used (Harris and Littleton, 2015). To assay NMJ morphology, synaptic bouton and active zone (AZ) number were quantified by immunostaining for neuronal membranes (anti-HRP) and the AZ protein Bruchpilot (Brp) (**Figure 2B, F, G**). In contrast to the large increase in bouton (72%) and AZ (65%) number in cpx^{SH1}, synaptic growth was largely unaffected in $cpx^{\Delta 7A}$ and $cpx^{\Delta 7B}$ mutants. Despite the differences in overall levels of the two splice isoforms at NMJs (**Figure 2B**), $cpx^{\Delta 7A}$ mutants had similar NMJ morphology to $cpx^{\Delta 7B}$. We conclude that Cpx7A and Cpx7B are functionally redundant in their ability to regulate synaptic growth, with Cpx7B having a more robust role than expected based on its lower expression level.

To assay synaptic function, two-electrode voltage-clamp (TEVC) was used to measure evoked and spontaneous neurotransmitter release at 3rd instar larval muscle 6 in abdominal segment A3. In contrast to the dramatic increase in spontaneous release rates observed in cpx^{SH1} (>55-fold compared to control), endogenously expressed Cpx7A or Cpx7B was able to substantially lower mini frequency (**Figure 3A, B**). The presence of only Cpx7A in the $cpx^{\Delta 7B}$ mutant returned spontaneous release rates to control levels (p=0.52). Residual Cpx7B in $cpx^{\Delta 7A}$ mutants was not able to fully clamp spontaneous fusion, displaying a 2-fold increase in mini frequency compared to controls (p<0.0001). In contrast to spontaneous release, the presence of

only one of the two splice isoforms was not as effective in driving normal levels of evoked fusion (**Figure 3C, D**). A 71% reduction in the peak amplitude of the evoked excitatory junctional current (eEJC) was observed in cpx^{SH1} compared to control ($p<0.0001$). Although less severe, $cpx^{\Delta 7A}$ displayed a 46% reduction ($p<0.0001$) and $cpx^{\Delta 7B}$ a 25% reduction ($p=0.0269$) compared to control. These data indicate Cpx7A and Cpx7B are both required to recapitulate evoked responses observed in controls, though the higher levels of Cpx7A in $cpx^{\Delta 7B}$ mutants supports more evoked fusion than the lower levels of Cpx7B in $cpx^{\Delta 7A}$.

In addition to the total number of SVs that fuse during an action potential, Cpx also modulates SV release kinetics by promoting fast synchronous fusion and reducing the slower asynchronous pathway (Jorquera et al., 2012). While peak eEJC amplitude primarily captures synchronous release, assays for eEJC charge, half-width, and timecourse of cumulative release provide kinetic insights into both synchronous and asynchronous fusion. As such, these evoked response variables were compared across control, $cpx^{\Delta 7A}$, $cpx^{\Delta 7B}$ and cpx^{SH1} NMJs (**Figure 3E-I**). Like eEJC amplitude, release kinetics in $cpx^{\Delta 7B}$ mutants were more similar to controls. Loss of Cpx7A in the $cpx^{\Delta 7A}$ line resulted in reduced charge transfer (**Figure 3E**) and a mild increase in asynchronous release (**Figure 3F, G**), though far less than the large amount of asynchronous fusion in *cpx* nulls. The onset of synchronous release was slightly enhanced in $cpx^{\Delta 7A}$ mutants (**Figure 3G, H**), consistent with prior data showing overexpression of Cpx7B enhanced the speed of onset of evoked fusion (Jorquera et al., 2012). In summary, we conclude the endogenous levels of either Cpx isoform is sufficient to can clamp spontaneous SV fusion. The requirement for both isoforms to fully recapitulate control evoked responses indicate they have some shared and independent roles for Ca^{2+}-dependent SV release. Given the severe behavioral defects observed in larvae and adults lacking Cpx7A, some neuronal subtypes are likely to be more highly reliant on this splice variant for supporting synaptic transmission, in contrast to motoneurons.

Single-cell RNAseq reveals stochastic RNA editing of Cpx7A in larval motoneurons

Having analyzed functions for the two C-terminal splice isoforms of Cpx, we next examined the profile of RNA editing for the Cpx7A transcript in larval motoneurons. Larval abdominal muscles are innervated by several populations of motoneurons in *Drosophila*, including tonic Type Ib and phasic Type Is glutamatergic subclasses (Johansen et al., 1989; Hoang and Chiba, 2001; Aponte-Santiago and Littleton, 2020). Type Ib and Is motoneurons are the major

drivers of muscle contraction and display unique morphological and functional properties (Lnenicka and Keshishian, 2000; Aponte-Santiago et al., 2020; Wang et al., 2020b; Han et al., 2022; Newman et al., 2022; Jetti et al., 2023). Given Ib and Is neurons have distinct presynaptic release output, we hypothesized RNA editing of Cpx7A could contribute to these differences if: (1) Cpx7A edit variants were differentially expressed between the two neuronal populations; and (2) editing of Cpx7A altered its function. To determine the abundance and diversity of Cpx7A edit variants (I125M, N130G, N130S, N130D), single-cell RNAseq datasets we previously generated from ~200 larval Ib and Is motoneurons were analyzed (Jetti et al., 2023). For these experiments, whole cell electrodes were used to collect cytosolic and nuclear content from individual Ib or Is neurons that expressed GFP via Gal4 drivers specific to each cell type (Aponte-Santiago et al., 2020). High-resolution paired-end deep single-cell RNA sequencing was performed on RNA extracted from each individual motoneuron, generating ~4 million reads per cell and allowing identification of RNA editing diversity at single neuron resolution. Prior studies using mRNA obtained from pooled neuronal populations proposed RNA editing occurs in an "all or none" fashion at individual edit sites within a cell. For example, more than 99% of mammalian AMPA GluA2 receptor subunit transcripts undergo RNA editing at specific times during brain development (Sommer et al., 1991; Higuchi et al., 1993). Given our method provides individual neuron resolution of RNA editing, we could directly test the "all or none" model. Strikingly, individual larval motoneurons showed highly stochastic RNA editing of the three adenosine bases (position 375, 388 and 389) that can be edited in exon 7A. Editing rates for these adenosines ranged from 0 to 100% across the ~200 neurons, with 98% of Ib cells and 94% of Is cells showing some level of exon 7A editing (**Figure 4A, B**). For the upstream I125 edit site at adenosine 375, 3% of Ib and 1% of Is neurons fully edited all Cpx mRNA to I125M (adenosine 375 to inosine 375). The average I125M transcript level per neuron was 31.7±2.4% in Ib (*n*=95 cells) and 30.3±2.4% in Is (*n*=86 cells). For all Cpx7A mRNA edit variants, the average Ib motoneuron expressed 53% unedited Cpx, 32% Cpx^{I125M}, 0.0% Cpx^{N130D}, 1.5% Cpx^{N130S}, 0.3% Cpx^{N130G}, 0.2% $Cpx^{I125M,N130D}$, 9.5% $Cpx^{I125M,N130S}$ and 3.7% $Cpx^{I125M,N130G}$ (**Figure 4A, B**). The average Is motoneuron expressed a similar ratio of edited Cpx7A transcripts (**Figure 4A, B**). As such, differential RNA editing of Cpx7A is unlikely to drive the distinct release properties of Ib and Is motoneurons, though stochastic editing of Cpx7A could contribute to individual neuron heterogeneity in

presynaptic output. We conclude that RNA editing of Cpx exon 7A is stochastic across individual edit sites and generates similar diversity of edited isoforms in Is and Ib motoneurons.

Prior studies proposed RNA editing at adenosine 375 serves to enhance exon-intron base pairing within 7A to generate a more favorable double-stranded RNA structure for ADAR to edit downstream adenosines 388 and 389 that form the AAT codon (N130) (Buhl et al., 2013). Consistent with this model, RNAseq data from single motoneurons showed editing for both I125 and N130 was far more common than single edits to N130 alone (**Figure 4A**). Ib neurons expressing $Cpx^{I125M,N130S}$ mRNA were six-fold more abundant that those expressing Cpx^{N130S} alone (I125M, N130S: 9.5±1.5 edit % per cell; N130S: 1.47±0.51 edit % per cell, p=0.0035). A similar ratio was observed in Is neurons (**Figure 4A, B**). In the 56% of Ib cells expressing $Cpx^{I125M,N130S}$ edited transcripts, an average of 17% of total *cpx* mRNA were of this variant, similar to the 16% of total *cpx* mRNA in the 59% of Is cells that expressed $Cpx7A^{I125M,N130S}$. Rarely, $Cpx^{I125M,N130S}$ represented the only Cpx mRNA detected within a neuron (**Figure 4A**). In contrast to the more abundant $Cpx^{I125M,N130S}$, only 6% of Ib neurons expressed $Cpx^{I125M,N130D}$ and it represented just 3% of the total *cpx* mRNA in these cells. The $Cpx^{I125M,N130G}$ variant, which requires A-to-I editing at all three adenosines, was observed in 40% of Ib neurons, representing 9% of total *cpx* mRNA in cells in which it was expressed. Similar patterns were observed in Is neurons (**Figure 4A, B**). For the most abundant edit variant (Cpx^{I125M}), no correlation of editing percentage at this site and expression levels of *adar* mRNA in that cell was observed for Ib or Is motoneurons (**Figure 4C, D**). We conclude that $Cpx^{I125M,N130S}$ is the highest expressed variant in larval motoneurons that alters the N130 residue on the amphipathic helix in Cpx7A.

To determine if RNA editing of other synaptic target genes showed similar stochastic single neuron editing, additional mRNAs known to undergo RNA editing were examined in the single neuron RNAseq dataset. RNA editing percentages at three sites (N15D, R19G, R20G) within Synapsin (Syn) and one site (M244V) in Syntaxin 1A (Syx1A) were compared in the same motoneurons that edited Cpx7A to I125M (**Figure 4E**). Both Syn and Syx1A displayed stochastic editing rates that ranged from 0-100% across motoneurons. For example, Syn R20G editing was observed at an average of 55±11.6% (n=11 Is cells), while Syx1A M244V was edited in the same neurons at a rate of only 5.4±3.8% per cell (n=11 Is cells). Similar to Cpx^{I125M}, no significant difference in editing percent was found when comparing the same edit site between Ib and Is neurons (**Figure 4E**). We conclude ADAR-mediated RNA editing is not an all-or-none process in

individual *Drosophila* motoneurons, with stochastic editing at single adenosine base sites and across multiple mRNAs having the potential to generate unique synaptic proteomes within the same population of neurons.

RNA editing of Cpx7A alters its subcellular localization and functional properties

Given Cpx7A^{I125M,N130S} is the most abundant editing variant on the hydrophilic face of the amphipathic C-terminal helix and resides near the Cpx7B S126 phosphorylation site, the functional significance of RNA editing to N130S or the potential phospho-mimetic version N130D was examined. Unlike Cpx7B, PKA did not phosphorylate unedited Cpx7A or Cpx7A^{I125M,N130S} in *in vitro* phosphorylation assays (data not shown). As such, N130S might represent a target for different kinases or instead alter structural properties of the amphipathic helix independent of phosphorylation. Computational analysis of candidate phosphorylation motifs in Cpx7A predict a casein kinase 2 (CK2) consensus sequence of S/T E/D at the N130S site that is found in some CK2 targets (Bulat et al., 2014). To determine if Cpx7A^{I125M,N130S} can be phosphorylated by CK2, *in vitro* phosphorylation assays were performed. Indeed, Cpx7A^{I125M,N130S} was phosphorylated by CK2 while unedited Cpx7A^{I125,N130} was not (**Figure 4F, G**), pinpointing N130S as a potential target for CK2 phosphorylation *in vivo*. Although it is unknown if CK2 phosphorylation alters Cpx7A^{I125M,N130S} function, it provides a potential regulatory mechanism downstream of RNA editing.

To examine if RNA editing alters Cpx function at synapses, transgenic UAS rescue lines expressing Cpx7A^{I125M,N130S}, Cpx7A^{I125M,N130D} or unedited Cpx7A were generated and expressed pan-neuronally using *elav^{C155}*-Gal4 in the *cpx^{SH1}* null that lacks both Cpx7A and Cpx7B. All three Cpx7A transgenic proteins were overexpressed at similar levels when assayed by western analysis of adult brain lysates (**Figure 5A, B**) or anti-Cpx immunostaining at larval muscle 4 NMJs (**Figure 5C, D**). Given N130S and N130D alter the hydrophilic face of the C-terminal amphipathic helix that facilitates SV membrane binding and Cpx localization (**Figure 1E**), Cpx subcellular distribution at the NMJ was assayed by immunostaining controls (*elav^{C155};; cpx^{PE}* (precise excision control for *cpx^{SH1}*)), *cpx* nulls (*elav^{C155};; cpx^{SH1}*) and the three rescue strains: (1) *elav^{C155};; cpx^{SH1}*, UAS-Cpx7A^{I125,N130}; (2) *elav^{C155};; cpx^{SH1}*, UAS-Cpx7A^{I125M,N130S}; (3) *elav^{C155};; cpx^{SH1}*, UAS-Cpx7A^{I125M,N130D}. Endogenous Cpx accumulates along the periphery of presynaptic boutons (**Figure 5E**), co-localizing with other SV protein markers (Buhl et al., 2013). Lower Cpx levels

are found in non-synaptic regions of the axon, resulting in a 3.6-fold synaptic enrichment (Cpx synapse/axon fluorescence ratio) at control NMJs (**Figure 5E, F**). Expression of unedited Cpx7A in the null background resulted in a shift to more Cpx enrichment at synapses, significantly increasing the synapse/axon ratio to 4.7 (**Figure 5E, F**, p=0.0174). Expression of Cpx7A^{I125M,N130S} or Cpx7A^{I125M,N130D} in the null background had the opposite effect, with a greater fraction of Cpx in non-synaptic regions of the axon (**Figure 5E, F**). Cpx7A^{I125M,N130D} was enriched 2-fold at synapses, decreasing ~44% compared to controls (p=0.0003) and ~57% compared to unedited Cpx7A (p<0.0001). Cpx7A^{I125M,N130S} had a more striking subcellular change, with a nearly one-to-one ratio of its abundance at synapses and along axons (1.16±0.09, p<0.0001 to control). Taken together, these data indicate the normal Cpx subcellular distribution in wildtype neurons likely represents a combinatorial expression of both unedited and edited Cpx proteins. Unedited Cpx7A is more strongly enriched at synapses, while the predominant splice variant altering the C-terminal amphipathic helix (Cpx7A^{I125M,N130S}) distributes equally between axons and synapses.

Given the observed changes to Cpx7A localization induced by RNA editing, structural and functional synaptic assays were performed in rescue lines. Quantification of synaptic bouton and AZ number revealed significant differences in the ability of different Cpx7A proteins to rescue synaptic overgrowth in *cpx*^{SH1} null larvae (**Figure 5G, H**). Cpx7A^{I125M,N130D} fully rescued the increased number of AZs (p=0.25, **Figure 5G**) and boutons (p=0.47, **Figure 5H**), returning synaptic morphology to control levels. In contrast, Cpx7A^{I125M,N130S} displayed the weakest rescue, with ~80% more AZs and boutons than controls (p<0.0001), slightly less than the doubling of AZ and bouton number observed in *cpx*^{SH1} (**Figure 5G, H**). Expression of unedited Cpx7A in the null background resulted in a partial rescue of the morphological defects. Electrophysiological analysis of spontaneous fusion rates revealed a similar pattern of rescue as observed for synaptic growth (**Figure 6A, B**), consistent with enhanced mini frequency being the primary driver for synaptic over-proliferation in *cpx* mutants. Like the full rescue of synaptic overgrowth, Cpx7A^{I125M,N130D} returned mini frequency to control levels (p=0.99). In contrast, Cpx7A^{I125M,N130S} expression failed to properly clamp spontaneous release, similar to its inability to rescue synaptic overgrowth. Compared to the 102 Hz mini frequency at *cpx*^{SH1} null NMJs, Cpx7A^{I125M,N130S} expression was able to reduce spontaneous fusion by only ~50% to 47 Hz. Rescue with unedited Cpx7A created a more effective fusion clamp, decreasing mini frequency to 13 Hz, although this rate was still ~3-fold higher than controls or the Cpx7A^{I125M,N130D} rescue. RNA editing of Cpx7A also impacted

evoked release, but the effects were less pronounced. Both unedited and edited Cpx7A rescue lines were able to improve eEJC amplitude and release kinetics over null mutants (**Figure 6C-F**). Similar to spontaneous release, Cpx7A^{I125M,N130D} showed the strongest rescue for evoked release. We conclude that RNA editing of Cpx7A regulates the functional properties of the protein, with N130D and N130S displaying several opposing effects compared to unedited Cpx7A. The N130D edit improved Cpx's ability to clamp spontaneous release while the N130S edit reduced the ability of the protein to act as a fusion clamp and failed to prevent synaptic overgrowth. Based on the distinct properties of N130S and N130D, it seems unlikely the primary effect of N130S would be downstream of phosphorylation, but instead reflect a change to the functional properties of the C-terminal amphipathic helix. Alternatively, the N130D change does not act as a phospho-mimetic in the case of Cpx, but rather alters the C-terminal helix in a distinct manner.

RNAseq analysis of single neuron editing demonstrated most motoneurons express a combination of edited Cpx7A proteins (**Figure 4A B**), with Cpx7A^{I125M,N130S} representing the most abundant edit to the N130 residue. To determine if co-expression of unedited Cpx7A with Cpx7A^{I125M,N130S}, as would be observed *in vivo*, drives competition for interactions with the fusion machinery to regulate release, the two proteins were co-expressed in the *cpx^{SH1}* null background. If unedited Cpx7A restored mini frequency to baseline rates, RNA editing would likely have effects on synaptic transmission only when neurons predominantly express the edited Cpx protein. Alternatively, if co-expression of Cpx7A^{I125M,N130S} increased mini frequency beyond unedited Cpx7A rescues alone, a combinatorial role for unique Cpx variants to modulate presynaptic output from a neuron would be more likely. Indeed, an intermediate effect on spontaneous fusion was observed when unedited Cpx7A and Cpx7A^{I125M,N130S} were both expressed in *cpx^{SH1}*. Co-expression of the two proteins resulted in a spontaneous release rate of 23 Hz (**Figure 6A, G**), distinct from the 13 Hz in unedited Cpx7A (p=0.041) or 47 Hz in Cpx7A^{I125M,N130S} (p=0.0013). Co-expression of unedited Cpx7A and Cpx7A^{I125M,N130S} also displayed a larger evoked response than unedited Cpx7A alone (p=0.043) and similar to that observed in Cpx7A^{I125M,N130S} (p=0.48), suggesting the N130S acts in a dominant fashion for promoting evoked release (**Figure 6C, H**). These data suggest co-expression of different Cpx variants can independently interface with the SV release machinery, consistent with stochastic RNA editing of Cpx acting as a mechanism for generating release heterogeneity across neurons.

2.4 Discussion

Mechanisms that control SNARE complex assembly dynamics provide attractive sites for regulatory control of presynaptic neurotransmitter release. Several SNARE binding proteins act at multiple steps of the SV cycle to chaperone SNARE proteins and regulate their ability to zipper together to form the four-stranded alpha-helical bundle that drives fusion (Wickner and Rizo, 2017; Brunger et al., 2019; Sauvola and Littleton, 2021). Cpx and Syt1 play key roles at a late stage of SNARE assembly to control whether SVs fuse through the evoked or spontaneous release pathway. The Cpx C-terminal amphipathic helix has emerged as an important site for regulatory control of the protein (Lottermoser and Dittman, 2023). In addition to acting as a membrane curvature sensor that can tether Cpx to SVs (Wragg et al., 2013; Snead et al., 2014, 2017; Gong et al., 2016; Grasso et al., 2023), the C-terminal domain can clamp fusion by blocking SNARE assembly (Makke et al., 2018), remodel membranes to regulate fusion pore dynamics (Courtney et al., 2022), directly stimulate SNARE-mediated assembly (Malsam et al., 2009; Seiler et al., 2009) or compete with Syt1 for membrane binding (Liang et al., 2022). In addition, post-translational modifications to this domain can alter Cpx function (Hill et al., 2006; Shata et al., 2007; Malsam et al., 2009; Cho et al., 2015; Robinson et al., 2018; Bulgari et al., 2022), identifying presynaptic plasticity mechanisms that directly impinge on SNARE-mediated fusion.

In the current study, we examined the functional consequences of alternative splicing or RNA editing of the C-terminus of *Drosophila* Cpx. Endogenous expression of either the Cpx7A or Cpx7B isoform was sufficient to prevent synaptic overgrowth and the dramatic elevation of spontaneous release rates observed in null mutants. Indeed, across all manipulations of Cpx splicing and RNA editing, large increases in mini frequency were always associated with over proliferation of synapses. These observations support the linkage between spontaneous fusion and retrograde signaling mechanisms that drive one form of activity-dependent synaptic growth at *Drosophila* NMJs (McCabe et al., 2003; Yoshihara et al., 2005; Huntwork and Littleton, 2007; Choi et al., 2014; Cho et al., 2015; Harris et al., 2016; Banerjee et al., 2021). Endogenously expressed Cpx7A or Cpx7B alone were not sufficient to fully recapitulate evoked release observed in controls, suggesting both are required *in vivo*. Given differences in expression level between Cpx7A and Cpx7B, it was surprising that endogenous Cpx7B could support Cpx function at larval NMJs. Loss of the predominant Cpx7A isoform in the $cpx^{\Delta 7A}$ splicing mutant reduced overall levels of Cpx by 87% in adult heads and by 85% at NMJs. In contrast, loss of Cpx7B in $cpx^{\Delta 7B}$ reduced

total Cpx levels by only 10% in adult heads and did not cause a detectable decrease at NMJs. We considered the possibility that a truncated Cpx might still be produced that lacked the 7A exon in $cpx^{\Delta 7A}$ mutants that supported some release on its own. However, western analysis showed that only traces of a truncated protein as a much fainter lower molecular weight band that was barely detectable in $cpx^{\Delta 7A}$, dramatically less than the already reduced levels of Cpx7B. This observation indicates loss of the C-terminal domain destabilizes Cpx and leads to its degradation, similar to observations with a truncating mutant with a stop codon in exon 6 (Buhl et al., 2013).

Given Cpx7B clamped spontaneous fusion and promoted evoked release with only ~15% of the expression level of Cpx7A, the two splice variants likely have intrinsic differences in their activity. Like mammalian CPX1 and CPX2 that are present at most central nervous system (CNS) synapses, Cpx7B lacks the C-terminal CAAX motif, potentially endowing these non-prenylated Cpx proteins with greater mobility to interface with Syt1 and SNAREs and enhance release kinetics. Indeed, the onset of evoked release was slightly faster in larvae expressing only Cpx7B. While Cpx7B was able to reduce elevated mini frequency 28-fold compared to null mutants, it was only able to rescue ~50% of evoked amplitude, suggesting Cpx abundance is more important for promoting evoked release than clamping spontaneous fusion. The estimated requirements for zippering of 3 to 11 SNARE complexes in a radial assembly for a single SV to undergo action potential-triggered fusion (Hua and Scheller, 2001; Montecucco et al., 2005; Domanska et al., 2009; Karatekin et al., 2010; Shi et al., 2012; Bao et al., 2018; McDargh et al., 2018; Rizo et al., 2022) provides a candidate mechanism for Cpx expression to differentially impact the two release pathways. For spontaneous release, a smaller number of Cpx proteins could block enough SNARE zippering events to prevent reaching the minimum required for fusion. For rapid Ca^{2+}-triggered release, excess Cpxs would be needed to bind more SNARE complexes in the radial assembly at the SV-plasma membrane interface to control Syt1 activity and SNARE zippering. In contrast to Cpx7B, elevated levels of Cpx7A and prenylation of its C-terminus could increase local concentration at release sites to provide more effective clamping and triggering activity. Given the more severe behavioral deficits in $cpx^{\Delta 7A}$ animals, we hypothesize some CNS synapses are more sensitive to loss of Cpx7A than motoneurons.

We previously discovered that PKA phosphorylation of S126 in the Cpx7B C-terminus enhances spontaneous release and promotes structural and functional synaptic plasticity at larval NMJs (Cho et al., 2015). PKA phosphorylation of S126 also controls fusion pore dilation and

cargo release from *Drosophila* dense core vesicles (Bulgari et al., 2022), indicating changes to the C-terminal amphipathic domain of Cpx modulate its function in membrane fusion. Although Cpx7A lacks this PKA phosphorylation site, it undergoes RNA editing to generate up to eight unique C-terminal sequence variants (I125 with N130, S130, D130, or G130 and M125 with N130, S130, D130 or G130). Single-cell RNAseq revealed multiple Cpx7A editing variants are simultaneously expressed in Ib and Is motoneurons. As such, ADAR-mediated RNA editing does not act in an "all-or-none" fashion, but instead stochastically deaminates A-to-I residues with distinct efficiencies depending upon the local environment of its unspliced exon-intron double-stranded mRNA substrate. Generally, unedited Cpx7A was the dominant form of Cpx in motoneurons, with editing variants represented at lower levels. However, in rare cases, a single edited variant was the only Cpx mRNA expressed in that neuron (**Figure 4A**). The amount of Cpx editing was not correlated with ADAR expression, similar to the dissociation of editing percentage and ADAR abundance in pooled RNAseq data from adult *Drosophila* neurons over a broader range of RNA editing targets (Sapiro et al., 2019). The percentage of Cpx editing variants were similarly expressed in the Ib and Is motoneuron subgroups. However, analysis of FACS-sorted neuronal populations from adult *Drosophila* brains revealed RNA editing of Cpx7A was even more robust and diverse in these neurons, with 22% of *cpx* mRNAs encoding N130S and 23% encoding N130G (Sapiro et al., 2019). As *Drosophila* ADAR itself is subject to developmentally-regulated auto-editing that can change its enzymatic activity (Palladino et al., 2000), the frequency of Cpx editing might be modulated by intrinsic activity, allowing more dynamic changes to Cpx function within single neurons.

To determine if Cpx7A edit variants within a single neuron alter presynaptic output, transgenic rescues were used to assay their function. The most prominent variant $Cpx7A^{I125M,N130S}$ displayed an altered synaptic distribution, with more of the protein observed in axons. It also failed to clamp spontaneous fusion, resulting in synaptic overgrowth. We found that $Cpx7A^{I125M,N130S}$ could be phosphorylated by CK2 *in vitro*. CK2 phosphorylates multiple synaptic proteins, including Syx1A (Foletti et al., 2000; Shi et al., 2021; Shekar et al., 2023), Syt1 (Bennett et al., 1993) and mammalian CPX1 (Shata et al., 2007). Phosphorylation of the C-terminus of mammalian CPX1 by CK2 alters its SNARE-binding affinity (Shata et al., 2007), while mutation of the CK2 phosphorylation site (S115) prevents CPX1 from stimulating liposomal fusion (Malsam et al., 2009). In *Drosophila*, presynaptic CK2 has been demonstrated to control synaptic

stability by regulating Ankyrin2 function (Bulat et al., 2014). Although CK2 can phosphorylate Cpx7A^{I125M,N130S} *in vitro*, it remains unclear if this is relevant to Cpx function *in vivo*. In particular, the putative phospho-mimetic variant Cpx7A^{I125M,N130D} was able to fully clamp spontaneous release and support normal synaptic growth, outperforming even unedited Cpx. This was surprising given expression of a similarly phospho-mimetic Cpx7B^{S126D} failed to clamp spontaneous fusion and occluded synaptic plasticity expression at larval NMJs (Cho et al., 2015). As such, Cpx7A^{I125M,N130S} may instead alter the structure or binding properties of the amphipathic helix in unique ways to prevent normal interactions with SNAREs or other protein/lipid targets.

Given stochastic expression of Cpx edited proteins within single motoneurons, and the previously described model with multiple SNARE complexes driving fusion, we assayed if co-expression of Cpx7A^{I125M,N130S} with unedited Cpx7A could independently contribute to presynaptic release output. Indeed, the N130S isoform acted in a partially dominant manner, preventing unedited Cpx7A from fully clamping spontaneous fusion, while supporting higher levels of evoked release. These data support a model where each Cpx variant may have access to assembling SNAREs, allowing them to fine-tune presynaptic output. The redistribution of Cpx edit variants within NMJs might also contribute to changes in their functional properties. Further studies will be required to determine how N130, N130S and N130D alter the structure and properties of the C-terminal amphipathic helix. However, disruptions of the amphipathic helix in *C. elegans* Cpx reduce inhibition of SV release (Wragg et al., 2013; Snead et al., 2014), further highlighting a key role for this domain.

Beyond stochastic RNA editing of Cpx7A across single motoneurons, we observed heterogeneity in the percent of RNA editing for sites in both Synapsin and Syx1A. If similar rules apply for other editing sites in the genome, stochastic RNA editing across multiple mRNAs could generate unique synaptic proteomes within the same neuronal population and contribute to heterogenous properties of individual cells with similar transcriptomes. Such a mechanism would be a robust way to alter multiple features of neuronal function, given ADAR editing alters the function of proteins that contribute to both synaptic function and membrane excitability (Hoopengardner et al., 2003; Barlati and Barbon, 2005; Diegelmann et al., 2006; Maldonado et al., 2013; Li et al., 2014; Robinson et al., 2016; Kliuchnikova et al., 2020; Shumate et al., 2021).

References

Ali YO, Escala W, Ruan K, Zhai RG (2011) Assaying locomotor, learning, and memory deficits in Drosophila models of neurodegeneration. J Vis Exp.

Aponte-Santiago NA, Littleton JT (2020) Synaptic properties and plasticity mechanisms of invertebrate tonic and phasic neurons. Front Physiol 11:611982.

Aponte-Santiago NA, Ormerod KG, Akbergenova Y, Littleton JT (2020) Synaptic plasticity induced by differential manipulation of tonic and phasic motoneurons in drosophila. J Neurosci 40:6270–6288.

Astacio H, Vasin A, Bykhovskaia M (2022) Stochastic properties of spontaneous synaptic transmission at individual active zones. J Neurosci 42:1001–1019.

Banerjee S, Vernon S, Jiao W, Choi BJ, Ruchti E, Asadzadeh J, Burri O, Stowers RS, McCabe BD (2021) Miniature neurotransmission is required to maintain Drosophila synaptic structures during ageing. Nat Commun 12:4399.

Bao H, Das D, Courtney NA, Jiang Y, Briguglio JS, Lou X, Roston D, Cui Q, Chanda B, Chapman ER (2018) Dynamics and number of trans-SNARE complexes determine nascent fusion pore properties. Nature 554:260–263.

Barlati S, Barbon A (2005) RNA editing: a molecular mechanism for the fine modulation of neuronal transmission. Acta Neurochir Suppl 93:53–57.

Bennett MK, Miller KG, Scheller RH (1993) Casein kinase II phosphorylates the synaptic vesicle protein p65. J Neurosci 13:1701–1707.

Bera M, Ramakrishnan S, Coleman J, Krishnakumar SS, Rothman JE (2022) Molecular determinants of complexin clamping and activation function. Elife 11.

Brunger AT, Choi UB, Lai Y, Leitz J, White KI, Zhou Q (2019) The pre-synaptic fusion machinery. Curr Opin Struct Biol 54:179–188.

Buhl LK, Jorquera RA, Akbergenova Y, Huntwork-Rodriguez S, Volfson D, Littleton JT (2013) Differential regulation of evoked and spontaneous neurotransmitter release by C-terminal modifications of complexin. Mol Cell Neurosci 52:161–172.

Bulat V, Rast M, Pielage J (2014) Presynaptic CK2 promotes synapse organization and stability by targeting Ankyrin2. J Cell Biol 204:77–94.

Bulgari D, Cavolo SL, Schmidt BF, Buchan K, Bruchez MP, Deitcher DL, Levitan E (2022) Ca^{2+} and cAMP open differentially dilating synaptic fusion pores. BioRxiv.

Bykhovskaia M, Jagota A, Gonzalez A, Vasin A, Littleton JT (2013) Interaction of the complexin accessory helix with the C-terminus of the SNARE complex: molecular-dynamics model of the fusion clamp. Biophys J 105:679–690.

Cho RW, Buhl LK, Volfson D, Tran A, Li F, Akbergenova Y, Littleton JT (2015) Phosphorylation of Complexin by PKA Regulates Activity-Dependent Spontaneous Neurotransmitter Release and Structural Synaptic Plasticity. Neuron 88:749–761.

Cho RW, Kümmel D, Li F, Baguley SW, Coleman J, Rothman JE, Littleton JT (2014) Genetic analysis of the Complexin trans-clamping model for cross-linking SNARE complexes in vivo. Proc Natl Acad Sci USA 111:10317–10322.

Cho RW, Song Y, Littleton JT (2010) Comparative analysis of Drosophila and mammalian complexins as fusion clamps and facilitators of neurotransmitter release. Mol Cell Neurosci 45:389–397.

Choi BJ, Imlach WL, Jiao W, Wolfram V, Wu Y, Grbic M, Cela C, Baines RA, Nitabach MN, McCabe BD (2014) Miniature neurotransmission regulates Drosophila synaptic structural maturation. Neuron 82:618–634.

Courtney KC, Wu L, Mandal T, Swift M, Zhang Z, Alaghemandi M, Wu Z, Bradberry MM, Deo C, Lavis LD, Volkmann N, Hanein D, Cui Q, Bao H, Chapman ER (2022) The complexin C-terminal amphipathic helix stabilizes the fusion pore open state by sculpting membranes. Nat Struct Mol Biol 29:97–107.

Diegelmann S, Nieratschker V, Werner U, Hoppe J, Zars T, Buchner E (2006) The conserved protein kinase-A target motif in synapsin of Drosophila is effectively modified by pre-mRNA editing. BMC Neurosci 7:76.

Domanska MK, Kiessling V, Stein A, Fasshauer D, Tamm LK (2009) Single vesicle millisecond fusion kinetics reveals number of SNARE complexes optimal for fast SNARE-mediated membrane fusion. J Biol Chem 284:32158–32166.

Foletti DL, Lin R, Finley MA, Scheller RH (2000) Phosphorylated syntaxin 1 is localized to discrete domains along a subset of axons. J Neurosci 20:4535–4544.

Gautier R, Douguet D, Antonny B, Drin G (2008) HELIQUEST: a web server to screen sequences with specific alpha-helical properties. Bioinformatics 24:2101–2102.

Gong J, Lai Y, Li X, Wang M, Leitz J, Hu Y, Zhang Y, Choi UB, Cipriano D, Pfuetzner RA, Südhof TC, Yang X, Brunger AT, Diao J (2016) C-terminal domain of mammalian complexin-1 localizes to highly curved membranes. Proc Natl Acad Sci USA 113:E7590–E7599.

Grasso EM, Terakawa MS, Lai AL, Xue Xie Y, Ramlall TF, Freed JH, Eliezer D (2023) Membrane Binding Induces Distinct Structural Signatures in the Mouse Complexin-1C-Terminal Domain. J Mol Biol 435:167710.

Gratz SJ, Ukken FP, Rubinstein CD, Thiede G, Donohue LK, Cummings AM, O'Connor-Giles KM (2014) Highly specific and efficient CRISPR/Cas9-catalyzed homology-directed repair in Drosophila. Genetics 196:961–971.

Han Y, Chien C, Goel P, He K, Pinales C, Buser C, Dickman D (2022) Botulinum neurotoxin accurately separates tonic vs. phasic transmission and reveals heterosynaptic plasticity rules in Drosophila. Elife 11.

Harris KP, Littleton JT (2015) Transmission, development, and plasticity of synapses. Genetics 201:345–375.

Harris KP, Zhang YV, Piccioli ZD, Perrimon N, Littleton JT (2016) The postsynaptic t-SNARE Syntaxin 4 controls traffic of Neuroligin 1 and Synaptotagmin 4 to regulate retrograde signaling. Elife 5.

Higuchi M, Single FN, Köhler M, Sommer B, Sprengel R, Seeburg PH (1993) RNA editing of AMPA receptor subunit GluR-B: a base-paired intron-exon structure determines position and efficiency. Cell 75:1361–1370.

Hill JJ, Callaghan DA, Ding W, Kelly JF, Chakravarthy BR (2006) Identification of okadaic acid-induced phosphorylation events by a mass spectrometry approach. Biochem Biophys Res Commun 342:791–799.

Hoang B, Chiba A (2001) Single-cell analysis of Drosophila larval neuromuscular synapses. Dev Biol 229:55–70.

Hobson RJ, Liu Q, Watanabe S, Jorgensen EM (2011) Complexin maintains vesicles in the primed state in C. elegans. Curr Biol 21:106–113.

Hoopengardner B, Bhalla T, Staber C, Reenan R (2003) Nervous system targets of RNA editing identified by comparative genomics. Science 301:832–836.

Hua Y, Scheller RH (2001) Three SNARE complexes cooperate to mediate membrane fusion. Proc Natl Acad Sci USA 98:8065–8070.

Huntwork S, Littleton JT (2007) A complexin fusion clamp regulates spontaneous neurotransmitter release and synaptic growth. Nat Neurosci 10:1235–1237.
Jetti SK, Crane ASB, Akbergenova Y, Aponte-Santiago NA, Cunningham KL, Whittaker CA, Littleton JT (2023) Molecular logic of synaptic diversity between drosophila tonic and phasic motoneurons. BioRxiv.
Johansen J, Halpern ME, Johansen KM, Keshishian H (1989) Stereotypic morphology of glutamatergic synapses on identified muscle cells of Drosophila larvae. J Neurosci 9:710–725.
Jorquera RA, Huntwork-Rodriguez S, Akbergenova Y, Cho RW, Littleton JT (2012) Complexin controls spontaneous and evoked neurotransmitter release by regulating the timing and properties of synaptotagmin activity. J Neurosci 32:18234–18245.
Jumper J et al. (2021) Highly accurate protein structure prediction with AlphaFold. Nature 596:583–589.
Karatekin E, Di Giovanni J, Iborra C, Coleman J, O'Shaughnessy B, Seagar M, Rothman JE (2010) A fast, single-vesicle fusion assay mimics physiological SNARE requirements. Proc Natl Acad Sci USA 107:3517–3521.
Kashima R, Redmond PL, Ghatpande P, Roy S, Kornberg TB, Hanke T, Knapp S, Lagna G, Hata A (2017) Hyperactive locomotion in a Drosophila model is a functional readout for the synaptic abnormalities underlying fragile X syndrome. Sci Signal 10.
Katz B, Miledi R (1967) The timing of calcium action during neuromuscular transmission. J Physiol (Lond) 189:535–544.
Kliuchnikova AA, Goncharov AO, Levitsky LI, Pyatnitskiy MA, Novikova SE, Kuznetsova KG, Ivanov MV, Ilina IY, Farafonova TE, Zgoda VG, Gorshkov MV, Moshkovskii SA (2020) Proteome-Wide Analysis of ADAR-Mediated Messenger RNA Editing during Fruit Fly Ontogeny. J Proteome Res 19:4046–4060.
Li X, Overton IM, Baines RA, Keegan LP, O'Connell MA (2014) The ADAR RNA editing enzyme controls neuronal excitability in Drosophila melanogaster. Nucleic Acids Res 42:1139–1151.
Liang Q, Ofosuhene AP, Kiessling V, Liang B, Kreutzberger AJB, Tamm LK, Cafiso DS (2022) Complexin-1 and synaptotagmin-1 compete for binding sites on membranes containing PtdInsP2. Biophys J 121:3370–3380.
Lnenicka GA, Keshishian H (2000) Identified motor terminals in Drosophila larvae show distinct differences in morphology and physiology. J Neurobiol 43:186–197.
Lottermoser JA, Dittman JS (2023) Complexin membrane interactions: implications for synapse evolution and function. J Mol Biol 435:167774.
Mahoney RE, Azpurua J, Eaton BA (2016) Insulin signaling controls neurotransmission via the 4eBP-dependent modification of the exocytotic machinery. Elife 5.
Makke M, Mantero Martinez M, Gaya S, Schwarz Y, Frisch W, Silva-Bermudez L, Jung M, Mohrmann R, Dhara M, Bruns D (2018) A mechanism for exocytotic arrest by the Complexin C-terminus. Elife 7.
Maldonado C, Alicea D, Gonzalez M, Bykhovskaia M, Marie B (2013) Adar is essential for optimal presynaptic function. Mol Cell Neurosci 52:173–180.
Malsam J, Bärfuss S, Trimbuch T, Zarebidaki F, Sonnen AF-P, Wild K, Scheutzow A, Rohland L, Mayer MP, Sinning I, Briggs JAG, Rosenmund C, Söllner TH (2020) Complexin Suppresses Spontaneous Exocytosis by Capturing the Membrane-Proximal Regions of VAMP2 and SNAP25. Cell Rep 32:107926.

Malsam J, Seiler F, Schollmeier Y, Rusu P, Krause JM, Söllner TH (2009) The carboxy-terminal domain of complexin I stimulates liposome fusion. Proc Natl Acad Sci USA 106:2001–2006.
Martin JA, Hu Z, Fenz KM, Fernandez J, Dittman JS (2011) Complexin has opposite effects on two modes of synaptic vesicle fusion. Curr Biol 21:97–105.
McCabe BD, Marqués G, Haghighi AP, Fetter RD, Crotty ML, Haerry TE, Goodman CS, O'Connor MB (2003) The BMP homolog Gbb provides a retrograde signal that regulates synaptic growth at the Drosophila neuromuscular junction. Neuron 39:241–254.
McDargh ZA, Polley A, O'Shaughnessy B (2018) SNARE-mediated membrane fusion is a two-stage process driven by entropic forces. FEBS Lett 592:3504–3515.
Montecucco C, Schiavo G, Pantano S (2005) SNARE complexes and neuroexocytosis: how many, how close? Trends Biochem Sci 30:367–372.
Newman ZL, Bakshinskaya D, Schultz R, Kenny SJ, Moon S, Aghi K, Stanley C, Marnani N, Li R, Bleier J, Xu K, Isacoff EY (2022) Determinants of synapse diversity revealed by super-resolution quantal transmission and active zone imaging. Nat Commun 13:229.
Nichols CD, Becnel J, Pandey UB (2012) Methods to assay Drosophila behavior. J Vis Exp.
Nishikura K (2016) A-to-I editing of coding and non-coding RNAs by ADARs. Nat Rev Mol Cell Biol 17:83–96.
Palladino MJ, Keegan LP, O'Connell MA, Reenan RA (2000) A-to-I pre-mRNA editing in Drosophila is primarily involved in adult nervous system function and integrity. Cell 102:437–449.
Port F, Bullock SL (2016) Augmenting CRISPR applications in Drosophila with tRNA-flanked sgRNAs. Nat Methods 13:852–854.
Quiñones-Frías MC, Littleton JT (2021) Function of Drosophila Synaptotagmins in membrane trafficking at synapses. Cell Mol Life Sci 78:4335–4364.
Radhakrishnan A, Li X, Grushin K, Krishnakumar SS, Liu J, Rothman JE (2021) Symmetrical arrangement of proteins under release-ready vesicles in presynaptic terminals. Proc Natl Acad Sci USA 118.
Reim K, Wegmeyer H, Brandstätter JH, Xue M, Rosenmund C, Dresbach T, Hofmann K, Brose N (2005) Structurally and functionally unique complexins at retinal ribbon synapses. J Cell Biol 169:669–680.
Rizo J (2022) Molecular mechanisms underlying neurotransmitter release. Annu Rev Biophys 51:377–408.
Rizo J, Sari L, Qi Y, Im W, Lin MM (2022) All-atom molecular dynamics simulations of Synaptotagmin-SNARE-complexin complexes bridging a vesicle and a flat lipid bilayer. Elife 11.
Robinson JE, Paluch J, Dickman DK, Joiner WJ (2016) ADAR-mediated RNA editing suppresses sleep by acting as a brake on glutamatergic synaptic plasticity. Nat Commun 7:10512.
Robinson JT, Thorvaldsdóttir H, Winckler W, Guttman M, Lander ES, Getz G, Mesirov JP (2011) Integrative genomics viewer. Nat Biotechnol 29:24–26.
Robinson SW, Bourgognon J-M, Spiers JG, Breda C, Campesan S, Butcher A, Mallucci GR, Dinsdale D, Morone N, Mistry R, Smith TM, Guerra-Martin M, Challiss RAJ, Giorgini F, Steinert JR (2018) Nitric oxide-mediated posttranslational modifications control neurotransmitter release by modulating complexin farnesylation and enhancing its clamping ability. PLoS Biol 16:e2003611.
Sapiro AL, Shmueli A, Henry GL, Li Q, Shalit T, Yaron O, Paas Y, Billy Li J, Shohat-Ophir G

(2019) Illuminating spatial A-to-I RNA editing signatures within the Drosophila brain. Proc Natl Acad Sci USA 116:2318–2327.
Sauvola CW, Littleton JT (2021) SNARE regulatory proteins in synaptic vesicle fusion and recycling. Front Mol Neurosci 14:733138.
Schindelin J, Arganda-Carreras I, Frise E, Kaynig V, Longair M, Pietzsch T, Preibisch S, Rueden C, Saalfeld S, Schmid B, Tinevez J-Y, White DJ, Hartenstein V, Eliceiri K, Tomancak P, Cardona A (2012) Fiji: an open-source platform for biological-image analysis. Nat Methods 9:676–682.
Seiler F, Malsam J, Krause JM, Söllner TH (2009) A role of complexin-lipid interactions in membrane fusion. FEBS Lett 583:2343–2348.
Shata A, Saisu H, Odani S, Abe T (2007) Phosphorylated synaphin/complexin found in the brain exhibits enhanced SNARE complex binding. Biochem Biophys Res Commun 354:808–813.
Shekar A, Mabry SJ, Cheng MH, Aguilar JI, Patel S, Zanella D, Saleeby DP, Zhu Y, Romanazzi T, Ulery-Reynolds P, Bahar I, Carter AM, Matthies HJG, Galli A (2023) Syntaxin 1 Ser14 phosphorylation is required for nonvesicular dopamine release. Sci Adv 9:eadd8417.
Shi L, Shen Q-T, Kiel A, Wang J, Wang H-W, Melia TJ, Rothman JE, Pincet F (2012) SNARE proteins: one to fuse and three to keep the nascent fusion pore open. Science 335:1355–1359.
Shi VH, Craig TJ, Bishop P, Nakamura Y, Rocca D, Wilkinson KA, Henley JM (2021) Phosphorylation of Syntaxin-1a by casein kinase 2α regulates pre-synaptic vesicle exocytosis from the reserve pool. J Neurochem 156:614–623.
Shumate KM, Tas ST, Kavalali ET, Emeson RB (2021) RNA editing-mediated regulation of calcium-dependent activator protein for secretion (CAPS1) localization and its impact on synaptic transmission. J Neurochem 158:182–196.
Snead D, Lai AL, Wragg RT, Parisotto DA, Ramlall TF, Dittman JS, Freed JH, Eliezer D (2017) Unique Structural Features of Membrane-Bound C-Terminal Domain Motifs Modulate Complexin Inhibitory Function. Front Mol Neurosci 10:154.
Snead D, Wragg RT, Dittman JS, Eliezer D (2014) Membrane curvature sensing by the C-terminal domain of complexin. Nat Commun 5:4955.
Sommer B, Köhler M, Sprengel R, Seeburg PH (1991) RNA editing in brain controls a determinant of ion flow in glutamate-gated channels. Cell 67:11–19.
Varadi M et al. (2022) AlphaFold Protein Structure Database: massively expanding the structural coverage of protein-sequence space with high-accuracy models. Nucleic Acids Res 50:D439–D444.
Wang J, Youkharibache P, Zhang D, Lanczycki CJ, Geer RC, Madej T, Phan L, Ward M, Lu S, Marchler GH, Wang Y, Bryant SH, Geer LY, Marchler-Bauer A (2020a) iCn3D, a web-based 3D viewer for sharing 1D/2D/3D representations of biomolecular structures. Bioinformatics 36:131–135.
Wang Y, Lobb-Rabe M, Ashley J, Carrillo RA (2020b) Structural and functional synaptic plasticity induced by convergent synapse loss requires co-innervation in the Drosophila neuromuscular circuit. BioRxiv.
Wickner W, Rizo J (2017) A cascade of multiple proteins and lipids catalyzes membrane fusion. Mol Biol Cell 28:707–711.
Wragg RT, Gouzer G, Bai J, Arianna G, Ryan TA, Dittman JS (2015) Synaptic activity regulates the abundance and binding of complexin. Biophys J 108:1318–1329.

Wragg RT, Parisotto DA, Li Z, Terakawa MS, Snead D, Basu I, Weinstein H, Eliezer D, Dittman JS (2017) Evolutionary Divergence of the C-terminal Domain of Complexin Accounts for Functional Disparities between Vertebrate and Invertebrate Complexins. Front Mol Neurosci 10:146.

Wragg RT, Snead D, Dong Y, Ramlall TF, Menon I, Bai J, Eliezer D, Dittman JS (2013) Synaptic vesicles position complexin to block spontaneous fusion. Neuron 77:323–334.

Yoshihara M, Adolfsen B, Galle KT, Littleton JT (2005) Retrograde signaling by Syt 4 induces presynaptic release and synapse-specific growth. Science 310:858–863.

Figures

Figure 1. Alternative splicing and RNA editing generate diversity in the conserved Complexin C-terminal amphipathic helix. (**A**) Diagram of the *Drosophila cpx* genomic locus with protein-coding exons indicated by black boxes and noncoding exons with gray. The ATG start codon is noted, together with the 7A (orange) and 7B (yellow) alternative splicing events. The location of CRISPR-generated *cpx* deletions removing 7A ($cpx^{\Delta 7A}$) or 7B ($cpx^{\Delta 7B}$) are also shown. (**B**) Alignment of Cpx C-termini from several species (Dm – *Drosophila melanogaster*, Hs – *Homo sapiens*, Mm – *Mus musculus*) highlights the two subfamilies that contain or lack a CAAX prenylation motif (orange). The amphipathic helix region is underlined, with asterisks denoting residues modified by RNA editing (I125, N130) in *Dm*Cpx7A or phosphorylation (S126) in *Dm*Cpx7B. (**C**) AlphaFold predictions of Cpx structure for homologs with and without the CAAX prenylation motif. The dashed line box denotes the SNARE-binding central helix and the solid line box highlights the C-terminal amphipathic helix. Cpx7A RNA editing sites and the Cpx7B phosphorylation site are denoted with *. AlphaFold per-residue confidence scores (pLDDT) are color-coded: blue=very high (pLDDT>90), cyan=confident (90>pLDDT>70), yellow=low (70>pLDDT>50), orange=very low (pLDDT<50). Cpx7B was generated using a simplified AlphaFold version without confidence scores and visualized with iCn3D (Wang et al., 2020a). (**D**) HELIQUEST predictions of the Cpx C-terminal amphipathic helix show the conserved hydrophilic and hydrophobic faces, with amino acid properties noted in the legend on the right. Arrows indicate the Cpx7A edit sites and the Cpx7B phosphorylation site. (**E**) Amphipathic helix models for non-edited (left) and edited (right) Cpx7A proteins.

Figure 2. Morphological and behavioral phenotypes in CRISPR-generated splicing mutants lacking Cpx exon 7A or 7B. (A) Quantification and representative western blot of Cpx levels from adult head extracts normalized to the loading control (anti-Tubulin) for the indicated genotypes (control (*white*), $cpx^{\Delta 7A}$, $cpx^{\Delta 7B}$, and cpx^{SH1}). **(B)** Immunostaining of 3rd instar larval muscle 4 NMJs at segment A3 for the indicated genotypes with antibodies against Cpx (gray, upper panels), Brp (green) and anti-HRP (magenta) show the large decrease in total Cpx levels in $cpx^{\Delta 7A}$ mutants lacking the predominant Cpx7A isoform. Scale bar=10 μm. **(C)** Quantification of total Cpx fluorescence within the HRP-positive area at muscle 4 NMJs for the indicated genotypes. **(D)** Quantification of climbing rate in negative geotaxis assays for adult males of the indicated

genotypes demonstrates severe motor deficits in $cpx^{\Delta 7A}$ mutants compared to $cpx^{\Delta 7B}$. Each point represents the average climbing rate for a cohort of 10 males. **(E)** Quantification of 3rd instar larval crawling velocity for the indicated genotypes. **(F)** Quantification of mean AZ number per muscle area at muscle 4 NMJs of the indicated genotypes. **(G)** Quantification of mean synaptic bouton number per muscle area at muscle 4 NMJs of the indicated genotypes. Data are shown as mean±SEM; *p<0.05, **p<0.01, ***p<0.001, ****p<0.0001, ns=not significant.

Figure 3. Electrophysiological analysis of synaptic function in mutants lacking Cpx7A or Cpx7B. (A) Representative postsynaptic current recordings of spontaneous release at muscle 6 NMJs in control (blue), cpx^{SH1} (gray), $cpx^{\Delta 7A}$ (orange), or $cpx^{\Delta 7B}$ (yellow) 3rd instar larvae. This genotypic color scheme is maintained for all figure panels. **(B)** Quantification of average spontaneous release rate for the indicated genotypes. Note the y-axis gap between 10-60 Hz due to the extreme elevation of mini frequency in cpx^{SH1} null mutants, which was excluded from one-way ANOVA comparison as its sample mean fell outside of a normal distribution. **(C)** Average traces of evoked EJC responses for the indicated genotypes. **(D)** Quantification of average eEJC amplitude for the indicated genotypes. **(E)** Quantification of average evoked release charge obtained by measuring total release over time following single action potentials. **(F)** Average normalized evoked responses for each genotype. **(G)** Average normalized responses plotted on a semi-logarithmic graph to display release components for each genotype. Note the large increase in the slower asynchronous release component in cpx^{SH1} null mutants (gray line). **(H)** Cumulative release normalized for the maximum response in 2.0 mM external Ca^{2+} for each genotype. Each trace was adjusted to a double exponential fit. **(I)** Average evoked EJC half-width change for each genotype. All recordings were performed in 2.0 mM external Ca^{2+} saline. Data are shown as mean±SEM; *p<0.05, **p<0.01, ***p<0.001, ****p<0.0001, ns=not significant.

Figure 4. Stochastic expression of Cpx7A RNA editing variants in single neurons. (A) Quantification of unedited and edited Cpx7A mRNAs from single Ib and Is motoneuron RNAseq datasets. Each point represents the number of edit variant reads as percent of total Cpx reads in an individual neuron. **(B)** Sorted single-cell RNA editing profiles for Cpx7A across the sampled population of Ib and Is motoneurons. Each neuron is displayed as a stacked bar with corresponding edit and unedited read percentages that total 100% of *cpx* mRNA for that cell. Cells 1-95 are Ib

motoneurons and cells 96-181 are Is motoneurons. Neurons are sorted by the largest unedited percent for both Ib and Is groups. (**C**) Comparison of ADAR transcripts per million (TPM) profile in Ib motoneuron with the corresponding percent of Cpx7A I125M RNA editing. **(D)** Comparison of ADAR transcripts per million (TPM) profile in Is motoneuron with the corresponding percent of Cpx7A I125M RNA editing. **(E)** Quantification of RNA editing percentage for known edit sites in genes encoding the synaptic proteins Synapsin (Syn) and Syntaxin 1A (Syx1A) in comparison to Cpx. Each point represents the percent of editing occurring at the base position of interest in one cell. All cells included for quantification (Ib=9 cells, Is=11 cells) contained at least ten reads at all base positions of interest (Syn N15, Syn R19, Syn R20, Cpx I125, and Syx1A M244). **(F)** Representative images of protein loading control (Coomassie blue, top panel) and CK2 phosphorylation ([^{32}P] incorporation on autoradiograph, bottom panel) for Cpx7A I125M, N130S (Cpx7A^{N130S}) compared to unedited Cpx7A I125, N130 (Cpx7A^{N130}) in *in vitro* phosphorylation assays. The absence (-) or presence (+) CK2 in labeling reactions is denoted. **(G)** Quantification of [^{32}P] incorporation for the indicated Cpx proteins in *in vitro* CK2 phosphorylation assays. Data are shown as mean±SEM; *p<0.05, **p<0.01, ***p<0.001, ****p<0.0001, ns=not significant.

Figure 5. RNA editing of Cpx7A alters its ability to regulate synaptic growth. (A) Representative western blot from adult head extracts stained for Cpx or Tubulin (loading control) for the indicated genotypes (control (*elav^{C155}-GAL4*, *cpx^{PE}*), *cpx^{SH1}* (*elav^{C155}-GAL4*, *cpx^{SH1}*), unedited rescue (*elav^{C155}-GAL4*, *cpx^{SH1}*, UAS- Cpx7A^{I125,N130}), I125M, N130S rescue (*elav^{C155}-GAL4*, *cpx^{SH1}*, UAS- Cpx7A^{I125M,N130S}) and I125M, N130D rescue (*elav^{C155}-GAL4*, *cpx^{SH1}*, UAS-Cpx7A^{I125M,N130D}). **(B)** Quantification of Cpx protein levels normalized to Tubulin from western blots of the indicated genotypes. **(C)** Immunostaining of 3rd instar larval muscle 4 NMJs at segment A3 for the indicated genotypes with antibodies against Cpx (gray, upper panels), Brp (green) and anti-HRP (magenta). Scale bar=10 μm. **(D)** Quantification of total Cpx fluorescence within the HRP-positive area at muscle 4 NMJs for the indicated genotypes. **(E)** Representative staining of 3rd instar muscle 4 NMJs and axons of the indicated genotypes from segment A3 with antibodies against Cpx (gray) and HRP (magenta). Cpx staining in axons is denoted with white arrows. The brightness of anti-Cpx staining was enhanced in controls to demonstrate the lower amounts of Cpx normally found in non-synaptic regions of the axon. Scale bar=10 μm. **(F)** Quantification of the Cpx NMJ/axon fluorescent ratio for the indicated genotypes. **(G)** Quantification of mean AZ

number per muscle area at muscle 4 NMJs of the indicated genotypes. **(H)** Quantification of mean synaptic bouton number per muscle area at muscle 4 NMJs of the indicated genotypes. Data are shown as mean±SEM; *p<0.05, **p<0.01, ***p<0.001, ****p<0.0001, ns=not significant.

Figure 6. RNA editing of Cpx7A alters its role in synaptic transmission. (A) Representative postsynaptic current recordings of spontaneous release at muscle 6 NMJs in control (blue, *elav*^{C155}-*GAL4*, *cpx*^{PE}), *cpx*^{SH1} (gray, *elav*^{C155}-*GAL4*, *cpx*^{SH1}), unedited Cpx rescue (orange, *elav*^{C155}-*GAL4*, *cpx*^{SH1}, UAS-Cpx7A^{I125,N130}), I125M, N130S rescue (yellow, *elav*^{C155}-*GAL4*, *cpx*^{SH1}, UAS-Cpx7A^{I125M,N130S}), I125M, N130D rescue (green, *elav*^{C155}-*GAL4*, *cpx*^{SH1}, UAS- Cpx7A^{I125M,N130D}) and co-expression of unedited and I125M, N130S (purple, *elav*^{C155}-*GAL4*, *cpx*^{SH1}, UAS-Cpx7A^{I125M,N130S}/*cpx*^{SH1}, UAS-Cpx7A^{I125,N130}). **(B)** Quantification of average spontaneous release rate for the indicated genotypes. **(C)** Average traces of evoked EJC responses for the indicated genotypes. **(D)** Quantification of average eEJC amplitude for the indicated genotypes. **(E)** Quantification of average evoked release charge obtained by measuring total release over time following single action potentials. **(F)** Average evoked EJC half-width change for each genotype. **(G)** Quantification of average spontaneous release rate for co-expression of Cpx7A$^{N130/N130S}$ rescue compared to Cpx7A^{N130} rescue and Cpx7A^{N130S} rescue alone in *cpx*^{SH1} mutant background. **(H)** Quantification of average eEJC amplitude for co-expression of Cpx7A$^{N130/N130S}$ rescue compared to Cpx7A^{N130} rescue and Cpx7A^{N130S} rescue alone in *cpx*^{SH1} mutant background. All recordings were performed in 2.0 mM external Ca^{2+} saline. Data are shown as mean±SEM; *p<0.05, **p<0.01, ***p<0.001, ****p<0.0001, ns=not significant.

Figure 1

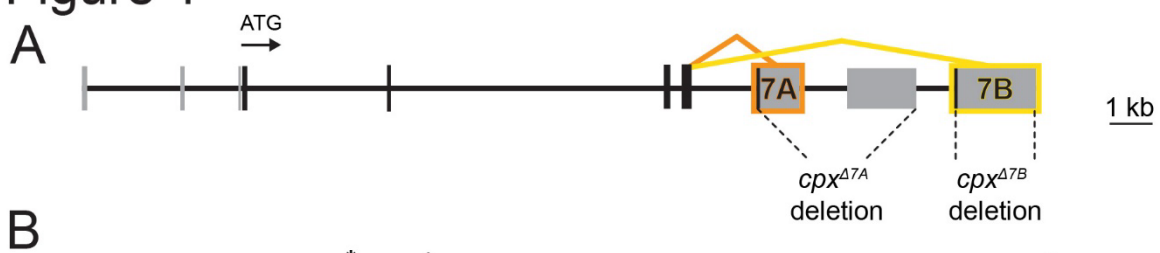

B

***Dm*7A**	EQEELDDFTKLKNQIETQVNELKTQIEGKCVMQ	***Dm*7B**	AEQEELDDFTTKLKKRLSDAFKNCPLRNLF
***Hs*3**	LASLPGLNLGSLKDKAQATLGDLKQSAEKCHVM	***Hs*1**	CGDEVEEEDESILDTVIKYLPGPLQDMLKK
***Mm*3**	LASLPGLDLSSLKDKAQTTLGDLKQSAEKCHIM	***Mm*1**	CGDEPEEEDESILDTVIKYLPGPLQDMFKK

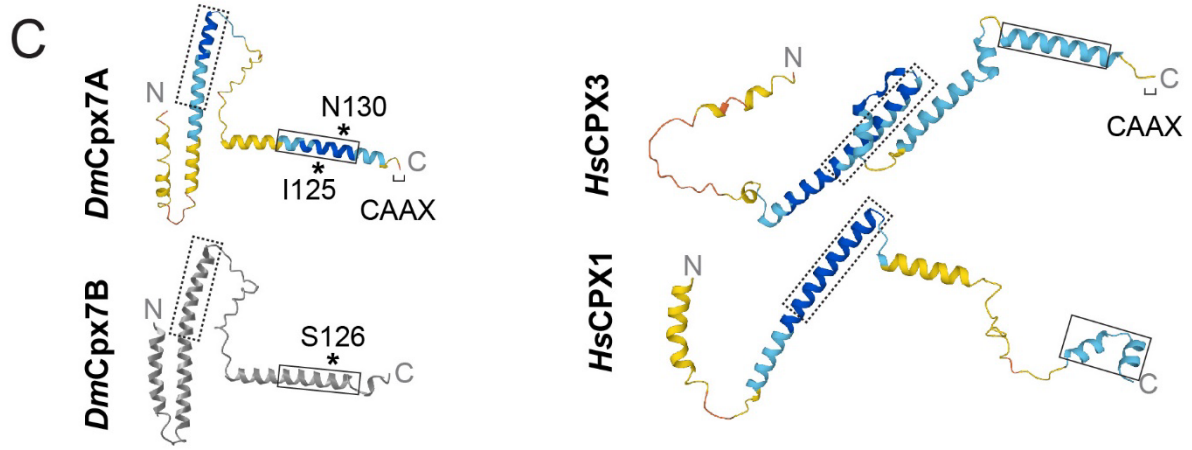

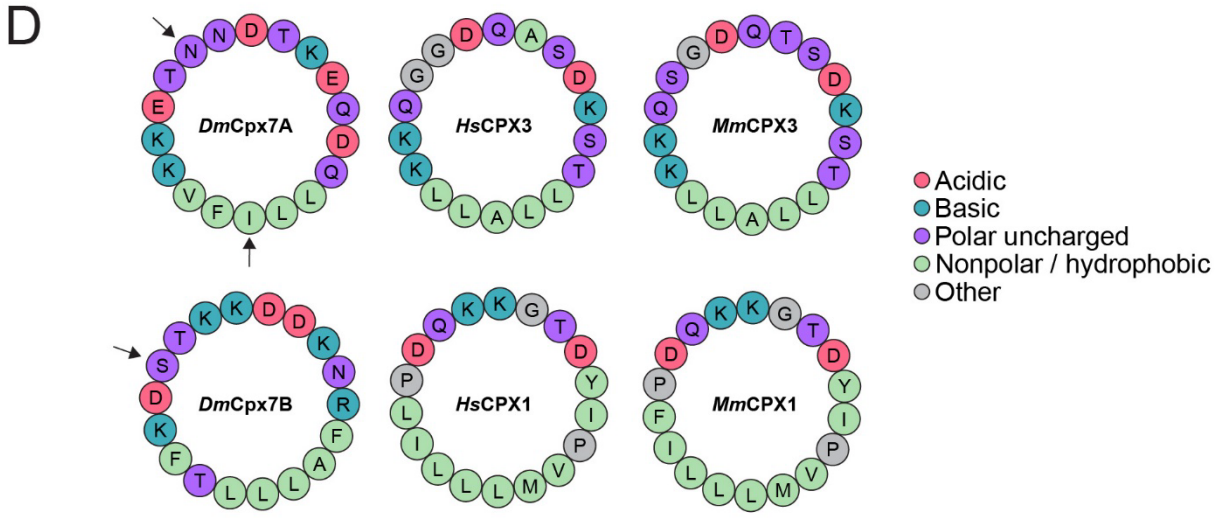

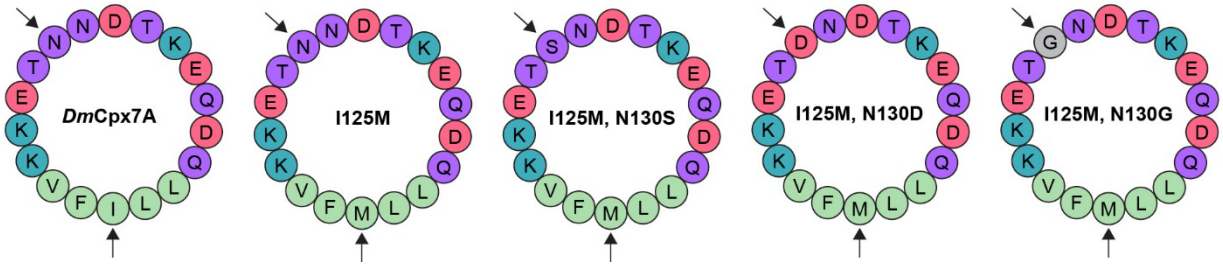

Figure 2

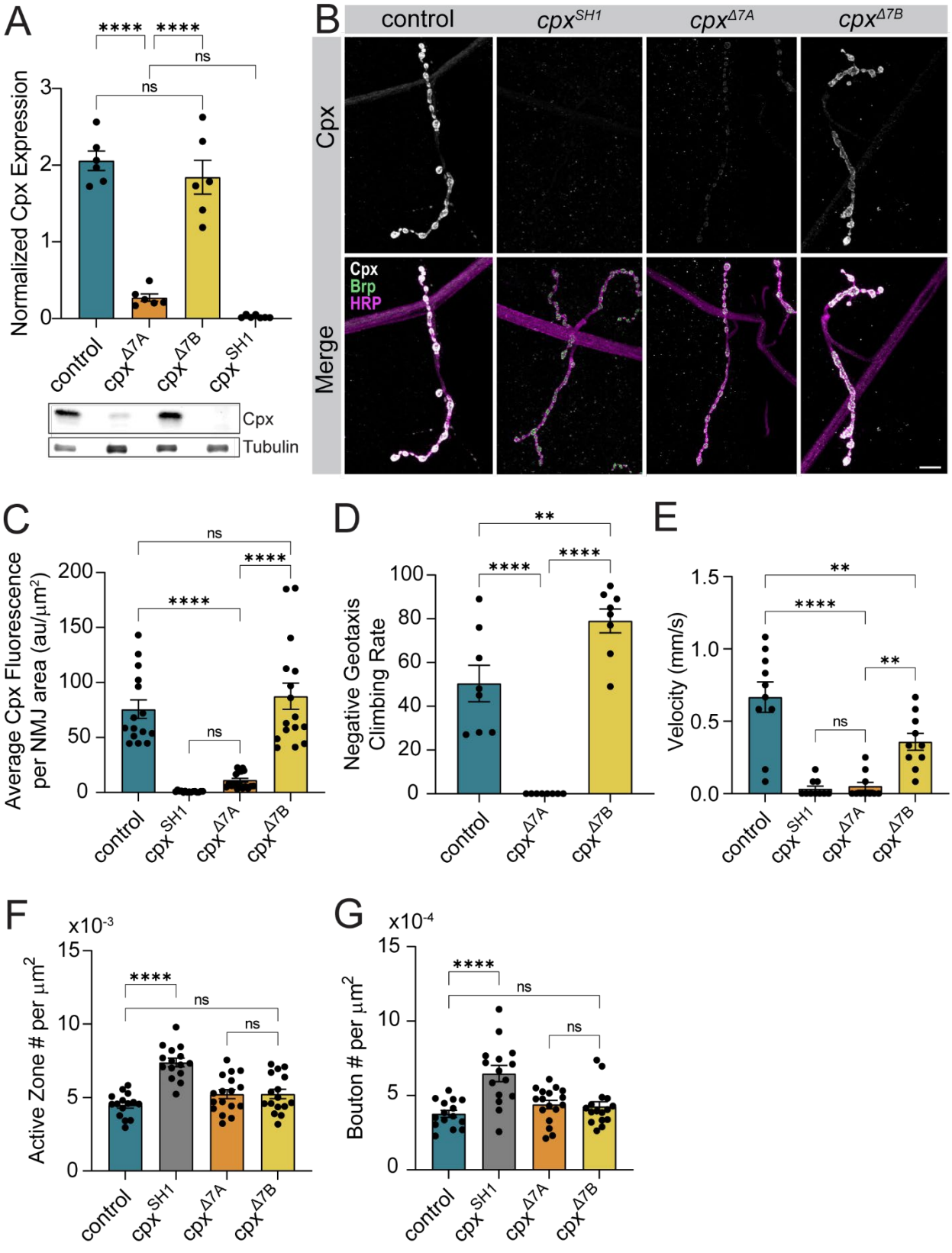
A
Normalized Cpx Expression
control
cpxΔ7A
cpxΔ7B
cpxSH1
Cpx
Tubulin
B
control
cpxSH1
cpxΔ7A
cpxΔ7B
Cpx
Merge
Cpx
Brp
HRP
C
Average Cpx Fluorescence per NMJ area (au/µm²)
D
Negative Geotaxis Climbing Rate
E
Velocity (mm/s)
F
Active Zone # per µm²
x10-3
G
Bouton # per µm²
x10-4

Figure 3

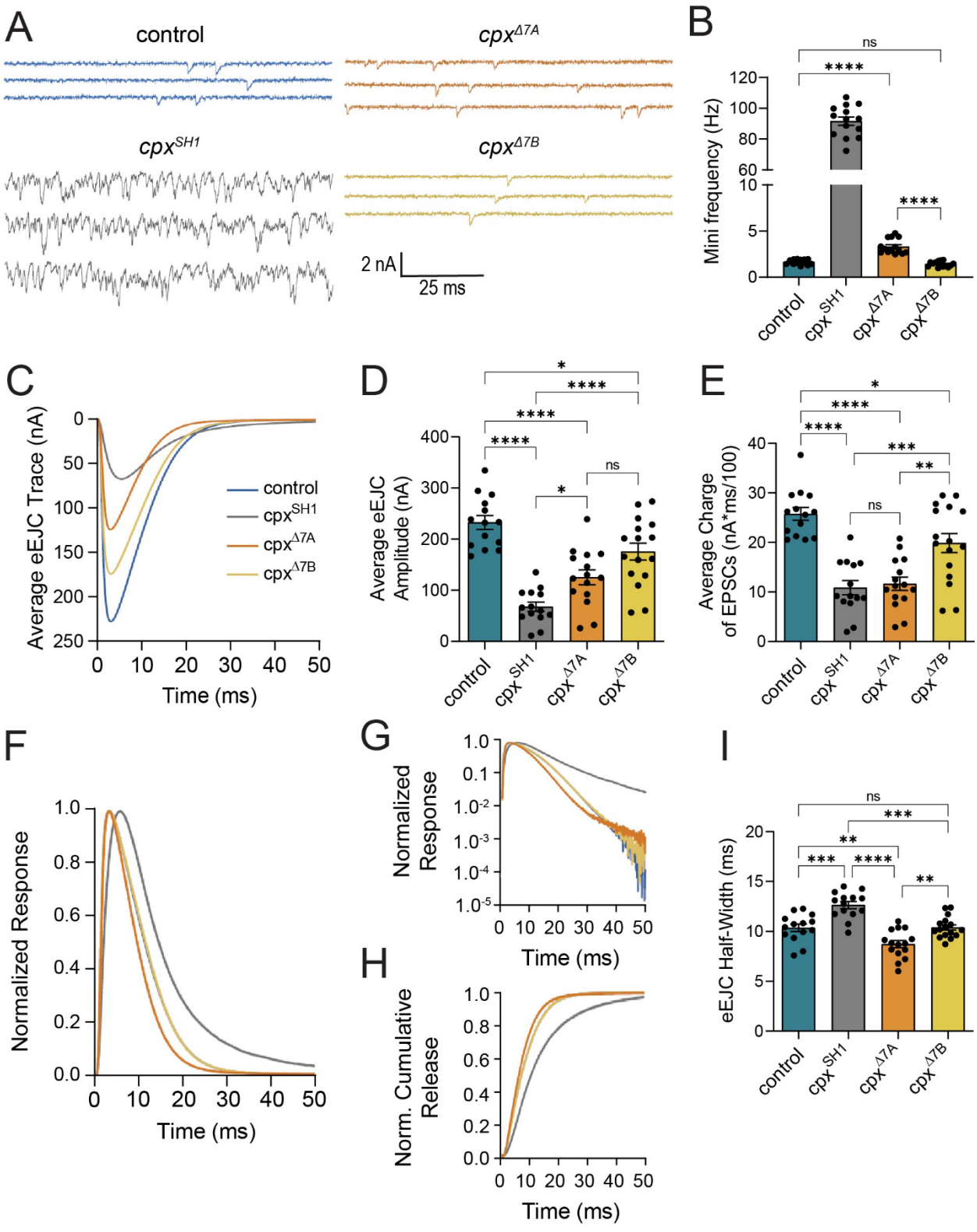
A
control
cpx^Δ7A
cpx^SH1
cpx^Δ7B
2 nA
25 ms
B
Mini frequency (Hz)
ns
****
****
control
cpx^SH1
cpx^Δ7A
cpx^Δ7B
C
Average eEJC Trace (nA)
Time (ms)
control
cpx^SH1
cpx^Δ7A
cpx^Δ7B
D
Average eEJC Amplitude (nA)
E
Average Charge of EPSCs (nA*ms/100)
F
Normalized Response
Time (ms)
G
Normalized Response
Time (ms)
H
Norm. Cumulative Release
Time (ms)
I
eEJC Half-Width (ms)

Figure 4

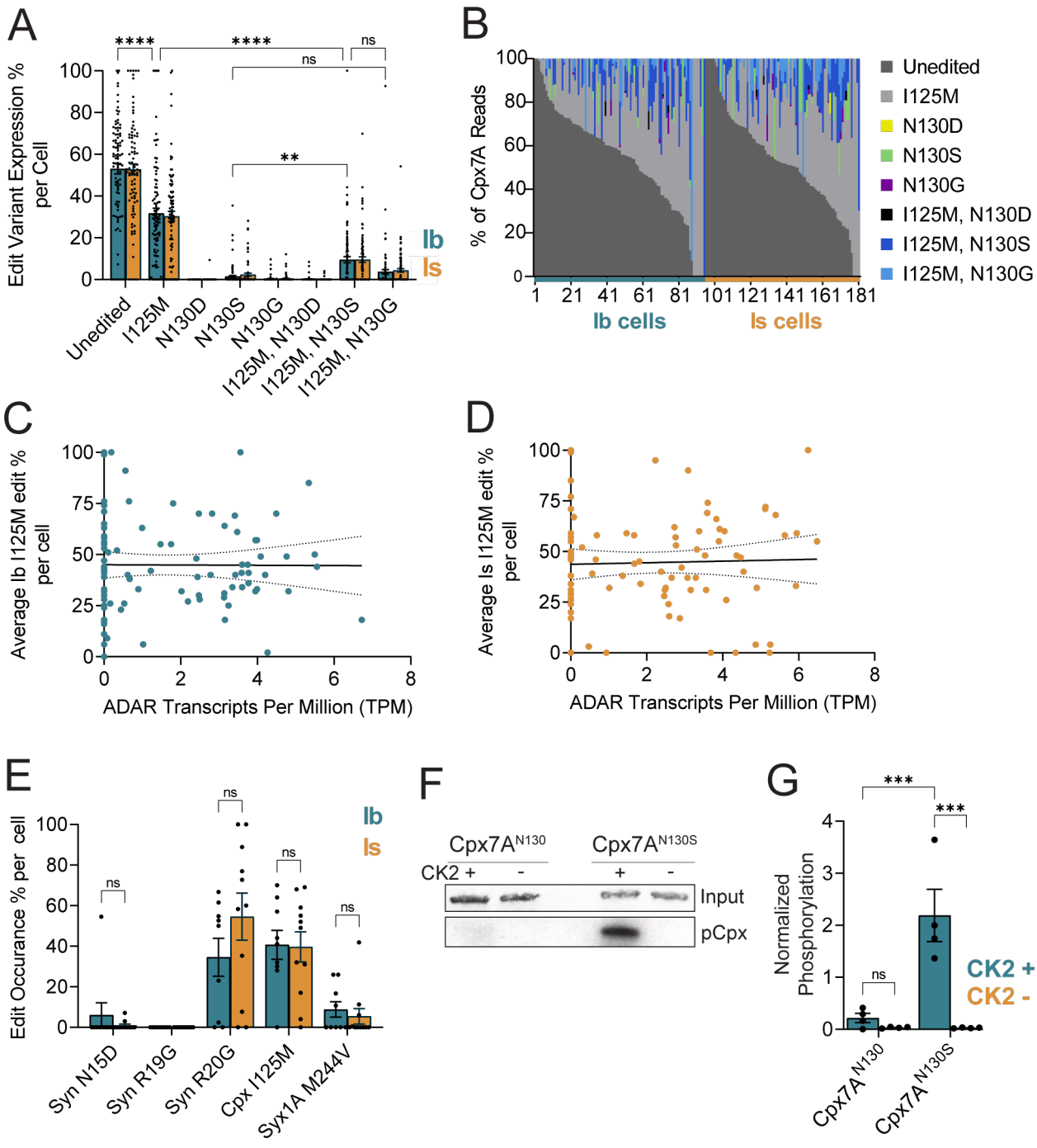
A
Edit Variant Expression % per Cell
****
****
ns
ns
**
Ib
Is
Unedited
I125M
N130D
N130S
N130G
I125M, N130D
I125M, N130S
I125M, N130G
B
% of Cpx7A Reads
Unedited
I125M
N130D
N130S
N130G
I125M, N130D
I125M, N130S
I125M, N130G
Ib cells
Is cells
C
Average Ib I125M edit % per cell
ADAR Transcripts Per Million (TPM)
D
Average Is I125M edit % per cell
ADAR Transcripts Per Million (TPM)
E
Edit Occurance % per cell
Ib
Is
Syn N15D
Syn R19G
Syn R20G
Cpx I125M
Syx1A M244V
F
Cpx7A N130
Cpx7A N130S
CK2 +
-
Input
pCpx
G
Normalized Phosphorylation
***
***
CK2 +
CK2 -
Cpx7A N130
Cpx7A N130S

Figure 5

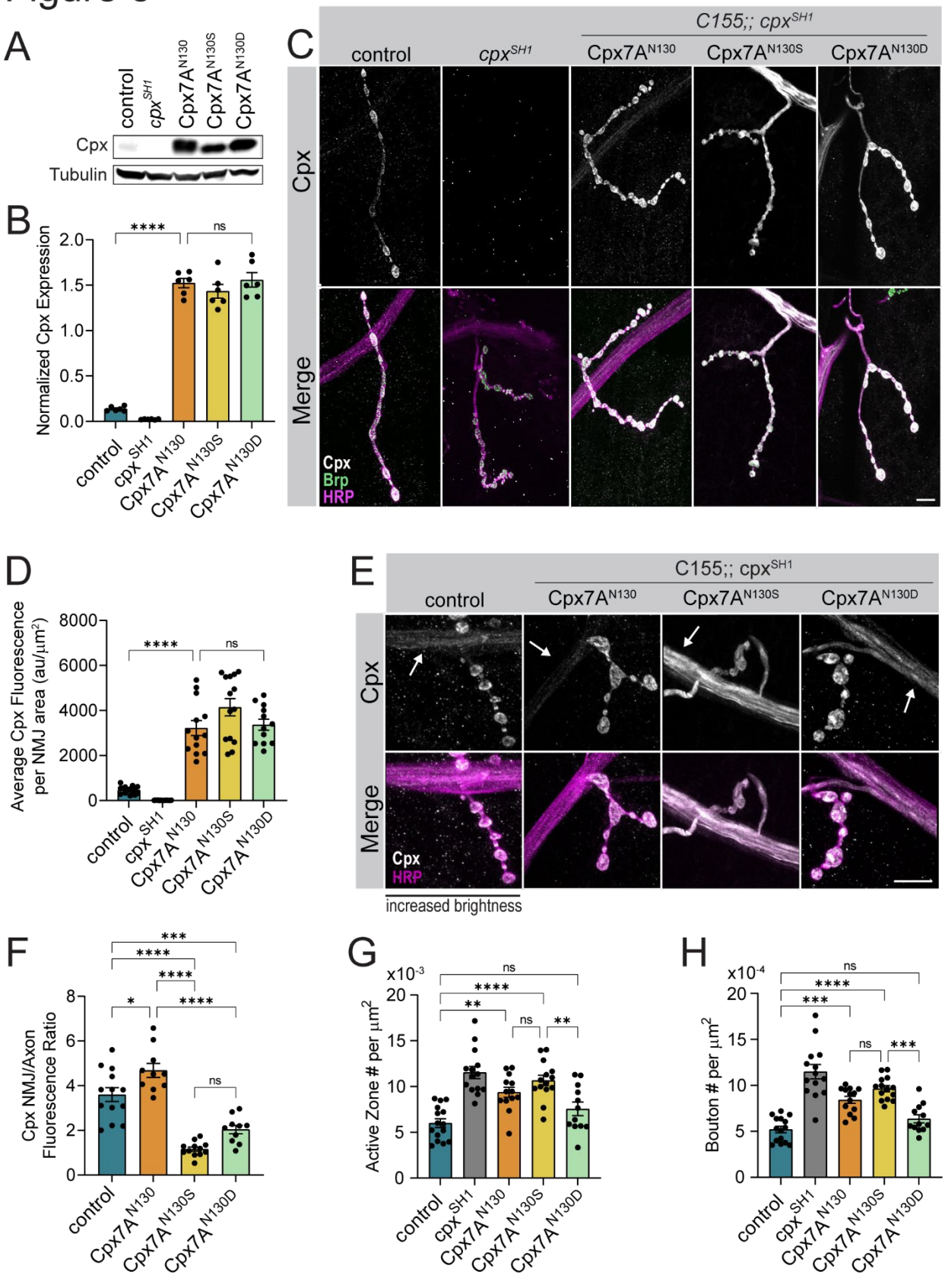
A
control
cpxSH1
Cpx7AN130
Cpx7AN130S
Cpx7AN130D
Cpx
Tubulin
B
Normalized Cpx Expression
2.0
1.5
1.0
0.5
0.0
****
ns
control
cpxSH1
Cpx7AN130
Cpx7AN130S
Cpx7AN130D
C
C155;; cpxSH1
control
cpxSH1
Cpx7AN130
Cpx7AN130S
Cpx7AN130D
Cpx
Merge
Cpx
Brp
HRP
D
Average Cpx Fluorescence per NMJ area (au/µm2)
8000
6000
4000
2000
0
****
ns
control
cpxSH1
Cpx7AN130
Cpx7AN130S
Cpx7AN130D
E
C155;; cpxSH1
control
Cpx7AN130
Cpx7AN130S
Cpx7AN130D
Cpx
Merge
Cpx
HRP
increased brightness
F
Cpx NMJ/Axon Fluorescence Ratio
8
6
4
2
0
***
****
****
*
****
ns
control
Cpx7AN130
Cpx7AN130S
Cpx7AN130D
G
Active Zone # per µm2
x10-3
20
15
10
5
0
ns
****
**
ns
**
control
cpxSH1
Cpx7AN130
Cpx7AN130S
Cpx7AN130D
H
Bouton # per µm2
x10-4
20
15
10
5
0
ns
****
***
ns
***
control
cpxSH1
Cpx7AN130
Cpx7AN130S
Cpx7AN130D

Figure 6

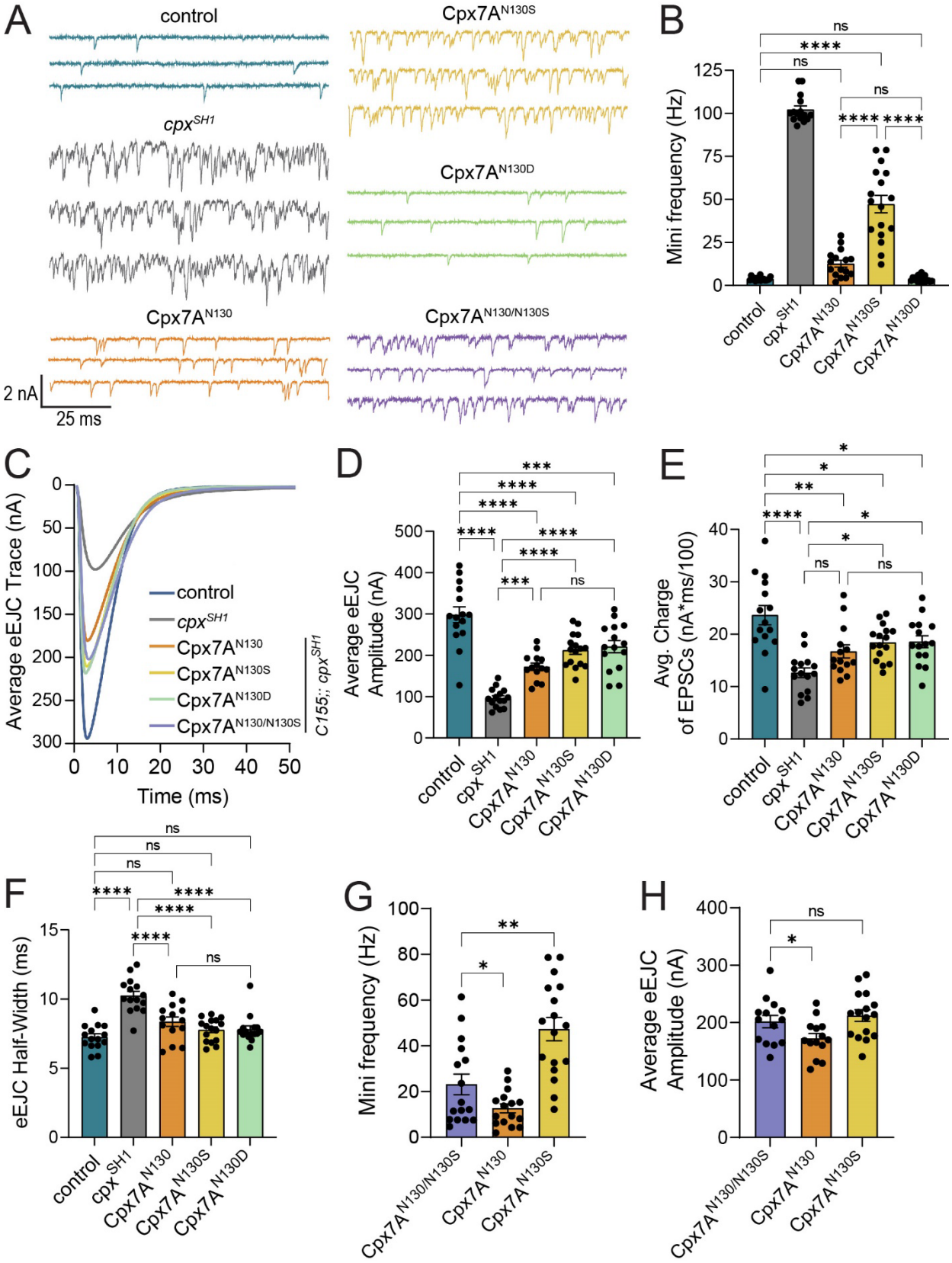
A
control
Cpx7A^N130S
cpx^SH1
Cpx7A^N130D
Cpx7A^N130
Cpx7A^N130/N130S
2 nA
25 ms
B
Mini frequency (Hz)
control
cpx SH1
Cpx7A N130
Cpx7A N130S
Cpx7A N130D
C
Average eEJC Trace (nA)
Time (ms)
control
cpx^SH1
Cpx7A^N130
Cpx7A^N130S
Cpx7A^N130D
Cpx7A^N130/N130S
C155;; cpx^SH1
D
Average eEJC Amplitude (nA)
E
Avg. Charge of EPSCs (nA*ms/100)
F
eEJC Half-Width (ms)
G
Mini frequency (Hz)
Cpx7A N130/N130S
Cpx7A N130
Cpx7A N130S
H
Average eEJC Amplitude (nA)

Chapter 3

Conclusions and Future Directions

Elizabeth A. Brija[1]

[1]Picower Institute for Learning and Memory, Department of Brain and Cognitive Sciences, Massachusetts Institute of Technology, Cambridge, MA 02139

3.1 Major Conclusions

In this thesis, I characterized functional roles for alternative splicing and RNA editing of the Cpx C-terminus. Cpx is a key regulatory protein for SV fusion that arrests SNAREs in a partially-zippered state (Bera et al., 2022; Brady et al., 2021; Bykhovskaia et al., 2013). Loss of the protein disrupts neurotransmission, leading to changes in synchronous, asynchronous, and spontaneous release (Huntwork & Littleton, 2007; Jorquera et al., 2012; Reim et al., 2001; Yang et al., 2010). In *Drosophila,* a single *cpx* gene produces two isoforms with different C-termini due to alternative splicing of exon 7 (Buhl et al., 2013), in which the Cpx7A isoform contains a conserved membrane-tethering prenylation CAAX motif (like mammalian Cpx3 and 4), while Cpx7B lacks this motif (like mammalian Cpx1 and 2) (Cho et al., 2010). Previous studies demonstrated Cpx7B is regulated by PKA phosphorylation of S126 residing within its C-terminal amphipathic helix (Cho et al., 2015; Lottermoser & Dittman, 2023). PKA phosphorylation of Cpx7B reduces its clamping function at NMJs, leading to elevated spontaneous release that triggers activity-induced structural plasticity (Cho et al., 2015). Cpx7A lacks this serine and is instead subject to RNA editing by ADAR at adjacent adenosine residues in the amphipathic C-terminal region to generate multiple Cpx7A proteins with unique C-terminal sequences: unedited N130, phospho-incompetent N130G, a phospho-mimetic N130D, or a potentially phospho-competent N130S near the Cpx7B S126 site implicated in plasticity (Buhl et al., 2013; Hoopengardner et al., 2003). Given Cpx7A is expressed at much higher levels than Cpx7B and is the dominant isoform in the *Drosophila* nervous system (Buhl et al., 2013), RNA editing at the N130 residue represents an attractive mechanism for regulating spontaneous release and structural plasticity across a larger population of neurons. However, no functional role for Cpx7A editing at *Drosophila* NMJs has previously been described.

Here I establish that splice isoforms Cpx7A and Cpx7B redundantly support synaptic transmission, with differential RNA editing of Cpx7A in single neurons altering Cpx7A clamping properties to fine-tune SV release and presynaptic output at NMJs. CRISPR gene-editing of Cpx7A and Cpx7B demonstrates striking expression level differences between the two isoforms in adult brains and larval NMJs, consistent with previous *in situ* hybridization and transcript expression data demonstrating Cpx7A is the predominant isoform (Buhl et al., 2013). However, despite a drastic difference in expression levels, we find both proteins are individually efficient at maintaining normal synaptic morphology and are largely functionally redundant at NMJs.

Expression of only the minor isoform Cpx7B ($cpx^{\Delta 7A}$) demonstrates a mild disruption in clamping abilities from control, but can largely rescue the increased spontaneous fusion rate (~90 Hz) seen in *cpx* null animals. These animals also demonstrate a mild increase in asynchronous release and a 46% reduction of synchronous release compared to control. Interestingly, these mutants also increase the speed of the onset of evoked release, suggesting Cpx7B has a unique role in regulating speed of evoked release that may be due to greater mobility of this non-prenylated protein. Expression of only the predominant Cpx7A isoform ($cpx^{\Delta 7B}$) demonstrates release kinetics that more closely resemble control with a mild 25% reduction in synchronous fusion, indicating both isoforms are required to support normal levels of evoked fusion. The higher Cpx expression found in $cpx^{\Delta 7B}$ mutants supports synchronous neurotransmission more than the reduced Cpx expression of $cpx^{\Delta 7A}$ mutants. These results are consistent with transgenic rescue data demonstrating Cpx7A is functionally better at clamping spontaneous release while Cpx7B is better at facilitating evoked fusion by enhancing the speed of evoked release, though both proteins largely rescue *cpx* null neurotransmission deficits (Buhl et al., 2013).

Although neurotransmitter release at the NMJ is largely intact, $cpx^{\Delta 7A}$ mutants demonstrate severe behavioral abnormalities in both larvae and adults, indicating Cpx7A has a more prominent role in supporting behavior. It is possible that other cell types not assayed in this study, such as cells of the CNS, are more reliant on Cpx7A expression than motoneurons. Additionally, other synaptic processes, such as vesicle cycling and synaptic plasticity, may be altered in $cpx^{\Delta 7A}$ mutants leading to behavioral deficits. In *cpx* null animals, synaptic vesicle recycling and maintenance dynamics are altered, affecting the immediate releasable pool (IRP) and the ready releasable pool (RRP), which are comprised of docked SVs and mobilized SVs to prevent vesicle depletion at AZs during stimulation, respectively (Jorquera et al., 2012). Assessment of vesicle pool kinetics within these isoform mutants will be imperative in characterizing a differential role for Cpx7A in regulating behavior and provide potential insights into why loss of Cpx7A is tolerated better at the NMJ. Alternatively, other neuronal subtypes may be more reliant on the Cpx7A splice isoform to support normal levels of synaptic transmission required for behavior. Taken together, both proteins function similarly at NMJs to clamp spontaneous fusion and facilitate evoked events, despite drastic differences in expression.

Although Cpx7A and Cpx7B can support spontaneous and evoked fusion, it is possible that different regulatory mechanisms are in place to alter the ability of Cpx proteins to interact with

SNARE complexes and lipid membranes. As previously discussed, Cpx7B function is regulated by activity-dependent PKA phosphorylation of its amphipathic C-terminus (Cho et al., 2015). However, a similar regulation of Cpx7A function had not been defined. To characterize Cpx7A regulation, we used single-neuron isoform Patch-seq RNA profiling, phosphorylation assays, and transgenic rescue to evaluate different possible regulatory mechanisms of Cpx7A function to examine the significance of Cpx7A RNA editing. Through use of previously published *Drosophila* single motoneuron RNAseq data (Jetti et al., 2023), we observed that single larval Ib and Is motoneurons maintain multiple Cpx7A edit transcripts, suggesting ADAR activity is not "all-or-none" in individual cells, but can instead vary the amount of editing per cell. Overall, Ib cells demonstrated an average editing transcript profile as follows: Unedited = 53%, I125M = 32%, N130D = 0.0%, N130S = 1.5%, N130G = 0.3%, I125M, N130D = 0.2%, I125M, N130S = 9.5%, I125M, N130G = 3.7%. Our results are generally consistent with editing values from previous individual cDNA sequencing (Buhl et al., 2013), supporting that I125M editing may make a potentially more stable or attractive substrate for ADAR to carry out editing at N130 sites, demonstrated by an increase in editing percent for all N130 variants in the presence of I125M editing. Additionally, a large percentage of unedited Cpx7A is maintained in cells with smaller amounts of edit variants N130S and N130G expressed, and notably, the N130D edit is rarely observed.

Since N130D editing originates from AAT to GAT codon editing, it is possible that all editing of GAT serves as a priming edit event for further editing to GGT, creating the glycine N130G edit variant. The region of RNA structure that immediately surrounds an editing site is thought to influence the binding surface for ADAR and may alter the efficiency of editing for adenosines with different 5' and 3' neighboring residues (Eggington et al., 2011; Polson & Bass, 1994; St Laurent et al., 2013). This may explain the extremely low percent of N130D edits observed, as most editing to create N130D (AAT to GAT) can be quickly converted to the double adenosine edit (GGT) of N130G, while editing to N130S (AGT) maybe be functionally stable itself and does not generally act as a priming event for N130G.

Interestingly, we observed no correlation between ADAR expression levels and Cpx7A editing, as measured by percent editing of the I125M site, suggesting that differential editing of Cpx7A in individual cells is not due to differential ADAR expression. However, it is possible that ADAR activity is still altered in individual cells, giving rise to cellular differences in editing

profiles. *Drosophila* ADAR is a target of developmentally- and activity-regulated auto-editing, which produces a less active form of the enzyme (Palladino et al., 2000a; Rieder et al., 2015). We attempted to characterize ADAR auto-editing in this dataset to correlate ADAR activity states with Cpx7A editing, but found that the ADAR editing site was not well-represented in the data. Future work will be needed to determine if auto-editing of ADAR contributes to cell-specific differences in Cpx7A editing rates.

As RNA editing of Cpx7A produces potential phospho-mimetic, phospho-incompetent, and phospho-competent substitutions in the amphipathic region of Cpx, we performed an *in vitro* kinase phosphorylation assay of unedited Cpx7A^{I125,N130} (termed Cpx7A^{N130}) and edit variant Cpx7A^{I125M,N130S} (termed Cpx7A^{N130S}) to understand if the N130S site is indeed phospho-competent, which may provide an avenue for Cpx regulation. We found CK2 can selectively phosphorylate Cpx7A^{N130S}, supporting editing of the N130 to a serine creates a phospho-competent variant of the Cpx7A protein. Further mass spectrometry analysis will be needed to determine if the N130 site is phosphorylated *in vivo*, however, these findings support an interesting model for Cpx7A regulation through CK2-dependent phosphorylation. Mammalian Cpx1 and 2 (non-CAAX proteins) have been shown to undergo CK2 phosphorylation which leads to a higher affinity for SNARE complexes (Shata et al., 2007), suggesting CK2 phosphorylation of the N130S site may similarly allow the Cpx7A^{N130S} edit variant to associate with SNAREs more efficiently to alter its clamping properties. Future perturbations of CK2 activity, such as CK2 activity mutants or phosphorylation inhibitors, will be required to understand if the N130S phospho-competent site serves as a regulatory switch for Cpx function, similar to the activity-dependent PKA phosphorylation of Cpx7B (Cho et al., 2015).

After observing expression of multiple Cpx7A edit variants, including a phospho-competent edit variant, we sought to functionally characterize the impact of Cpx7A RNA editing on its function as a neurotransmission regulatory protein. We used pan-neuronal transgenic rescue of *cpx* null animals which demonstrate increased spontaneous fusion rates and a corresponding synaptic overgrowth phenotype at NMJs. Surprisingly, we found that incorporation of the phospho-competent site N130S produced a Cpx protein that was functionally inferior to a Cpx protein that incorporates the N130D phospho-mimetic site. This contrasts to the observed role for phospho-competent Cpx7B S126 site, in which phospho-mimetic S126D expression is less efficient at clamping spontaneous fusion and displays an overgrowth phenotype (Cho et al., 2015).

Instead of SV association, animals expressing Cpx7A^{N130S} or Cpx7A^{I125M,N130D} (termed Cpx7A^{N130D}) showed Cpx mislocalization to axons, suggesting altered SV tethering abilities of both edit variants. Conversely, animals rescued with Cpx7A^{N130} largely expressed NMJ-localized Cpx that appeared enhanced at AZs, resembling the enhanced AZ localization observed when Cpx7A prenylation is perturbed (Iyer et al., 2013; Robinson et al., 2018).

Despite mislocalization to axons, Cpx7A^{N130D} animals rescued synaptic overgrowth and spontaneous clamping function, similar to control. Since Cpx7A^{N130S} demonstrated a more severe mislocalization, it is possible that the elevated transgenic expression levels of Cpx7A^{N130D} combined with some capabilities for SV localization is sufficient for Cpx7A^{N130D} to efficiently interact with SNAREs and lipids to regulate fusion, while Cpx7A^{N130S} cannot efficiently tether SVs and thus, cannot clamp spontaneous fusion as well as the other edit variants. Additionally, Cpx7A^{N130} may hyperlocalize to AZs where it can interact with nearby SNAREs but is not diffusible and thus, cannot move to new areas where its regulatory function is required, creating only a partial rescue of Cpx function. This may be due to altered stability of the amphipathic helix caused by RNA editing at N130, which may change membrane associations of Cpx proteins required for localization and function (Snead et al., 2014; Wragg et al., 2013).

An alternative model is that Cpx7A localization does not alter Cpx's abilities to function as an SV fusion regulator, but instead, the N130 site causes a structural change within the edit variants to modulate clamping function. In the case of Cpx7A^{N130S}, this change may be linked to CK2 phosphorylation of this site and perhaps, possession of a negative charge on the hydrophilic face (as seen in phospho-mimetic Cpx7A^{N130D} or by phosphorylation of Cpx7A^{N130S}) may help Cpx associate with assembling SNAREpins even with altered membrane-interactions, as seen with CK2 phosphorylation of the mammalian Cpx1 and 2 C-terminal amphipathic region (Shata et al., 2007). Interestingly, co-expression of Cpx7A^{N130} with Cpx7A^{N130S} produced an intermediate clamping phenotype, suggesting multiple Cpx proteins bind assembling SNAREpins simultaneously to assert independent forces to fine-tune SV fusion kinetics and presynaptic output. Taken together, the structure and localization of Cpx7A edit variants may play important roles in modulating Cpx control of SV fusion.

The data presented in this thesis establish and characterize a novel functional role for RNA editing of Cpx7A in regulating SV fusion at *Drosophila* NMJs. RNA editing of the amphipathic C-terminal region of Cpx7A produces multiple Cpx7A edit variants simultaneously within single

cells, in which phosphorylation of the phospho-competent Cpx7A variant may serve as a regulatory switch for Cpx function and localization within synapses. Future studies of the molecular mechanisms which underlie Cpx7A's ability to interact with membranes and assembling SNAREpins will be critical to dissecting a role for CK2 phosphorylation and activity-dependent regulation of ADAR-mediated editing in fine-tuning Cpx regulation of neurotransmission.

3.2 Future Directions

We have demonstrated that RNA editing of the C-terminus of the SNARE-binding protein Cpx regulates its ability to clamp SNARE-mediated SV fusion and can fine-tune presynaptic output. In addition, RNA editing of Cpx within single neurons is stochastic, generating multiple edit variants that fine-tune neurotransmitter release by altering its function. However, many questions remain about the regulatory mechanisms underlying Cpx7A and 7B function at synapses. A few possible future directions to address these questions will be discussed in this section.

Defining distinct roles for Cpx7A and Cpx7B

We demonstrated that alternative splicing to generate Cpx7A and Cpx7B creates two proteins with largely redundant roles in regulating SV fusion at NMJs. However, mutants that have lost Cpx7A, the dominant isoform that is subject to RNA editing, demonstrate a significant reduction in Cpx expression and have striking behavioral deficits, indicating these proteins have a capacity to serve different functional roles. One explanation is that specific cells not assayed in this study are more reliant on Cpx7A function than *Drosophila* Type I motoneurons. For instance, loss of Cpx expression seen in $cpx^{\Delta 7A}$ mutants may specifically affect excitatory or inhibitory neuronal populations in a synapse-specific manner in the brain that regulate locomotion. However, preliminary observations of heterozygote CRISPR $cpx^{\Delta 7A}/cpx^{\Delta 7B}$ double mutants (expressing one endogenous allele for each splice isoform) only partially rescue the severe behavioral deficit observed in $cpx^{\Delta 7A}$ mutant adults (data not shown). This observation suggests locomotion requires broader pan-neuronal Cpx7A expression and may be dosage-sensitive to Cpx7A.

In future studies, spatial transcriptomic analysis of the central and peripheral nervous systems may elucidate spatial expression profiles of both Cpx splice isoforms in distinct neuronal classes, such as excitatory, inhibitory, and peptidergic neurons. Based on spatial profiling data, we can use whole-cell patch-clamp and optical recordings of central synapses to physiologically

characterize cells that show robust differences in Cpx isoform expression. Taken together, cell-type specific profiling will help determine the role of each Cpx isoform in regulating neurotransmission properties across a broad range of synapses and may offer explanation for the striking behavioral differences seen between the splicing mutants.

Given this potentially dosage-sensitive rescue of behavior, it is possible that specific SV cycling kinetics are altered by loss of Cpx7A, such as use and maintenance of SV pools, which may function to regulate depression and facilitation dynamics associated with synaptic plasticity. Cpx expression is required for maintenance of the IRP and RRP of vesicles (Jorquera et al., 2012), supporting a model in which the reduced Cpx expression observed in $cpx^{\Delta 7A}$ mutants could change SV pools that are critical for neuronal communication during high-frequency tetanic stimulation. Examination of how Cpx7A regulates short-term plasticity and SV pools during high-frequency tetanic stimulation (10 Hz) will allow for assessment of the IRP and RRP size. The IRP is measured through initial SV depletion, observed as the rapid and transient depression of physiological response to a sustained lower response value observed within the first 10-15 stimuli. We can then calculate the RRP by measuring response recovery through recruitment of vesicles from the RRP, which is observed as a slower depression in physiological response out to the ~1000^{th} stimuli before the cell reaches steady-state SV recycling dynamics. Assessment of pool size can also be validated with electron microscopy of the synapse to examine the number of docked and AZ-associated SVs.

As Cpx7B lacks a membrane-tethering CAAX motif, we expect the Cpx7B isoform to have increased mobility within synapses, while Cpx7A will be more concentrated at release sites, allowing the Cpx isoforms to participate in different functional roles (discussed in section 1.4). However, no detectable mislocalization of Cpx7B to axons was observed in CRISPR mutants, unlike results from the transgenic Cpx7A edit variant rescue experiments. This may be due to lower endogenous Cpx expression instead of overexpression, making it more difficult to see changes in localization. Future experiments can be performed to determine whether Cpx7A and Cpx7B differentially localize within the larval NMJ. Isoform-specific CRISPR mutants were generated through a split-GFP system, in which either exon 7A or 7B is endogenously-tagged with a single GFP_{11} fragment (small tag) that will fluoresce when in contact with GFP_{1-10} (large cytosolic part of GFP, expressed through Gal4-UAS system) (Kamiyama et al., 2021). However, background fluorescence from GFP_{1-10} was too high to observe Cpx localization signals. This

system can be optimized by creating CRISPR Cpx strains with tandem GFP_{11} fragments to multiply the observed signal associated with the Cpx proteins. Additionally, super-resolution microscopy or immuno-electron microscopy of the CRISPR mutants can provide the necessary resolution to distinguish subcellular localization of each isoform and determine if Cpx7B is indeed more diffuse than Cpx7A, potentially allowing different functions for each splice isoform.

Taken together, the altered behavior of $cpx^{\Delta 7A}$ mutants, along with a possible toolkit to assess subcellular localization specific to Cpx7A, provides an excellent opportunity to screen for interacting proteins that suppress the behavioral phenotype seen when Cpx7A is lost. A suppressor screen will provide insight into the interacting components of spontaneous and evoked SV fusion pathways, as well as Cpx7A membrane interactions that help localize Cpx proteins to release sites where it is needed to regulate assembling SNARE complexes. This work will continue to define distinct roles for splice isoforms Cpx7A and 7B and elucidate the molecular pathways involved in the regulation of neurotransmission.

Phosphorylation as a regulatory mechanism for Cpx7A function

In this thesis, we demonstrated that the Cpx7A edit variant $Cpx7A^{N130S}$ is subject to phosphorylation by CK2. As previously discussed, phosphorylation of the Cpx7B splice isoform plays an important role in functional and structural synaptic plasticity, but a similar regulatory phosphorylation event for Cpx7A function has not been characterized. Using *in vitro* kinase assays, we determined that the $Cpx7A^{N130S}$ edit variant was phospho-competent and phosphorylated by CK2. We have not yet recapitulated this Cpx7A phosphorylation *in vivo*. To that end, future studies of CK2 and $Cpx7A^{N130S}$ phosphorylation will be essential to understanding if Cpx7A function can be regulated by phosphorylation of its C-terminus. This work is especially pertinent given the established role for CK2 in synaptic organization and stability of *Drosophila* NMJs (Bandyopadhyay et al., 2016; Bulat et al., 2014), and evidence that CK2 pharmacological inhibition at the frog NMJ results in ~100-fold increase in spontaneous fusion (Rizzoli & Betz, 2002), suggesting CK2 activity plays an important role in SV fusion and synaptic stability pathways.

To address the question of N130S site-specific phosphorylation, we generated a Cpx7A protein with a mutated CK2 consensus sequence. Unlike unedited $Cpx7A^{N130}$, expression of the C-terminal N130S edit creates a predicted CK2 consensus sequence S/T E/D found in a small

percent of CK2 targets, in which phosphorylation of the serine residue (pS) in Cpx7A can also act as a "primed" consensus sequence for a more commonly observed S/T-x-x-E/D/pS sequence contained within the Cpx7A^{N130S} C-terminus (x=unspecified amino acid) (Bulat et al., 2014; Guerra et al., 1999; Meggio et al., 1998). Thus, we generated and purified Cpx7A^{I125M,T127A,N130S} (termed Cpx7A^{T127A}) to determine if phosphorylation of N130S can act as a priming phosphorylation event for T127. Preliminary results demonstrate that the altered CK2 consensus sequence created through phospho-incompetent T127A mutation reduces measured Cpx phosphorylation by half in comparison to Cpx7A^{N130S} when reactions were incubated with CK2 (**Figure 1A, B**; Cpx7A^{N130S}: 2.187±0.502 normalized pCpx level, n=4; Cpx7A^{T127A}: 0.900±0.732 normalized pCpx level, n=2, p=0.1333), indicating site T127 is important for Cpx7A^{N130S} phosphorylation, but T127 is not phospho-competent itself without the presence of N130S (Cpx7A^{N130}: 0.216±0.088 normalized pCpx level, n=4).

We attempted to validate phosphorylation of the endogenous Cpx7A N130S and Cpx7B S126 sites through mass spectrometry, but were only successful in observing Cpx7B S126 phosphorylation. Cpx7A edit variants were not detected by mass spectrometry, preventing observation of the C-terminal phosphorylation event. Sample preparation should be repeated and alignment of fragments carried out with the consideration of various C-terminal edit variants. Once edit variant representation is confirmed within sample preparations, detection of phosphorylation at N130S or T127 should be possible. Moreover, future functional and structural studies of Cpx7A^{N130S} in the context of CK2 inhibition, such as use of the CK2 *Drosophila* mutant, *Timekeeper* (*CK2α-Tik*), or other pharmacological CK2 inhibitors (reviewed in: Bandyopadhyay et al., 2016; Guerra et al., 1999), will be essential for testing phosphorylation-dependent regulation of Cpx7A^{N130S} function and localization at synapses. Since co-expression of unedited and phospho-competent Cpx7A demonstrated the Cpx7A^{N130S} edit variant can act in a dominant fashion, these experiments, along with SNARE binding assays, will elucidate the mechanism by which Cpx7A^{N130S} interacts with SNAREs and SV membrane to regulate fusion.

Role for RNA editing in synaptic plasticity

Although we characterized a functional role for RNA editing of the Cpx C-terminus, the role of RNA editing in Cpx-mediated synaptic plasticity is unknown. Previous work demonstrated an ability for ADAR activity to be modulated by spatial, temporal, and environmental factors

(discussed in section 1.5; Palladino et al., 2000a; Rieder et al., 2015; Sanjana et al., 2012), suggesting the frequency of Cpx editing may be modulated by intrinsic cellular activity, allowing dynamic changes to Cpx function within single cells. To assess RNA editing activity within single cells, we sought to characterize ADAR expression and ADAR editing states. Since ADAR is a target of auto-editing (Palladino et al., 2000a), we used expression of the edited ADAR transcript as a proxy for reduced ADAR activity. However, we found no correlation between ADAR expression and Cpx7A editing level, and we were unable to determine the editing state of ADAR within our RNAseq dataset. To address this issue, additional single-cell RNAseq of the adult brain and of activity mutants, such as the voltage-gated potassium channel mutant *Shaker*, can be completed to assess altered cellular activity levels and effects of activity on RNA editing. These experiments will provide access to define the dynamics of Cpx editing that contribute to altered synaptic properties in different cellular environments.

Additionally, we can characterize the role of RNA editing in activity-dependent structural and functional synaptic plasticity (discussed in section 1.4 and in Cho et al., 2015). Briefly, functional plasticity can be tested by using high-frequency stimulation and measuring changes in spontaneous fusion rates, in which plasticity is observed as an increase in mini frequency that is sustained for several minutes after stimulation. Structural plasticity can be induced by rearing animals at a higher temperature (29 °C) and measuring synaptic growth changes (AZ and bouton number) compared to low temperature rearing conditions (25 °C). The structural growth observed at high temperatures corresponds to an increase in synaptic signaling, as *Drosophila* NMJ growth is regulated by motoneuron activity and larval locomotion is enhanced at this elevated temperature (Banerjee et al., 2021; Budnik et al., 1990; Cho et al., 2015; Choi et al., 2014; Sigrist et al., 2003). Consequently, *cpx* null animals that demonstrate a baseline elevation of spontaneous fusion rates cannot participate in these activity-dependent synaptic plasticity pathways (Cho et al., 2015).

Preliminary structural growth analysis (muscle 6/7 Type Ib and Is motoneurons; abdominal segment A3) in *Drosophila adar* mutants ($adar^{5G1}$) indicates that loss of ADAR activity does not significantly alter baseline synaptic growth (**Figure 2A, B**; 14.6% reduction in normalized bouton number in *adar* mutants compared to control; p=0.2752), but does prevent activity-dependent structural plasticity (**Figure 2A, C**). At the higher temperature, control animals demonstrate a significant ~50% increase in bouton number per muscle area compared to the lower temperature (p=0.0165), while *adar* mutants exhibit a ~30% reduction in bouton number per muscle area in

these same conditions (p=0.4580), supporting a role for ADAR-mediated RNA editing in activity-dependent structural synaptic plasticity. However, it is worth noting that previous studies of *adar* mutants demonstrate a slight (~10%) baseline increase in bouton number at this same NMJ when compared to controls, though this percentage has not been normalized to muscle area as was done in **Figure 2B** (Maldonado et al., 2013). Given this discrepancy, future experiments should be completed to measure synaptic growth in *adar* mutants and determine if loss of *adar* leads to synaptic overgrowth at NMJs before proceeding with structural and functional synaptic plasticity assays.

After validating a role for ADAR in synaptic plasticity, the role of each Cpx7A edit variant in plasticity should be dissected. Using the same transgenic constructs described in this thesis, activity-dependent structural and functional plasticity can be evaluated with each rescue line. Preliminary results suggest all Cpx7A edit variants may support temperature-dependent structural synaptic plasticity except for $Cpx7A^{N130S}$, the edit variant that demonstrates limited spontaneous fusion clamping abilities and thus, most closely resembles *cpx* null animals that cannot participate in activity-dependent plasticity (**Figure 3A, B**; control: +35%; cpx^{SH1}: -13%; $Cpx7A^{N130}$: +39%; $Cpx7A^{N130S}$: -6%; $Cpx7A^{N130D}$: +44%; value represented is positive (+) or negative (-) percent change in bouton number normalized to muscle area between high and low temperature conditions per genotype). Due to the variability within this data and the difficulty in finding age-matched larvae, comparisons between temperature conditions within each genotype were not significant. This transgenic rescue plasticity experiment can be repeated using a greater temperature difference (18 °C and 29 °C) to exaggerate measurable synaptic growth.

Additionally, if ADAR regulates synaptic plasticity, double mutant experiments in $adar^{5G1}/cpx^{SH1}$ backgrounds with selective rescue by individual Cpx7A edit variant constructs will determine if ADAR's function in plasticity is through Cpx-mediated pathways or by ADAR-mediated editing of other synaptic proteins, such as the voltage-gated sodium channel *Para* (Palladino et al., 2000b). Together, these experiments will help define a role for RNA editing of the Cpx C-terminus in activity-dependent synaptic plasticity.

3.3 Materials and Methods

Drosophila stocks

Flies were cultured on standard medium and maintained at 25 °C (low) or 29 °C (high) incubator temperature. Age-matched late 3rd instar male larvae were used for imaging experiments. Experiments were performed with *adar*^{5G1} mutants and control (cantonized *adar*^{5G1}) generously gifted from Robert A. Reenan (Brown University, Providence, RI, USA) and with control, *cpx* null, and Cpx7A rescue lines described in Chapter 2.

Immunohistochemistry

Larvae were dissected in hemolymph-like HL3.1 solution (in mM: 70 NaCl, 5 KCl, 4 $MgCl_2$, 10 NaHCO3, 5 trehalose, 115 sucrose, 5 HEPES, pH 7.18) and fixed in 4% paraformaldehyde for 18 minutes. Larvae were washed three times for five minutes with PBST (PBS containing 0.1% Triton X-100), followed by a thirty-minute incubation in block solution (5% NGS in PBST). Fresh block solution and primary antibodies were added. Samples were incubated overnight at 4°C and washed with two short washes and three extended 20 minutes washed in PBST. PBST was replaced with block solution and fluorophore-conjugated secondary antibodies were added. Samples were incubated at room temperature for two hours. Finally, larvae were rewashed with PBST and mounted in Vectashield (Vector Laboratories, Burlingame, CA). Antibodies used for this study include: mouse anti-Brp, 1:500 (NC82; Developmental Studies Hybridoma Bank (DSHB), Iowa City, IA)); rabbit anti-Cpx, 1:5000 (Huntwork & Littleton, 2007); goat anti-rabbit Alexa Fluor 488, 1:500 (A-11008; ThermoFisher Scientific, Waltham, MA, USA); goat anti-mouse Alexa Fluor 546, 1:500 (A-11030; ThermoFisher); DyLight 649 conjugated anti-HRP, 1:500 (#123-605-021; Jackson Immuno Research, West Grove, PA, USA).

Confocal imaging and imaging data analysis

Immunoreactive proteins were imaged on a Zeiss Pascal confocal microscope (Carl Zeiss Microscopy, Jena, Germany) using 63X 1.3 NA oil-immersion objective (Carl Zeiss Microscopy). Images were processed with the Zen (Zeiss) software. A 3D image stack was acquired for each NMJ imaged (muscle 6/7 Ib/Is of abdominal segment A3) and merged into a single plane for 2D analysis using FIJI image analysis software (Schindelin et al., 2012). No more than two NMJs

were analyzed per larva. HRP labeling was used to identify neuronal tissue (NMJ) and quantify synaptic bouton number. Muscle 6/7 area was used to normalize quantifications.

Purification of Complexin for in vitro phosphorylation assays

QuikChange Lightning (Agilent) was used for site-directed mutagenesis of unedited Cpx7A to generate $Cpx7A^{I125M,N130S}$ (termed N130S) and $Cpx7A^{I125M,T127A,N130S}$ (termed T127A). Recombinant Cpx fused with GST was expressed in E. coli (BL21) and purified using glutathione sepharose 4B (Fisher Scientific). Peak fractions were concentrated and further purified by gel filtration as previously described (Cho et al., 2015). *In vitro* kinase assays were performed using purified recombinant Cpx proteins and the catalytic subunit of CK2 (C70-10G, SignalChem). Briefly, 10 mg of purified GST-fusion protein (unedited Cpx7A, N130S, or T127A) was used per reaction and incubated with 2,500 units of recombinant kinase and [^{32}P]ATP (Perkin Elmer). Reaction products were separated by SDS-PAGE and gels were stained with Bio-Safe Coomassie Blue (Bio-Rad), dried, and exposed to autoradiography film at room temperature. Mean integrated density of each band was quantified using FIJI and relative density of phospho-Cpx (pCpx) was calculated by normalizing to input band intensity determined by Coomassie staining.

Experimental design and statistical analysis

Statistical analysis and plot generation were performed using GraphPad Prism (San Diego, CA, USA). Appropriate sample size was determined using a normality test. Statistical significance for comparisons of two groups was determined by a Student's t-test. For comparisons of three or more groups of data, a one-way ANOVA followed by Tukey's Multiple Comparisons test was used to determine significance. For comparisons of two factors with three or more groups of data, a two-way ANOVA was used followed by Tukey's Multiple Comparisons test. The mean of each distribution is plotted in figures with individual datapoints also shown. Figure legends report mean±SEM, and *n*. Asterisks indicate the following *p*-values: *, $p < 0.05$; **, $p < 0.01$; ***, $p < 0.001$; ****, $p < 0.0001$, with ns=not significant.

References

Bandyopadhyay, M., Arbet, S., Bishop, C., & Bidwai, A. (2016). Drosophila Protein Kinase CK2: Genetics, Regulatory Complexity and Emerging Roles during Development. *Pharmaceuticals*, *10*(4), 4. https://doi.org/10.3390/ph10010004

Banerjee, S., Vernon, S., Jiao, W., Choi, B. J., Ruchti, E., Asadzadeh, J., Burri, O., Stowers, R. S., & McCabe, B. D. (2021). Miniature neurotransmission is required to maintain Drosophila synaptic structures during ageing. *Nature Communications*, *12*(1), 4399. https://doi.org/10.1038/s41467-021-24490-1

Bera, M., Ramakrishnan, S., Coleman, J., Krishnakumar, S. S., & Rothman, J. E. (2022). Molecular determinants of complexin clamping and activation function. *ELife*, *11*, e71938. https://doi.org/10.7554/eLife.71938

Brady, J., Vasin, A., & Bykhovskaia, M. (2021). The Accessory Helix of Complexin Stabilizes a Partially Unzippered State of the SNARE Complex and Mediates the Complexin Clamping Function *In Vivo*. *Eneuro*, *8*(2), ENEURO.0526-20.2021. https://doi.org/10.1523/ENEURO.0526-20.2021

Budnik, V., Zhong, Y., & Wu, C. (1990). Morphological plasticity of motor axons in Drosophila mutants with altered excitability. *The Journal of Neuroscience*, *10*(11), 3754–3768. https://doi.org/10.1523/JNEUROSCI.10-11-03754.1990

Buhl, L. K., Jorquera, R. A., Akbergenova, Y., Huntwork-Rodriguez, S., Volfson, D., & Littleton, J. T. (2013). Differential regulation of evoked and spontaneous neurotransmitter release by C-terminal modifications of complexin. *Molecular and Cellular Neuroscience*, *52*, 161–172. https://doi.org/10.1016/j.mcn.2012.11.009

Bulat, V., Rast, M., & Pielage, J. (2014). Presynaptic CK2 promotes synapse organization and stability by targeting Ankyrin2. *Journal of Cell Biology*, *204*(1), 77–94. https://doi.org/10.1083/jcb.201305134

Bykhovskaia, M., Jagota, A., Gonzalez, A., Vasin, A., & Littleton, J. T. (2013). Interaction of the Complexin Accessory Helix with the C-Terminus of the SNARE Complex: Molecular-Dynamics Model of the Fusion Clamp. *Biophysical Journal*, *105*(3), 679–690. https://doi.org/10.1016/j.bpj.2013.06.018

Cho, R. W., Buhl, L. K., Volfson, D., Tran, A., Li, F., Akbergenova, Y., & Littleton, J. T. (2015). Phosphorylation of Complexin by PKA Regulates Activity-Dependent Spontaneous Neurotransmitter Release and Structural Synaptic Plasticity. *Neuron*, *88*(4), 749–761. https://doi.org/10.1016/j.neuron.2015.10.011

Cho, R. W., Song, Y., & Littleton, J. T. (2010). Comparative analysis of Drosophila and mammalian complexins as fusion clamps and facilitators of neurotransmitter release. *Molecular and Cellular Neuroscience*, *45*(4), 389–397. https://doi.org/10.1016/j.mcn.2010.07.012

Choi, B. J., Imlach, W. L., Jiao, W., Wolfram, V., Wu, Y., Grbic, M., Cela, C., Baines, R. A., Nitabach, M. N., & McCabe, B. D. (2014). Miniature Neurotransmission Regulates Drosophila Synaptic Structural Maturation. *Neuron*, *82*(3), 618–634. https://doi.org/10.1016/j.neuron.2014.03.012

Eggington, J. M., Greene, T., & Bass, B. L. (2011). Predicting sites of ADAR editing in double-stranded RNA. *Nature Communications*, *2*(1), 319. https://doi.org/10.1038/ncomms1324

Guerra, B., Boldyreff, B., Sarno, S., Cesaro, L., Issinger, O.-G., & Pinna, L. A. (1999). CK2A Protein Kinase in Need of Control. *Pharmacology & Therapeutics*, *82*(2–3), 303–313. https://doi.org/10.1016/S0163-7258(98)00064-3

Hoopengardner, B., Bhalla, T., Staber, C., & Reenan, R. (2003). Nervous System Targets of RNA Editing Identified by Comparative Genomics. *Science*, *301*(5634), 832–836. https://doi.org/10.1126/science.1086763

Huntwork, S., & Littleton, J. T. (2007). A complexin fusion clamp regulates spontaneous neurotransmitter release and synaptic growth. *Nature Neuroscience*, *10*(10), 1235–1237. https://doi.org/10.1038/nn1980

Iyer, J., Wahlmark, C. J., Kuser-Ahnert, G. A., & Kawasaki, F. (2013). Molecular mechanisms of COMPLEXIN fusion clamp function in synaptic exocytosis revealed in a new Drosophila mutant. *Molecular and Cellular Neuroscience*, *56*, 244–254. https://doi.org/10.1016/j.mcn.2013.06.002

Jetti SK, Crane ASB, Akbergenova Y, Aponte-Santiago NA, Cunningham KL, Whittaker CA, Littleton JT (2023). Molecular logic of synaptic diversity between drosophila tonic and phasic motoneurons. BioRxiv.

Jorquera, R. A., Huntwork-Rodriguez, S., Akbergenova, Y., Cho, R. W., & Littleton, J. T. (2012). Complexin Controls Spontaneous and Evoked Neurotransmitter Release by Regulating the Timing and Properties of Synaptotagmin Activity. *Journal of Neuroscience*, *32*(50), 18234–18245. https://doi.org/10.1523/JNEUROSCI.3212-12.2012

Kamiyama, R., Banzai, K., Liu, P., Marar, A., Tamura, R., Jiang, F., Fitch, M. A., Xie, J., & Kamiyama, D. (2021). Cell-type–specific, multicolor labeling of endogenous proteins with split fluorescent protein tags in *Drosophila*. *Proceedings of the National Academy of Sciences*, *118*(23), e2024690118. https://doi.org/10.1073/pnas.2024690118

Lottermoser, J. A., & Dittman, J. S. (2023). Complexin Membrane Interactions: Implications for Synapse Evolution and Function. *Journal of Molecular Biology*, 167774. https://doi.org/10.1016/j.jmb.2022.167774

Maldonado, C., Alicea, D., Gonzalez, M., Bykhovskaia, M., & Marie, B. (2013). Adar is essential for optimal presynaptic function. *Molecular and Cellular Neuroscience*, *52*, 173–180. https://doi.org/10.1016/j.mcn.2012.10.009

Meggio F, Boulton AP, Marchiori F, Borin G, Lennon DP, Calderan A, Pinna LA. Substrate-specificity determinants for a membrane-bound casein kinase of lactating mammary gland. A study with synthetic peptides. Eur J Biochem. 1988 Nov 1;177(2):281-4. doi: 10.1111/j.1432-1033.1988.tb14374.x.

Palladino, M. J., Keegan, L. P., O'Connell, M. A., & Reenan, R. A. (2000a). DADAR, a Drosophila double-stranded RNA-specific adenosine deaminase is highly developmentally regulated and is itself a target for RNA editing. *RNA*, *6*(7), 1004–1018. https://doi.org/10.1017/S1355838200000248

Palladino, M. J., Keegan, L. P., O'Connell, M. A., & Reenan, R. A. (2000b). A-to-I Pre-mRNA Editing in Drosophila Is Primarily Involved in Adult Nervous System Function and Integrity. *Cell*, *102*(4), 437–449. https://doi.org/10.1016/S0092-8674(00)00049-0

Polson, A. G., & Bass, B. L. (1994). Preferential selection of adenosines for modification by double-stranded RNA adenosine deaminase. *The EMBO journal*, *13*(23), 5701-5711. https://doi.org/10.1002/j.1460-2075.1994.tb06908.

Reim, K., Mansour, M., Varoqueaux, F., McMahon, H. T., Südhof, T. C., Brose, N., & Rosenmund, C. (2001). Complexins Regulate a Late Step in Ca2+-Dependent Neurotransmitter Release. *Cell*, *104*(1), 71–81. https://doi.org/10.1016/S0092-8674(01)00192-1

Rieder, L. E., Savva, Y. A., Reyna, M. A., Chang, Y.-J., Dorsky, J. S., Rezaei, A., & Reenan, R. A. (2015). Dynamic response of RNA editing to temperature in Drosophila. *BMC Biology*, *13*(1), 1–16. https://doi.org/10.1186/s12915-014-0111-3

Rizzoli, S. O., & Betz, W. J. (2002). Effects of 2-(4-Morpholinyl)-8-Phenyl-4H-1-Benzopyran-4-One on Synaptic Vesicle Cycling at the Frog Neuromuscular Junction. *The Journal of Neuroscience*, *22*(24), 10680–10689. https://doi.org/10.1523/JNEUROSCI.22-24-10680.2002

Robinson, S. W., Bourgognon, J.-M., Spiers, J. G., Breda, C., Campesan, S., Butcher, A., Mallucci, G. R., Dinsdale, D., Morone, N., Mistry, R., Smith, T. M., Guerra-Martin, M., Challiss, R. A. J., Giorgini, F., & Steinert, J. R. (2018). Nitric oxide-mediated posttranslational modifications control neurotransmitter release by modulating complexin farnesylation and enhancing its clamping ability. *PLOS Biology*, *16*(4), e2003611. https://doi.org/10.1371/journal.pbio.2003611

Sanjana, N. E., Levanon, E. Y., Hueske, E. A., Ambrose, J. M., & Li, J. B. (2012). Activity-Dependent A-to-I RNA Editing in Rat Cortical Neurons. *Genetics*, *192*(1), 281–287. https://doi.org/10.1534/genetics.112.141200

Schindelin, J., Arganda-Carreras, I., Frise, E., Kaynig, V., Longair, M., Pietzsch, T., Preibisch, S., Rueden, C., Saalfeld, S., Schmid, B., Tinevez, J.-Y., White, D. J., Hartenstein, V., Eliceiri, K., Tomancak, P., & Cardona, A. (2012). Fiji: An open-source platform for biological-image analysis. *Nature Methods*, *9*(7), 676–682. https://doi.org/10.1038/nmeth.2019

Shata, A., Saisu, H., Odani, S., & Abe, T. (2007). Phosphorylated synaphin/complexin found in the brain exhibits enhanced SNARE complex binding. *Biochemical and Biophysical Research Communications*, *354*(3), 808–813. https://doi.org/10.1016/j.bbrc.2007.01.064

Sigrist, S. J., Reiff, D. F., Thiel, P. R., Steinert, J. R., & Schuster, C. M. (2003). Experience-Dependent Strengthening of *Drosophila* Neuromuscular Junctions. *The Journal of Neuroscience*, *23*(16), 6546–6556. https://doi.org/10.1523/JNEUROSCI.23-16-06546.2003

Snead, D., Wragg, R. T., Dittman, J. S., & Eliezer, D. (2014). Membrane curvature sensing by the C-terminal domain of complexin. *Nature Communications*, *5*(1), 4955. https://doi.org/10.1038/ncomms5955

St Laurent, G., Tackett, M. R., Nechkin, S., Shtokalo, D., Antonets, D., Savva, Y. A., Maloney, R., Kapranov, P., Lawrence, C. E., & Reenan, R. A. (2013). Genome-wide analysis of A-to-I RNA editing by single-molecule sequencing in Drosophila. *Nature Structural & Molecular Biology*, *20*(11), 1333–1339. https://doi.org/10.1038/nsmb.2675

Wragg, R. T., Snead, D., Dong, Y., Ramlall, T. F., Menon, I., Bai, J., Eliezer, D., & Dittman, J. S. (2013). Synaptic Vesicles Position Complexin to Block Spontaneous Fusion. *Neuron*, *77*(2), 323–334. https://doi.org/10.1016/j.neuron.2012.11.005

Yang, X., Kaeser-Woo, Y. J., Pang, Z. P., Xu, W., & Südhof, T. C. (2010). Complexin Clamps Asynchronous Release by Blocking a Secondary Ca2+ Sensor via Its Accessory α Helix. *Neuron*, *68*(5), 907–920. https://doi.org/10.1016/j.neuron.2010.11.001

Figures

Figure 1. Mutation of predicted CK2 consensus sequence alters Cpx7A phosphorylation. (**A**). Representative images of protein loading control (Coomassie blue, top panel) and CK2 phosphorylation ([^{32}P] incorporation on autoradiograph, bottom panel) for Cpx7A I125M, N130S (Cpx7A^{N130S}) and for Cpx7A I125M, T127A, N130S (Cpx7A^{T127A}) compared to unedited Cpx7A I125, N130 (Cpx7A^{N130}) in *in vitro* phosphorylation assays. The absence (-) or presence (+) CK2 in labeling reactions is denoted. Phosphorylation of Cpx7A isoforms by CK2 *in vitro* shows "priming" effect when predicted CK2 consensus sequence is mutated. **(B)** Quantification of [^{32}P] incorporation for the indicated Cpx proteins in *in vitro* CK2 phosphorylation assays demonstrates reduction in Cpx phosphorylation when additional T127 site is mutated to a phospho-incompetent residue (T127A), suggesting that residues T127 and S130 are both required for proper Cpx phosphorylation. Data are shown as mean±SEM.

Figure 2. ADAR is required for activity-dependent structural plasticity. (**A**) Immunostaining of developmentally-matched 3rd instar larval muscle 6/7 NMJs at segment A3 from control (Cantonized *adar^{5G1}*) and *adar* mutant (*adar^{5G1}*) animals with antibodies against Brp (green), Cpx (gray), and anti-HRP (magenta) after being raised in either low (25 °C, blue, top panel) or high (29 °C, orange, bottom panel) temperature conditions. Scale bar=10 µm. (**B**) Basal synaptic growth of control and *adar^{5G1}* mutant animals is similar, quantified as a bouton number normalized to muscle 6/7 area. (**C**) Controls show activity-dependent structural plasticity, whereas *adar* mutants lack this plasticity. Control animals have an increase in bouton number when raised at a high temperature compared to low temperature rearing conditions. Data are shown as mean±SEM; **p*<0.05, ***p*<0.01, ****p*<0.001, *****p*<0.0001, ns=not significant.

Figure 3. Phospho-competent Cpx7A does not display activity-dependent structural plasticity. (**A**) Immunostaining from developmentally-matched 3rd instar larval muscle 6/7 NMJs at segment A3 from control (*elav^{C155}-GAL4*, *cpx^{PE}* (precise excision (Huntwork & Littleton, 2007), *cpx^{SH1}* (*elav^{C155}-GAL4*, *cpx^{SH1}*), Cpx7A^{N130} (*elav^{C155}-GAL4*, *cpx^{SH1}*, UAS-Cpx7A^{I125,N130}), Cpx7A^{N130S} (*elav^{C155}-GAL4*, *cpx^{SH1}*, UAS-Cpx7A^{I125M,N130S}), and Cpx7A^{N130D} (*elav^{C155}-GAL4*, *cpx^{SH1}*, UAS-Cpx7A^{I125,N130D}) animals with antibodies against Brp (red), Cpx (green), and anti-HRP (blue) after being raised in either low (25 °C, blue, top panel) or high (29 °C, orange, bottom panel) temperature conditions. Scale bar=10 µm. (**B**) Quantification of activity-dependent

structural plasticity, quantified as a bouton number normalized to muscle 6/7 area. Control animals have an increase in bouton number when raised at a high temperature compared to low temperature rearing conditions. Data are shown as mean±SEM.

Figure 1

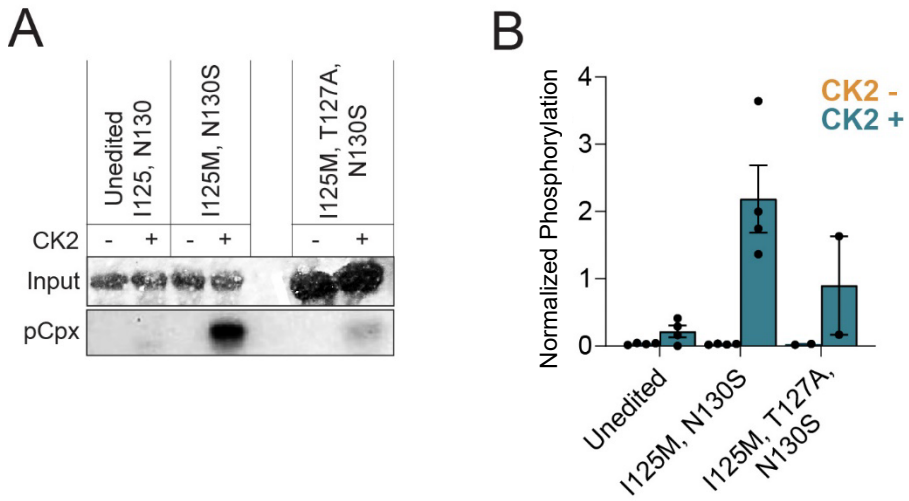
A
Unedited I125, N130
I125M, N130S
I125M, T127A, N130S
CK2
- + - + - +
Input
pCpx
B
Normalized Phosphorylation
0
1
2
3
4
CK2 -
CK2 +
Unedited
I125M, N130S
I125M, T127A, N130S

Figure 2

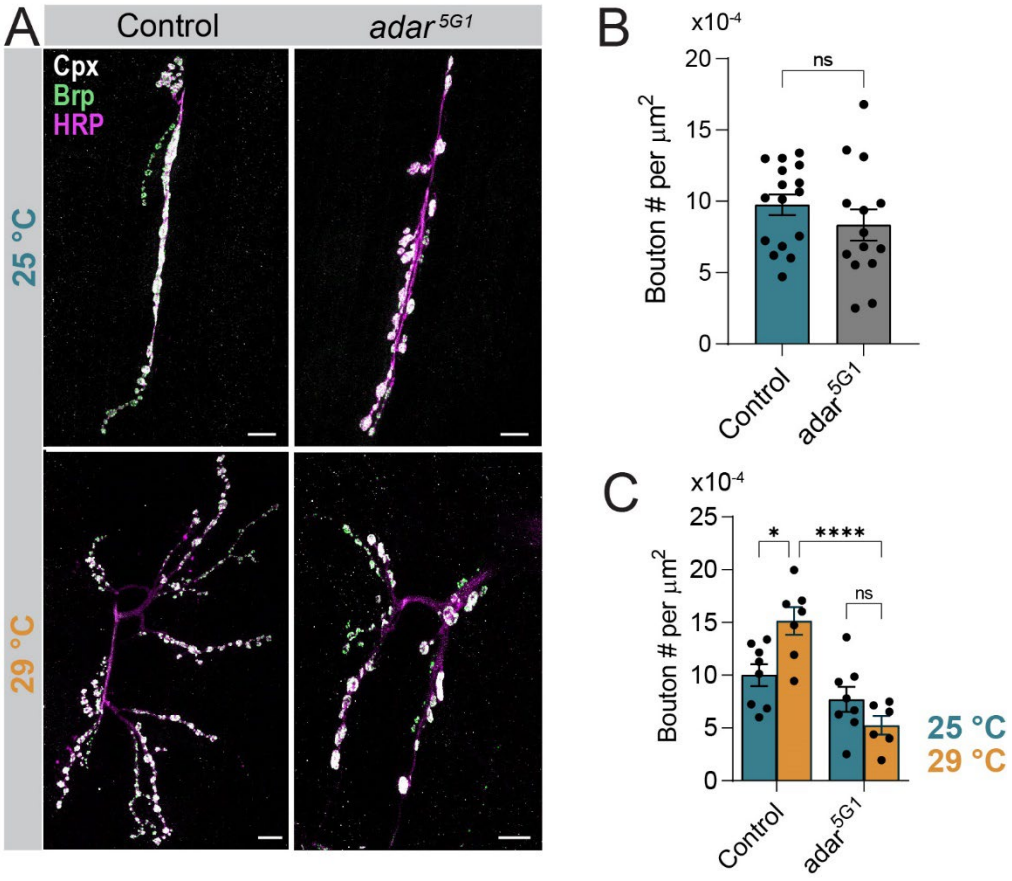
A
Control
adar5G1
Cpx
Brp
HRP
25 °C
29 °C
B
x10-4
Bouton # per µm2
ns
Control
adar5G1
C
x10-4
Bouton # per µm2
*
****
ns
25 °C
29 °C
Control
adar5G1

Figure 3

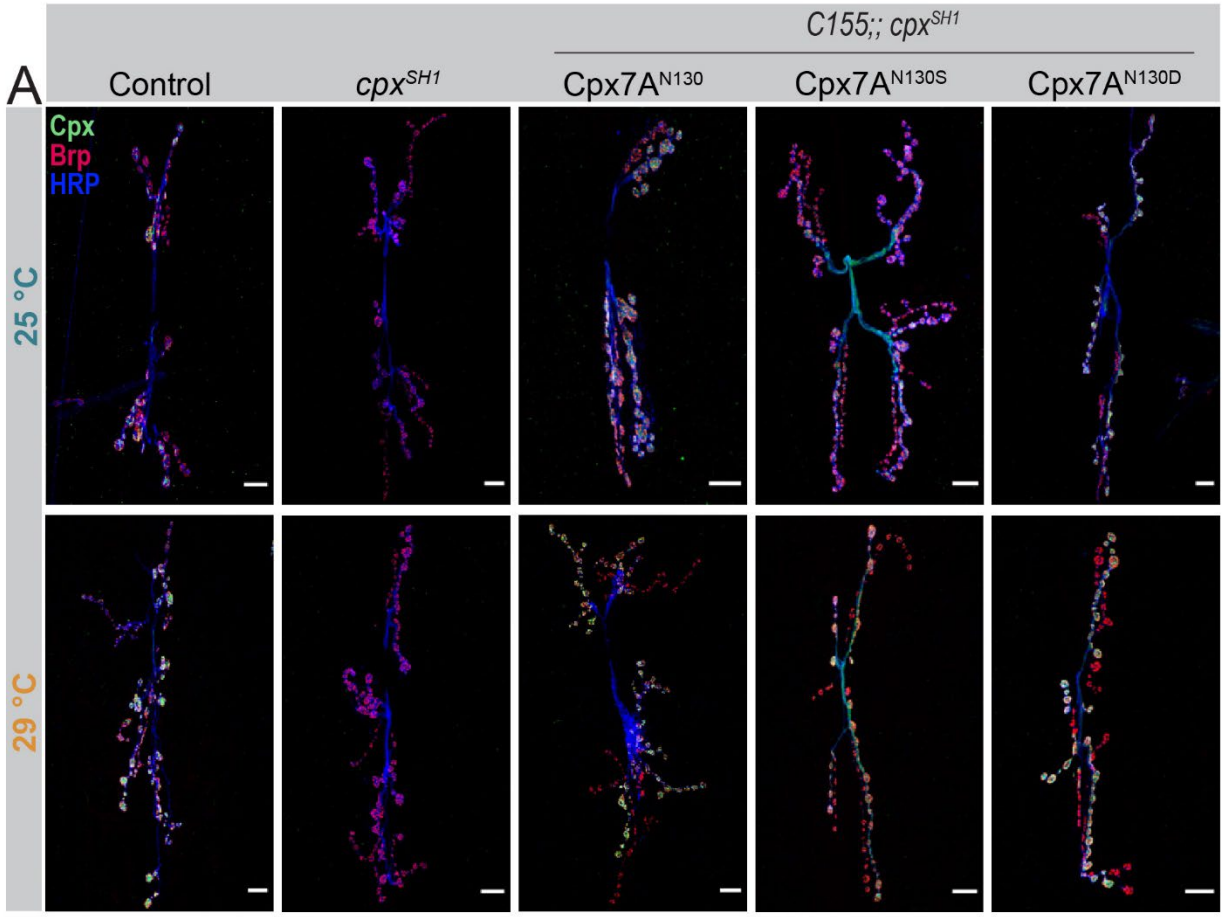
A
C155;; cpxSH1
Control
cpxSH1
Cpx7AN130
Cpx7AN130S
Cpx7AN130D
Cpx
Brp
HRP
25 °C
29 °C

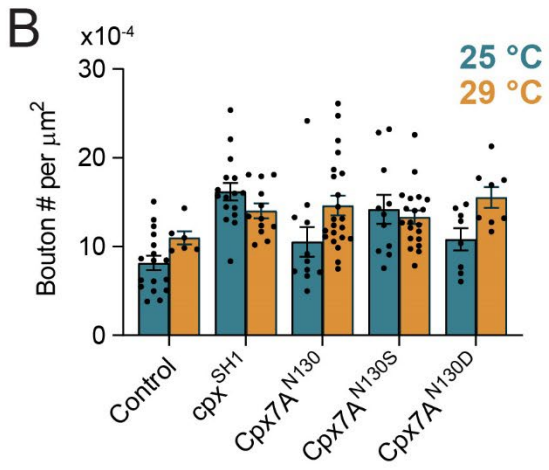
B
x10-4
30
20
10
0
Bouton # per µm2
25 °C
29 °C
Control
cpxSH1
Cpx7A N130
Cpx7A N130S
Cpx7A N130D